Deciphering the paleoceanographic and paleoclimatic changes of the Gulf of Cádiz during the past 2.6 million years

Utrecht Studies in Earth Sciences 114

Dissertation committee:

Prof. dr. David A. Hodell
Univeristy of Cambridge, United Kingdom

Prof. dr. Francisco J. Sierro
Universidad de Salamanca, Spain

Prof. dr. Antje Voelker
Instituto Português do Mar e da Atmosfera (IPMA), Portugal

Prof. dr. Friederike Wagner-Cremer
Utrecht University, Netherlands

Prof. dr. Gert-Jan Reichert
Utrecht University, Netherlands

ISBN 978-90-6266-437-5

Cover: "*Strait of Gibraltar*" courtesy of Lucas J. Lourens. Layout by Margot Stoete of GeoMedia

Printed in the Netherlands by WPS, Zutphen.

Deciphering the paleoceanographic and paleoclimatic changes of the Gulf of Cádiz during the past 2.6 million years

Ontrafelen van de paleoceanografische en paleoklimatologische veranderingen in de Golf van Cádiz in de laatste 2.6 miljoen jaar

(met een samenvatting in het Nederlands)

Die Entschlüsselung der paläozeanographischen und paläoklimatologischen Veränderungen im Golf von Cádiz der vergangenen 2,6 Millionen Jahre

(mit einer Zusammenfassung in deutscher Sprache)

PROEFSCHRIFT

ter verkrijging van de graad van doctor aan de Universiteit Utrecht
op gezag van de rector magnificus, prof.dr. G.J. van der Zwaan,
ingevolge het besluit van het college voor promoties
in het openbaar te verdedigen

vrijdag 9 september 2016 des middags te 12.45 uur

door

Stefanie Kaboth

geboren op 14 maart 1985
te Mühlhausen, Duitsland

Promotor:
Prof. dr. L. J. Lourens

This thesis was accomplished with the financial support from NWO-ALW grant (project number 865.10.001) to Prof. dr. L.J. Lourens. Parts were also funded by ECORD, AGU and Bristol University grants.

Deciphering the paleoceanographic and paleoclimatic changes of the Gulf of Cádiz during the past 2.6 million years

Stefanie Kaboth

Utrecht 2016

Tempora mutantur, nos et mutamur in illis.

Contents

Chapter 1

Introduction and summary

This thesis aims to shed new light on the climatic dependent evolution of Mediterranean Outflow Water (MOW) throughout the Pleistocene epoch which comprises the last ~2.8 million years. During this period of Earth`s history the global climate was predominately controlled by the waxing and waning of large continental ice sheets in the Northern Hemisphere and Antarctica paced by periodic changes in insolation. Although the warm and high-saline MOW is considered an important modulator of the North Atlantic salt budget that drives the oceanic northward heat distribution, and hence global climate, its potential role in affecting small- and large-scale climate variability has thus far remained poorly understood.

In this **first chapter**, I will briefly summarize the scientific consensus at the time this thesis was prepared and at the same time provide an introduction to the most import aspects and objectives of the conducted research (note that each of the following chapters contains an individual and more detailed introduction to the subject in question). At the end of this chapter, I will provide an overview of the individual thesis chapters.

1.1 Background and objectives

Since the re-opening of the Strait of Gibraltar at the end of the Messinian salinity crises (5.33 million years ago) a density driven exchange between Mediterranean Sea and the ambient North Atlantic established. The Atlantic-Mediterranean buoyancy drive is fostered by the net evaporation loss of the Mediterranean Sea itself (Baringer and Price, 1999; Bersch et al., 2007; Bryden et al., 1994; Hernández-Molina et al., 2014; Iorga and Lozier, 1999; Thorpe, 1976). The end-member of this circulation is the MOW exiting into the North Atlantic at the bottom of the Gibraltar Strait (Bryden et al., 1994; Sankey, 1973). These outflowing warm (10.5 to 14°C) and high saline (~38.5 PSU) water

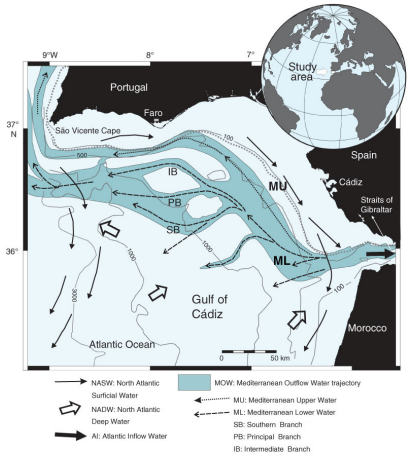

Figure 1.1: *Study area; Location map of the Gulf of Cadiz showing the recent flow pattern of MOW (Hernández-Molina et al., 2013; Stow et al., 2013)*

masses (Rogerson et al., 2012) can be traced due to their distinct fingerprint at intermediate water depth along the European continental margin until it mixes with the North Atlantic Current at Rockall Plateau (Hernandez-Molina et al., 2014).

After exiting the Strait of Gibraltar, the MOW plume cascades down and follows the seafloor morphology of the Gulf of Cadiz, while penetrating northwest along the continental slope (Ambar and Howe, 1979; Hernandez-Molina et al., 2014a; Hernández-Molina et al., 2006; Mulder et al., 2006). Within the Gulf of Cadiz, the MOW can be traced as two major flow cores located at 800-1400 m water depth alongside the middle slope (lower MOW), and at 500-700 m water depth (upper MOW) alongside the upper slope (Baringer and Price, 1997; Borenäs et al., 2002; Hernández-Molina et al., 2013) (see Fig. 1.1). Due to its increased salinity MOW is considered an important source for salt to the North Atlantic (see Fig. 1.2, Rogerson et al., 2012, 2006; Voelker et al., 2006). As the salt budget of the North Atlantic plays a crucial role in the modification of the thermohaline circulation – the oceanic conveyer belt driving the oceanic northward heat transport – it has become imperative to investigate the potential role of MOW not just as a reflection of Mediterranean climate variability but also in the context of global climate change. In light of the critical role of the modern northward heat transport by the Gulfstream and the indications that it has substantially weakened during the last decades, such knowledge is also important in order to forecast the potential consequences of anthropogenic climate change (Rahmstorf et al., 2015).

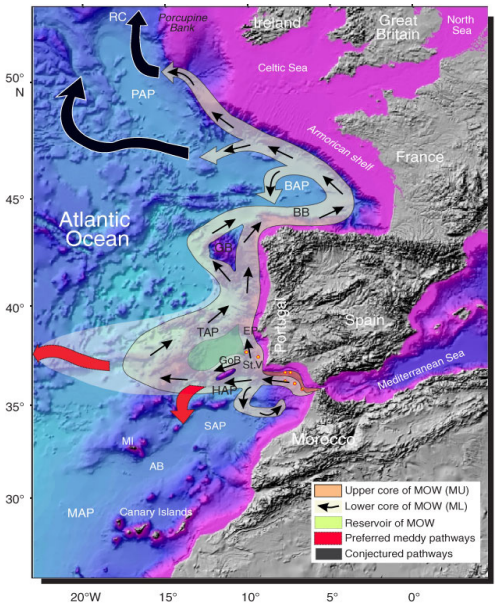

Figure 1.2: *General circulation pattern of the Mediterranean Outflow Water (MOW) pathway in the North Atlantic (modified from Iorga and Lozier, 1999). Red circles filled with yellow indicate relative location of proposed sites. AB = Agadir Basin, BAP = Biscay Abyssal Plain, BB = Bay of Biscay, EP = Extremadura Promontory, GaB = Galicia Bank, GoB = Gorringe Bank, HAP = Horseshoe Abyssal Plain, MAP = Madeira Abyssal Plain, MI = Madeira Island, PAP = Porcupine Abyssal Plain, RC = Rockall Channel, SAP = Seine Abyssal Plain, St.V = Cape São Vicente, TAP = Tagus Abyssal Plain (Hernández-Molina et al., 2013; Stow et al., 2013).*

Despite its potential global significance our current knowledge of the MOW is fragmented and mainly limited to data sets dating back not further than the climatic cycle (e.g. Bahr et al., 2014; Llave et al., 2007, 2006; Nelson et al., 1993, 1999; Rogerson et al., 2005; Schönfeld and Zahn, 2000; Schönfeld, 1997; Sierro et al., 1999; Toucanne et al., 2007; Voelker et al., 2006). From the available data it was inferred that MOW variability acts in concert with strong Milankovitch to millennial-scale oscillations in its source region, the Mediterranean Sea, and the ambient North Atlantic. Due to the direct interactions between the overflowing dense MOW and the sediments deposited in the Gulf of Cadiz, these climatic modulations have been eventually "recorded" in the sedimentological (e.g. grain-size, elementary composition) and microfossil (e.g. benthic foraminifera) properties of the sediments.

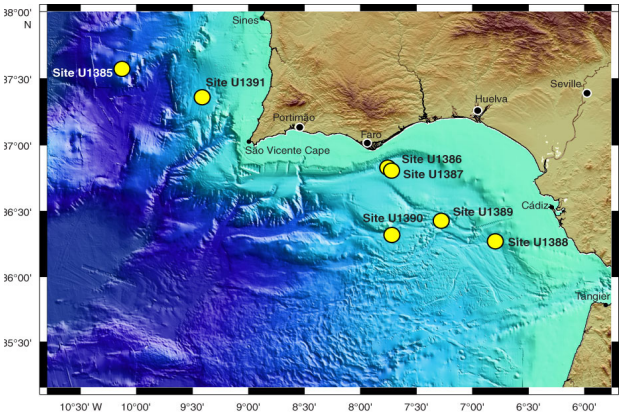

Figure 1.3: *Expedition 339 sites in the Gulf of Cádiz and West Iberian margin (Hernández-Molina et al., 2013; Stow et al., 2013).*

Only recently have we gained access to geological long paleoclimatic and paleoceanographic archives from the Pliocene epoch to the present day during the Integrated Ocean Drilling Program Expedition 339 in December 2011 to January 2012 (Hernández-Molina et al., 2013; Stow et al., 2013, see Fig. 1.3). This expedition specifically set out to provide constrains on MOW circulation patterns and its global impact beyond the last glaciations. From the total of seven sites (U1385-1391) drilled along the southern Iberian Margin we concentrated predominately on Sites U1386 along the upper slope and U1389 located along the middle slope for this thesis.

The main objectives of this thesis are:

- Reconstruction of the main features of MOW variability during the Late (last ~600.000 years) and Early Pleistocene (~2.6 to ~1.7 million years);
- Evaluating the influence of cold periods (e.g. glaciations, terminations, and ice-rafting events) on MOW behaviour; testing the concept of cold period intensification of MOW;
- Detailing the interconnection between hydrographic changes in the Mediterranean Sea and their impact on MOW variability;
- Analysing the response of MOW to low-latitude forcing and monsoonal influence, and;
- Investigating the role of MOW in the dynamics of the North Atlantic climate system and assessment of its potential global significance.

1.2 Chapter summary

In **Chapter 2** we investigated the upper MOW variability throughout the last climatic cycle. In an integrated approach, we correlate our benthic foraminiferal stable oxygen isotope ($\delta^{18}O$), grain-size and Zr/Al data with existing data from the Mediterranean Sea, open ocean and Gulf of Cadiz. We found clear indications for a vertical shift of the MOW from the upper to the middle slope of the Gulf of Cadiz during sea-level lowstands coinciding with MIS 4 and MIS 2, but also potentially during MIS 3. Additionally, our results indicate an increased upper MOW flow correlated with Heinrich Events 7 to 10 and the Younger Dryas, and also an inverse relationship with precession-forced monsoonal freshwater inputs into the Eastern Mediterranean.

The preliminary findings of low-latitude forcing on MOW variability are in-depth analysed in **Chapter 3** for the last 150 kyr based on the comparison of Zr/Al records from various drill sites of the IODP 339 Expedition located along the upper and middle slope. We document that enhanced MOW production was promoted by a weak East African Monsoon due to the reduction of freshwater input into the Eastern Mediterranean, and vice versa.
Consequently, high amounts of saline MOW discharged into the intermediate depth North Atlantic might have promoted deep water formation and stabilized the meridional overturning circulation. The direct coupling of MOW formation to low-latitude climate forcing represents a hitherto neglected way of propagating (sub)tropical climate signals into the high northern latitudes.

How applicable are the MOW characteristics identified throughout the last climatic cycle in regards to older glacial-interglacial cycles of the Late Pleistocene? This question is at the heart of **Chapter 4**. Here we present the first continuous and high-resolution benthic foraminiferal stable oxygen ($\delta^{18}O$) and carbon ($\delta^{13}C$) isotope as well as grain-size records representing the last ~570 kyr. Based on the comparison to its Mediterranean source region we identified three distinct phases of MOW variability throughout the Late Pleistocene at Site U1386 associated with distinct shifts in its composition and flow strength. It seems feasible that variability is caused predominately through changes in water mass sourcing from Mediterranean intermediate water by stronger contributions of the denser Western Mediterranean Deep-Water. This change in water mass sourcing is accompanied by the occurrence of distinct and precession paced $\delta^{18}O$ enrichment events during the interval between MIS 12 and MIS 6 contrasting the pattern of global ice volume change as inferred from the global mean $\delta^{18}O$ signal of the LR04 stack.

The origin of the MIS 8 and 6 $\delta^{18}O$ enrichment events is investigated in greater depth in **Chapter 5**. Our results point towards increased ice volume and associated colder bottom water conditions than inferred from the LR04 stack as most feasible driving mechanisms for these enrichment events. Particular interesting is that the enrichment events coincide with with substantial ice advance periods on continental Europe (Drenthe and Fuhne) and pre-date "cooling events" along the Iberian Margin linked to European sourced meltwater pulses. Their precession pacing is probably connected to the influence of MOW events linking their temperature and ice volume signal directly to its Mediterranean source region.

After concentrating on MOW variability throughout the Late Pleistocene we set out to test our earlier findings in the context of the different climatic background conditions of the Early Pleistocene in **Chapter 6**. Here we present the first benthic foraminifera $\delta^{18}O/\delta^{13}C$ and grain-size records from the upper MOW core in the Gulf of Cadiz for the time interval between 2.6 and 1.8 Ma. We find strong indications of MOW activity along the upper slope on glacial-interglacial timescales during the Early Pleistocene. We also find indications that the increasing presence of MOW in the Gulf of Cadiz during the investigated time interval aligns with the progressive

northward protrusion of Mediterranean sourced intermediate water masses into the North Atlantic, possibly modulating the intensification of the North Atlantic Meridional Overturning Circulation at the same time. Additionally, our results suggest that MOW flow strength was already governed by precession and semi-precession cyclicity during the Early Pleistocene against the background of glacial-interglacial variability dominated by the obliquity cycle of Earth`s inclination axis.

Chapter 2

New insights into upper MOW variability over the last 150 kyr from IODP 339 Site U1386 in the Gulf of Cadiz

published as: Kaboth, S., Bahr, A., Reichart, G.-J., Jacobs, B., Lourens, L.J., 2015. New insights into upper MOW variability over the last 150kyr from IODP 339 Site U1386 in the Gulf of Cadiz. Mar. Geol. doi:10.1016/j.margeo.2015.08.014

The upper Mediterranean Outflow (MOW) paleoceanographic history in the Gulf of Cadiz is poorly constrained due to the lack of high-resolution records that pre-date the last glaciation. Existing proxy records concentrate on MOW variability along the middle slope of the Gulf of Cadiz. Here we present a continuous high-resolution benthic foraminifera δ18O record from the upper MOW core at IODP Expedition 339 Site U1386 in the Gulf of Cadiz of the past 150.000 years. Based on δ18O, grain-size and Zr/Al variability comparison of our results with existing Mediterranean Sea (MD01-2472, MD95-2043), open ocean (LR04) and Gulf of Cadiz (MD99-2339) records we have gathered new insights into the evolution of the upper MOW core on glacial-interglacial timescales. The influence of the upper MOW at Site U1386 was strongest during MIS 5 and MIS 1. Similar δ18O variability can be seen in the Levantine Intermediate Water (LIW) originating from the Levantine Basin of the eastern Mediterranean Sea. We found clear indication for a vertical shift of the MOW from the upper to the middle slope of the Gulf of Cadiz during sea level lowstands coinciding with MIS 4 and MIS 2 but also during MIS 3. Additionally, our results indicate an increased upper MOW flow correlated with Heinrich Events 7 to 10 and the Younger Dryas, and also inversely relate to precession-forced monsoonal freshwater inputs into the Eastern Mediterranean. In the context of Sapropel formation, we could not find conclusive evidence of the proposed MOW shutdown in our data.

2.1 Introduction

Mediterranean Outflow Water (MOW) is an end-member of the thermohaline exchange between the Mediterranean Sea and the adjacent North Atlantic Ocean, providing a source for warm, highly saline water to the eastern North Atlantic through the Gibraltar Gateway (Baringer and Price, 1999; Bersch et al., 2007; Bryden et al., 1994; Hernández-Molina et al., 2014; Iorga and Lozier, 1999; Thorpe, 1976) (Fig. 2.1A). The present-day Atlantic-Mediterranean exchange through the Gibraltar Gateway is driven by the evaporation loss of the Mediterranean Sea itself (Bryden et al., 1994; Sankey, 1973). This results in the inflow of colder and less-dense North Atlantic water at the surface and the outflow of warmer and denser Mediterranean sourced water masses at depth (Ambar and Howe, 1979; Bryden and Stommel, 1984; Bryden et al., 1994) (Fig. 2.1A).

The outflowing water masses consist predominately (~70%) of Levantine Intermediate Water (LIW), formed in the Eastern Mediterranean Basin, and changeable parts of Western Mediterranean Deep Water (WMDW) originating in the Alboran and Tyrrhenian Sea (Millot, 2014, 2009; Millot et al., 2006). Upon leaving the Strait of Gibraltar, the MOW plume cascades down and follows the

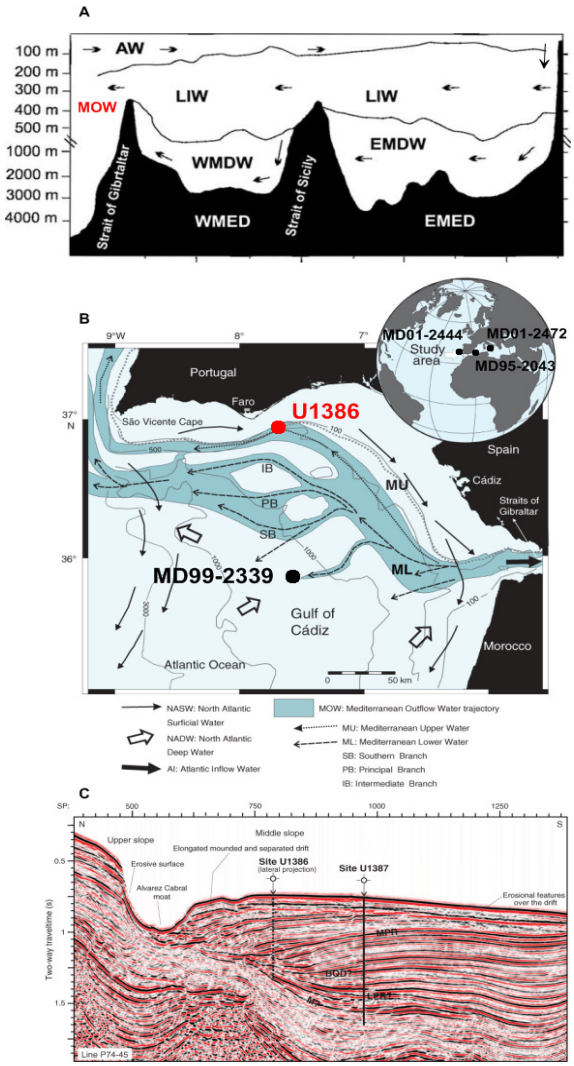

Figure 2.1: *Study area and Mediterranean Sea circulation (**A**) Simplified East – West cross section showing water mass circulation in the Mediterranean Sea (modified after Elshanawany et al., 2010). (Jansen et al., 1998)(Jansen et al., 1998)WMED = Western Mediterranean Sea; EMED =Eastern Mediterranean Sea; NASW = North Atlantic Water Surface Water; LIW = Levantine Intermediate Water; EMDW = Eastern Mediterranean Deep Water; WMDW = Western Mediterranean Deep Water; MOW: Mediterranean Outflow Water. (**B**) Location map of the Gulf of Cadiz showing the recent flow pattern of MOW modified after (Hernández-Molina et al., 2013; Stow et al., 2013); Site locations of U1386 (upper Mow core, this study), MD99-2339 (lower MOW core, Voelker et al., 2006), MD95-2043 (Alboran Sea, Cacho et al., 2006) and MD01-2472 (Corsica Through, Mediterranean Sea, Toucanne et al., 2012) are marked. (**C**) Multichannel seismic (MCS) reflection profile (Line P74-45) of Site U1386 and U1387 on the Faro- Drift (MCS lines provided by REPSOL Oil Company). SP = shot point. MPR = mid-Pleistocene revolution discontinuity, BQD = base Quaternary discontinuity, LPR = intra-lower Pliocene discontinuity, M = late Miocene discontinuity (Hernández-Molina et al., 2013).*

seafloor morphology of the Gulf of Cadiz, while penetrating northwest along the continental slope (Ambar and Howe, 1979; Hernandez-Molina et al., 2014a; Hernández-Molina et al., 2006; Mulder et al., 2006) overlying North Atlantic Deep Water (NADW), and underlying North Atlantic Central Water (NACW) and Antarctic Intermediate Water (AIW) (Baringer and Price, 1999; Hernandez-Molina et al., 2014a). As a water mass, the MOW can be traced within the Gulf of Cadiz in two major flow cores located at 800-1400 m water depth alongside the middle slope (lower MOW core), and at 500-700 m water depth alongside the upper slope including our study area (upper MOW core, Fig. 2.1B) (Baringer and Price, 1997; Borenäs et al., 2002; Hernández-Molina et al., 2013).

Since the reopening of the Strait of Gibraltar at 5.3 Ma (Hernández-Molina et al., 2014; Maldonado and Nelson, 1999) the Gulf of Cadiz is a key area to study MOW variability on glacial-interglacial time scales as its contourite depositional system has been shaped under the direct influence of the MOW (Hernandez-Molina et al., 2014a; Hernández-Molina et al., 2006; Llave et al., 2007, 2006; Nelson et al., 1993, 1999; Schönfeld and Zahn, 2000; Schönfeld, 1997; Stow et al., 2002; Toucanne et al., 2007; Voelker et al., 2006).

Previous studies have demonstrated the sensitivity of the upper and lower MOW core to climatic forcing on diverse time scales (e.g. Bahr et al., 2014; Llave et al., 2007, 2006; Nelson et al., 1993, 1999; Rogerson et al., 2005; Schönfeld and Zahn, 2000; Schönfeld, 1997; Sierro et al., 1999; Toucanne et al., 2007; Voelker et al., 2006). A variable spatial MOW influence was considered on glacial-interglacial timescales. It was argued that the lower MOW core was enhanced during cool (sea level lowstand) periods, favoring the development of sandy contourites whereas during warm climatic periods (sea level highstand) sandy contourites developed in shallower areas where the upper MOW was enhanced (Hernández-Molina et al., 2006; Llave et al., 2007, 2006; Schönfeld and Zahn, 2000; Voelker et al., 2006; Zahn et al., 1987). To explain this apparent pattern, an approximate doubling of the settling depth of the MOW plume during glacial periods was suggested due to increased density (Rogerson et al., 2012, 2005; Schönfeld and Zahn, 2000). On millennial time scales, evidence was found that North Atlantic Climate Oscillations such as Heinrich Events (HE1 to HE6) caused a short-term strengthening of the MOW alongside the upper and middle slope (Llave et al., 2006; Schönfeld and Zahn, 2000; Schönfeld, 2002a; Toucanne et al., 2007; Voelker et al., 2006). In addition, it was argued that the absence of MOW would reduce the Atlantic Meridional Overturning Circulation by as much as 15% compared to modern (Rogerson et al., 2012). The lack of sufficient long sediment records has so far hampered a full understanding of MOW variability on orbital and millennial timescales but also the assessment of its global impact. This is changing now rapidly with the Plio-/Pleistocene contourite drift sequences retrieved during IODP Expedition 339 from the Gulf of Cadiz (Hernández-Molina et al., 2013; Stow et al., 2013).

In this paper, we present a new benthic foraminifera oxygen isotope and a grain-size record from IODP 339 Site U1386 located on the upper slope of the Gulf of Cadiz (Fig. 2.1B). In an integrated approach, we correlate our data to existing Mediterranean Sea, open ocean and Gulf of Cadiz

Table 2.1: *Coordinates, water depth and corresponding water mass of used sites for $\delta^{18}O$ and grain-size comparison (Fig. 2.1B). [1]this study, [2]Toucanne et al., 2012, [3]Voelker et al., 2006, [4]Cacho et al., 2006*

Site	Lat (N)	Lon	Water Depth (m)	Water Mass
U1386	36°49.68	7°45.32 W	561	Upper MOW[1]
MD01-2472	42°36.42	9°43.97 E	501	LIW[2]
MD99-2339	35°52.80	7°31.80 W	1170	Lower MOW[3]
MD95-2043	36°8.58	2°37.26 E	1841	WMDW[4]

records (Fig. 2.1B). We aim to relate our data to glacial-interglacial induced sea level variations, Heinrich Events (HEs) and Sapropel (S) formation in the Eastern Mediterranean Sea. This study is a contribution to deepen our understanding on how these climatic oscillations affected upper MOW variability at Site U1386 in the past, how upper MOW core variations relate to changes in the lower MOW core at the same time, and how hydrographic changes within the Mediterranean Sea contributed to these variations over the last 150 kyr.

2.2 Material & Methods

2.2.1 Site U1386

Integrated Ocean Drilling Program (IODP) Site U1386 was drilled during Expedition 339 in November to January 2011/2012 and is located southeast of the Portuguese Margin mounded on the Faro Drift along the Alvarez Cabral Moat at 36°49.68'N; -7°45.32'W in 561 m water depth (Fig. 2.1B and C). The Faro drift is part of the Contourite Depositional System (CDS) of the Gulf of Cadiz (Stow et al., 2013). At present, IODP Site U1386 is directly influenced by the upper MOW core (Hernández-Molina et al., 2013; Stow et al., 2013, 2002). The composite depth scale (meters composite depth, MCD) was developed from parallel holes at Site U1386 during the expedition (Hernández-Molina et al., 2013), and has been applied in this study. For this study 161 sediment samples were analyzed for $\delta^{18}O$ and grain-size at 30 cm intervals between 0 to 45.08 mcd (~150 kyr) resulting in an approximately 1 kyr resolution.

2.2.2 Oxygen isotopes

The freeze-dried sediment samples were wet sieved into three fractions: (>150 μm, >63 μm and >38 μm), and their residues oven dried at 40°C. Stable oxygen isotope analyses were carried out on 4 to 6 specimens of the epifaunal living foraminifera species *Planulina ariminensis* from the >150 μm size fraction. All selected specimens were crushed, sonicated in ethanol, and dried at 35˚C. Stable isotope analyses were carried out on a CARBO-KIEL automated carbonate preparation device linked to a Finnigan MAT253 mass spectrometer at Utrecht University. The precision of the measurements is ±0.08‰ for $\delta^{18}O$. The results were calibrated using the international standard NBS-19, and the in-house standard NAXOS. Isotopic values are reported in standard delta notation (δ) relative to the Vienna Pee Dee Belemnite (VPDB).

Changes in the $\delta^{18}O$ of foraminifera reflect a combination of global ice volume (sea level), temperature and local hydrographic influences such as salinity (Hodell et al., 2010). For our site-to-site comparison (see section 2.2.6) one can assume that the global ice volume contributions within the same time frame for the different $\delta^{18}O$ records are equal. Consequently, differences in $\delta^{18}O$ are caused by temperature and/or salinity differences of the water masses at the different sites. With this approach we are able to utilize $\delta^{18}O$ as a water mass tracer for MOW variability at Site U1386.

2.2.3 X-Ray Fluorescence analyses

The geochemical composition of sediment from Site U1386 was analyzed using a XRF Core Scanner II, (AVAATECH Serial No. 2) at the Royal Netherlands Institute for Sea Research (NIOZ). XRF scanning provides semi-quantitative estimates of light

atomic weight (e.g. aluminum) to heavy elements such as e.g. barium in a nondestructive manner (Jansen et al., 1998; Richter et al., 2006). XRF Core Scanner data were collected every 1 cm down-core over a 1.2 cm^2 area with down-core slit size of 10 mm in three separate runs using generator settings of 10, 30, and 50 kV, and a current of 1.5 mA respectively. Sampling time was set to 10, 20 and 40 s respectively and scanning took place directly at the split core surface of the archive half. The split core surface was covered with a 4 micron thin SPEXCerti Prep Ultralene1 foil to avoid contamination of the XRF measurement unit and desiccation of the sediment. The data were acquired by a Canberra X-PIPS Silicon Drift Detector (SDD; Model SXD 15C-150-500) with 150 eV X-ray resolution and the Canberra Digital Spectrum Analyzer DAS 1000. Raw data spectra were processed with the Iterative Least square software (WIN AXIL) package from Canberra Eurisys. To account for XRF signal distortions such as porosity variations, sediment surface roughness and the formation of a water film from condensation below the covering foil we "normalized" the raw total counts of a given element to the total counts of all processed elements for the same measurement position. This step of "normalization" reduces signal artifacts related to pronounced lithological changes (Bahr et al., 2014). The relative standard deviations of selected element counts for Site U1386 are aluminum (Al) = 1.43%, bromine (Br) = 3.57% and zirconium (Zr) = 1.45%.

2.2.4 Grain-size Analyses

The oxygen isotope sample preparation was used to obtain weight percentages of the grain-size fractions >150 µm, 150-63µm, 63-38 µm and <38 µm for every sample. We concentrate on the grain-size fraction between 63-150 µm which has been used previously as indicator for flow strength changes in the Gulf of Cadiz attributed to MOW variability (Rogerson et al., 2005). We disregard the size-fraction >150 µm to reduce the bias caused by planktic and benthic foraminifera abundances and test-size as well as IRD contributions.

To further account for the possible carbonate bias in the weight percentage of the size-fraction 63-150 µm we visually correlated these results to the Zr/Al ratios derived from the XRF scanning of the sediments. Bahr et al. (2014) argued that the Zr/Al ratio mainly reflects bottom current velocity and accumulation of heavy minerals linked to MOW variability.

Table 2.2: *Age control points used for the construction of the chronology at Site U1386 based on alignment of the normalized Br counts at Site U1386 to the planktic $\delta^{18}O$ Record of the Iberian Margin core MD01 – 2444 (Barker et al., 2011; Hodell et al., 2013) (Fig. 2.2A and B).*

Depth (MCD)	Age (ka)
0	0
2	10.642
2.7	11.302
3.7	16.831
12.5	31.12
13.4	32.419
13.7	33.341
14	34.64
14.7	35.902
15.5	37.702
16.2	38.6
16.4	39.23
16.75	40.401
17.1	41.178
17.5	41.995
18.2	43.33
18.7	44.249
19.4	46.25
19.5	47
20.2	48.11
24	56
25	58
27.21	65.037
28.05	70
28.1	71.24
29	74.95
29.55	75.544
30.05	84.194
30.15	86.174
34.5	104.6
37.7	110.11
40.45	116.53
43.7	127.6
44.4	133.12
45.04	134.77
48.05	150

2.2.5 Age control

Our chronology is based on the tuning of normalized bromine (Br) (Br/total counts) at Site U1386 derived from XRF scanning (Fig. 2.2A and B; Tab. 2.2) to the planktonic *G. bulloides* $\delta^{18}O$ record from core MD01 – 2444 (Barker et al., 2011; Hodell et al., 2013). This approach follows Bahr et al. (2014) who showed that conditions at the sea surface drive the Br content at Site U1387 which is located in vicinity and similar water depth as Site U1386 (Fig. 2.1C, Hernández-Molina et al. 2013). It was argued that Br is not distinctly influenced by varying lithology and its variations are not directly linked to other elements, making it an excellent tool for stratigraphic correlation (Bahr et al., 2014).

The chronology of the Marine Isotope Stages (MIS) follows Lisiecki and Raymo (2005). Heinrich Events (HEs) were identified following Sanchez-Goñi and Harrison, 2010 for HE1-6. The timing of the HE1-6 in the Hodell et al. (2013) chronology slightly differs from the GICC05 based chronology applied by Sanchez-Goñi and Harrison (2010). Following their description of the relationship of HEs and Greenland Stadials/Interstadials (GS/GI) we adapted their ages to our chronology. Following Bahr et al. (2014), the older HE 7-11 are based on the correlation of $\delta^{18}O$ and SST records of Site MD01-2444 (Martrat et al., 2007) put on the age model of Hodell et al. (2013). Heinrich Events 7 to 11 correspond to Iberian Margin Stadial (IMS) periods 1-IMS21, 22, 24, 25 and 2-IMS-1, respectively.

2.2.6 Site-to-Site comparison of $\delta^{18}O$

To evaluate changes in Mediterranean Outflow influence at Site U1386 during the last 150 kyr, we compared the $\delta^{18}O$ record from Site U1386 in the Gulf of Cadiz to the $\delta^{18}O$ records of cores MD01-2472 (Toucanne et al., 2012), MD99-2339 (Voelker et al., 2006) and MD95-2043 (Cacho et al., 2006) (Fig. 2.1B, Tab. 2.1). MD01-2472 is located at the Corsica Through (Northern Tyrrhenian Sea, Western Mediterranean) and bathes today in Levantine Intermediate Water (LIW). MD95-2043 is located in the western Alboran Sea within the Western Mediterranean Deep Water (WMDW) mass. WMDW is in addition to LIW the main contributor to MOW (Millot, 2009; Millot et al., 2006;

Figure 2.2: *Chronology of Site U1386; Blue columns represent MIS stages. Orange columns indicate Heinrich Events (H). Termination I and II are indicated by TI and TII, respectively and follow the chronology Lisiecki and Raymo (2005). (A) Normalized Br record of Site U1386 on shipboard MCD scale correlated to the planktonic $\delta^{18}O$ (G. bulloides) from core MD01 – 2444 (Barker et al., 2011; Hodell et al., 2013). The chronostratigraphy of MD01 – 2444 follows Hodell et al. (2013) which is based on tuning of the $\delta^{18}O$ record to the synthetic Greenland ice core of Barker et al. (2011). Lines with arrows indicate selected tie points used for the age model (a full list of tie points is available in Table 2.2). (B) Normalized Br record of Site U1386 on new time scale according to our tuning. (C) Comparison of the normalized benthic $\delta^{18}O$ record of Site U1386 on new time scale according to our tuning, and normalized global mean d18O LR04 stack on its respective age model (Lisiecki and Raymo, 2005) (D) Calculated Sedimentation rate for Site U1386. (E) Comparison of the planktic $\delta^{18}O$ record of MD01-2444 (blue line, Barker et al., 2011; Hodell et al., 2013), the SST record of MD01-2444,MD01-2443 (Martrat et al., 2007) and LR04 (Lisiecki and Raymo, 2005), on their respective age models. The correlation of Heinrich Events (brown columns) and Terminations I-II is shown between the different age chronologies.*

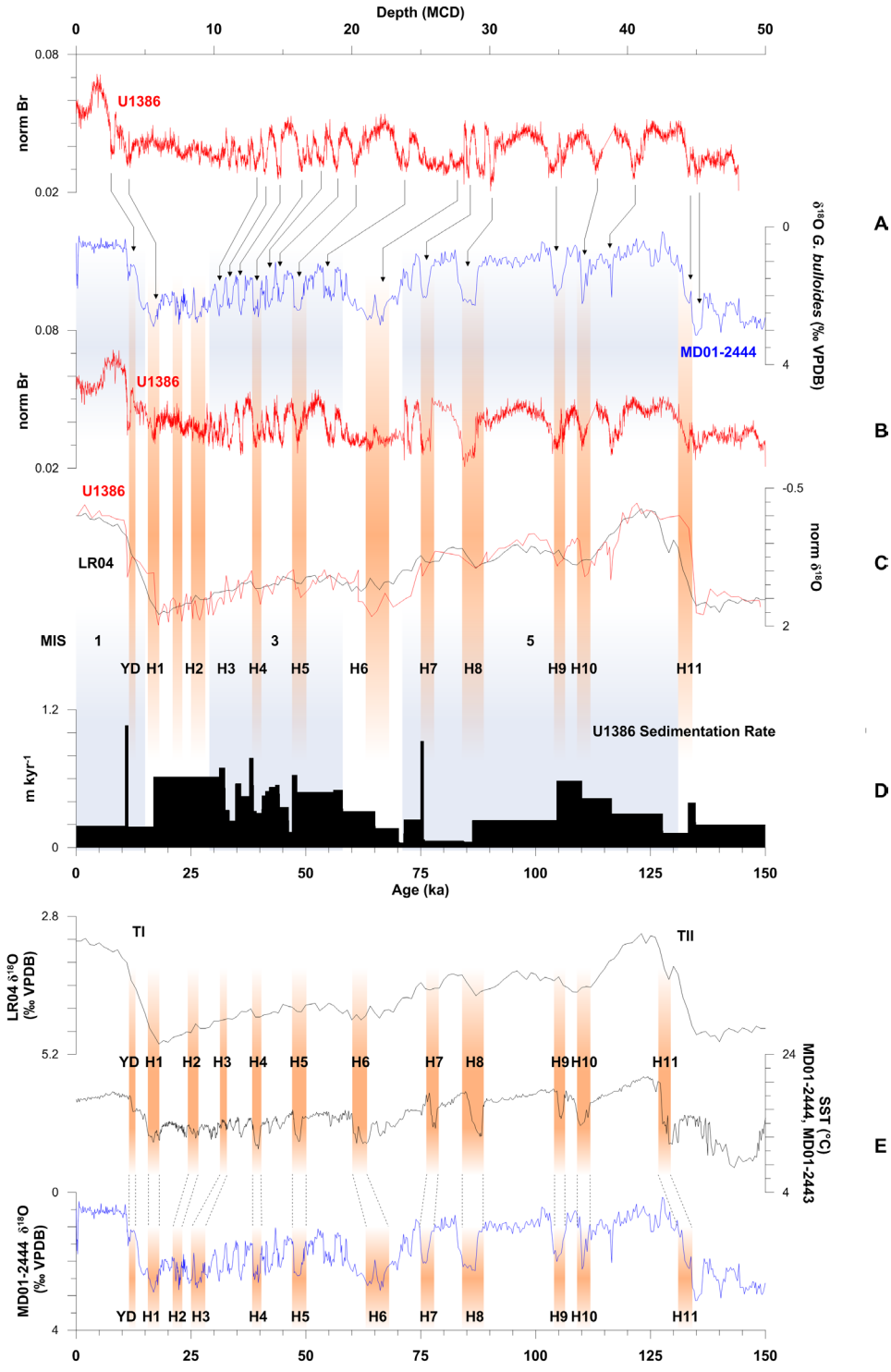
Depth (MCD)
0
10
20
30
40
50
0.08
0.02
norm Br
U1386
δ18O G. bulloides (‰ VPDB)
0
4
MD01-2444
A
B
C
D
E
-0.5
2
norm δ18O
LR04
MIS
1
3
5
YD H1 H2 H3 H4 H5 H6 H7 H8 H9 H10 H11
1.2
m kyr-1
U1386 Sedimentation Rate
0
25
50
75
100
125
150
Age (ka)
2.8
5.2
LR04 δ18O (‰ VPDB)
TI
TII
24
SST (°C) MD01-2444, MD01-2443
MD01-2444 δ18O (‰ VPDB)

Rogerson et al., 2012). MD99-2339 is located in the Eastern Gulf of Cadiz within the lower core of the MOW (Voelker et al., 2006).

For our comparison, we first corrected the four $\delta^{18}O$ records for interspecies offsets. For this purpose, we followed the calibration of Shackleton and Hall, 1984, who showed that *Uvigerina* spp. reliably represents calcite $\delta^{18}O$ in equilibrium with the ambient water mass, therefore setting the baseline for our comparison. The isotope record of core MD01-2472 is based on *Uvigerina* spp. therefore no further adjustment was necessary (Toucanne et al., 2012). The $\delta^{18}O$ records of cores MD95-2043 and MD99-2339, which are mainly based *on Cibicides* spp., were adjusted to those of *Uvigerina* by adding 0.64 ‰ to the $\delta^{18}O$ values following Shackleton and Hall, (1984) (see also Cacho et al., 2006; Voelker et al., 2006). Our oxygen isotope record of Site U1386 is based on *Planulina ariminensis*. Zahn et al., 1987 showed a small offset of -0.3‰ for $\delta^{18}O$ between *Planulina ariminensis* and *Cibicides wuellerstorfi*. To align Site U1386 to cores MD01-2472, MD99-2339 and MD95-2043 we adjusted the $\delta^{18}O$ values first to *C. wuellerstorfi* by -0.3 ‰ following Zahn et al. (1987), and secondly to *Uvigerina* by adding 0.64 ‰ following Shackleton and Hall (1984).

2.3 Results

2.3.1 Normalized Br and chronology

Normalized Br values (Br/total counts) at Site U1386 range between ~0.07 and ~0.02 within the time period investigated in this study. The highest values correlate to the early Holocene and the lowest values to late MIS 5. Despite the lack of an inherent glacial-interglacial pattern there is a good signal correlation on millennial and sub-millennial timescales between Br and planktonic *G. bulloides* $\delta^{18}O$ record from core MD01-2444 (Barker et al., 2011; Hodell et al., 2013; Martrat et al., 2007), as previously described by Bahr et al. (2014) (Fig. 2.2A).

However, the comparison of the $\delta^{18}O$ record of Site U1386, based on our age model, to LR04 (Lisiecki and Raymo, 2005) based on its respective age model yields a distinct offset between the records at the penultimate transition TII (~130 kyr) (Fig. 2.2C). This is not surprising since the LR04 stack, contrary to the absolute "Speleo-Age" timescale of MD01-2444 published by Hodell et al. (2013) and based on Barker et al. (2011), contain inherent assumptions about the time lag between insolation forcing and ice-sheet response (Hodell et al., 2013).

To qualitatively investigate TII time offset further we included the SST record of core MD01-2444 from the Iberian Margin based on its initial age model which is based on the GICC05 and EDC2 chronology (Martrat et al., 2007). Note, that the SST record was not used for the purpose of constructing our chronology.

The comparison of these three records, each drawn on their individual age scales, yields a good agreement for TI and obvious differences at TII (Fig. 2.2E). It seems feasible that the application of MD01-2444, based on the age scale of Hodell et al. (2013), as tuning target introduced the TII offset into our $\delta^{18}O$ record in comparison to LR04 and the SST record. This comparison showcases that independently from the age model used a TII offset would have occurred in comparison to LR04. Without better constraint at TII from possible tuning targets we are at this point unable to further validate our tuning for this time interval. As a consequence we exclude from our discussion TII and the preceding MIS6.

The estimated mean sedimentation rate for Site U1386 (Fig. 2.2D) is ~0.4 m/kyr which differs from the relatively uniform sedimentation rate of ~0.25 m/kyr that has been calculated from shipboard stratigraphy for the past 1.8 Myr (Hernández-Molina et al., 2013; Stow et al., 2013). For

the lower slope of the Gulf of Cadiz, Voelker et al. (2006) showed sedimentation rates between 0.3 and 0.5 m/kyr. However, average sedimentation rates do not fully characterize the history of accumulation. A doubling and tripling of the sedimentation rate coincides with the transition of MIS 5 to MIS 4 (~75 ka) and TI (~10 ka). Condensed sections with low sedimentation rates of <0.1 m/kyr correlate with two intervals at ~70 kyr and 75 to 85 kyr, respectively.

2.3.2 Oxygen isotopes

Figure 2.2 shows the comparison between our $\delta^{18}O$ record of U1386 with the global mean $\delta^{18}O$ stack LR04 (Lisiecki and Raymo, 2005). The good signal correlation of these records for the last 150 kyr highlights the ice volume induced glacial-interglacial variability at Site U1386 (Fig. 2.2C).
On glacial-interglacial timescales Site U1386 shows lightest values (~1.20-1.30 ‰) during interglacials MIS 5 and 1 and glacial enrichment in $\delta^{18}O$ (~3.33-3.17 ‰) during MIS 4 and MIS 2. The penultimate transition TII and the last termination TI show depletion of ~2.32 ‰ and ~1.90 ‰, respectively. In comparison, MIS 3 is ambiguous showing a mixed glacial/interglacial behavior (see Fig. 2.2C).

While the $\delta^{18}O$ signal of Site U1386 and LR04 are coherently in-phase, $\delta^{18}O$ amplitude variations between these two signals are visible especially during MIS 5 and MIS 1 (Fig. 2.2C). These periods at Site U1386 are marked by a series of millennial-scale oscillations of triangular shape coinciding with Heinrich Events (HE7-HE10 during MIS 5) (following Bahr et al., 2014), Iberian Margin Stadials (20-25 during MIS 5) (Martrat et al., 2007), and the Younger Dryas (MIS1). These perturbations are of the order of up to 0.5 ‰ (e.g. MIS 5e) compared to the global mean $\delta^{18}O$.

2.3.3 Grain-size and Zr/Al ratios

In general, the highest grain-size values (63-150 µm) of >15 %-wt. occur during interglacials MIS 5 and MIS 1 but are, with the exception of the late Holocene, correlated to the same short term variability observed in our $\delta^{18}O$ record (Fig. 2.3A). Highest values of up to ~33 %-wt. are correlated with MIS 5d. The lowest grain size values correspond to glacial periods MIS 4 and MIS 2 with values <5 %-wt (63 µm). The grain-size values during MIS 3 show, similar to the $\delta^{18}O$ values, a mixed glacial/interglacial character.

The Zr/Al ratio at Site U1386 (see Fig. 2.3A) shows a similar glacial-interglacial behavior as the grain-size values (Fig. 2.3A). Highest Zr/Al values (4.7 to 7.6) are linked to the same short-term variability observed in the grain-size values during MIS 5 and MIS 1. The weight percentages of 63-150 µm record mimics the Zr/Al signal at Site U1386.

2.4 Discussion

2.4.1 Glacial-Interglacial MOW variability

Site U1386 reveals similar $\delta^{18}O$ values as MD01-2472 during MIS 5e and MIS 1 (Fig. 2.3A). This correspondence emphasizes the direct influence of LIW variability on upper MOW and its influence at Site U1386 during these time intervals, similar to modern conditions. During the alternating full glacial periods MIS 4 and MIS 2, LIW is characterized by enriched $\delta^{18}O$ values at MD01-2472 relative to Site U1386. This results in a clear $\delta^{18}O$ gradient (gray shaded area in Fig. 2.3A) between these two locations, suggesting that at Site U1386 is no longer influenced by the upper MOW core

and baths in more open ocean waters during these glacial time periods. A reduced isotopic gradient between both sites during MIS 5d to MIS 5a and MIS 3 points furthermore to the absence or a substantially reduced MOW influence during these time intervals at Site U1386.

In the context of glacial periods, our findings corroborate the outcome of previous studies of the last glaciation that show a reduction in the upper MOW branch activity whilst the lower MOW limb increases in flow, i.e. an approximate doubling of the settling depth of the MOW plume (Rogerson et al., 2012, 2005; Toucanne et al., 2007; Voelker et al., 2006). The downslope shift of the MOW plume during glacials was related to the reduced cross-section of the Gibraltar-Gateway in combination with the glacial induced increase in salinity of the Mediterranean Sea itself (Hernández-Molina et al., 2006; Rogerson et al., 2012). Numerical simulations, however, indicate that the MOW flow speed within the Strait of Gibraltar does not change significantly in response to sea-level variations (Alhammoud et al., 2010). An increased salinity due to the lowered sea level during MIS 5d to 5a and MIS 3 compared to MIS 5e and MIS 1 could explain the increased isotopic gradient (Fig. 2.3A), and might also indicate a downslope shift of a denser MOW during these intervals.

To test the downslope shift of MOW during MIS 3 and MIS 2 we included the $\delta^{18}O$ record of piston core MD99-2339 from the middle slope of the Gulf of Cadiz (Voelker et al., 2006) into our comparison. MD99-2339 is argued to have been influenced by the lower MOW branch during the last 50 kyr (Voelker et al., 2006). During late MIS 3 and MIS 2 the $\delta^{18}O$ signal at MD99-2339 is slightly depleted relative to the $\delta^{18}O$ signal at MD01-2472 (Fig. 2.3B). This might be due to admixing of $\delta^{18}O$ depleted inflowing North Atlantic Surface Water (NASW) into the MOW during its passage through Gibraltar. The isotopic gradient related to MD01-2472 is smaller than the gradient between U1386 and MD01-2472 at the same time indicating a downslope shift of MOW during this interval, and are consistent with our initial findings of an reduced upper MOW influence at Site U1386 (Fig. 2.3B). During MIS 1, the isotopic gradient increases substantially between MD99-2339 and MD01-2472 while the gradient between U1386 and MD01-2472 reduces, coinciding with the proposed increase of upper MOW flow during the late Holocene (Bahr et al., 2014; Llave et al., 2006; Rogerson et al., 2005).

At first these results seem to contradict the findings of Bahr et al. (2014) where the observed MIS 3 variability at Site U1387, located in the vicinity of Site U1386 (Fig. 2.1C), was attributed to MOW variability. However, Site U1386 is located closer to the present day upper MOW flow core. With lowered sea-levels during MIS 3, and inferred denser MOW than compared to MIS 1 and MIS

Figure 2.3: *Orbital and millennial scale induced MOW variability over the last 150 kyr. Blue columns represent MIS stages. Orange columns indicate Younger Dryas (YD), Heinrich Events (H) and Greenland Stadials 20 to 25 (italic). Brown columns representing Sapropel (S) following the chronology of Ziegler et al., 2010. Termination I and II are indicated by TI and TII, respectively and follow the chronology Lisiecki and Raymo (2005). (A) Comparison of Precession derived from the astronomical solution of La2010 (Laskar et al., 2011), Sanbao-Hulu d18O speleothem record (Wang et al., 2008), normalized $\delta^{18}O$ of sites U1386 (upper MOW core, red line, this study) and MD01-2472 (Levantine Intermediate Water, blue line, Toucanne et al., 2012) over the last 150 kyr including the grain-size (63-150 µm) and Zr/Al records from Site U1386. Small red arrows indicate intervals of inverse relationship to precession-forced monsoonal freshwater input into the Eastern Mediterranean (B) Comparison of $\delta^{18}O$ records from Site U1386 (upper MOW core, red line, this study), MD01-2472 (Levantine Intermediate Water, blue line, Toucanne et al., 2012), MD99-2339 (lower MOW core, orange line, Voelker et al., 2006) and MD95-2043 (Western Mediterranean Deep Water, green line, Cacho et al., 2006) over the last 50 kyr.*

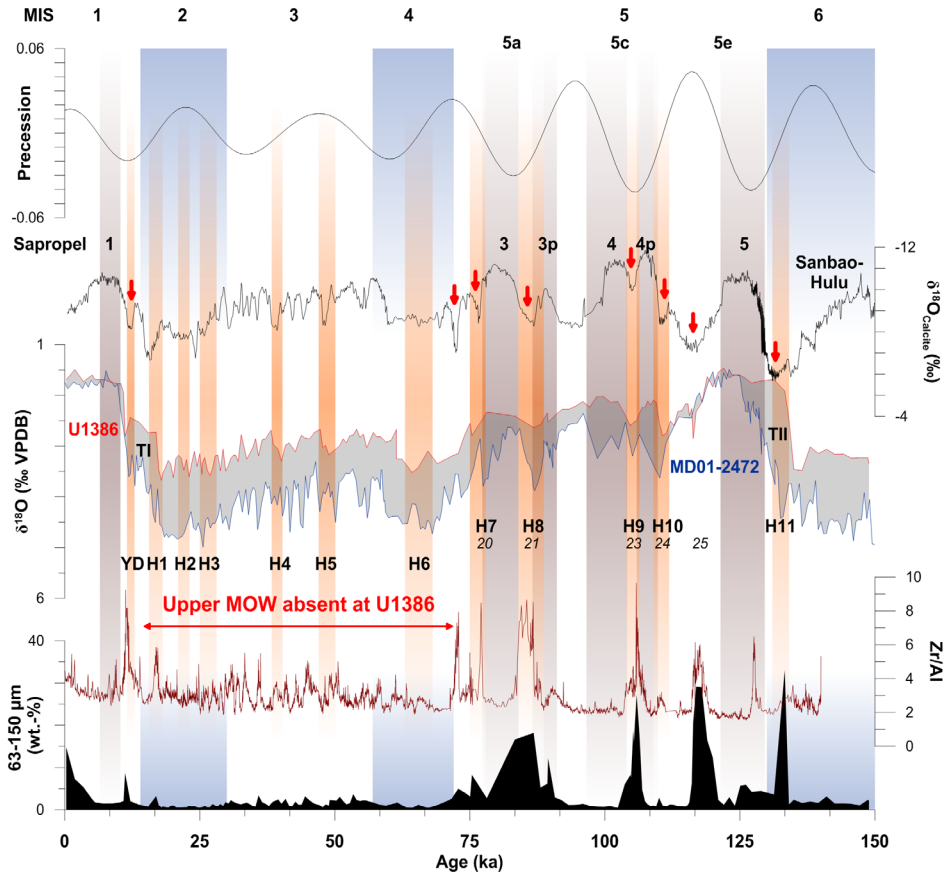
MIS
1
2
3
4
5
6
5a
5c
5e
Precession
0.06
-0.06
Sapropel
1
3
3p
4
4p
5
Sanbao-Hulu
δ18OCalcite (‰)
-12
-4
δ18O (‰ VPDB)
U1386
TI
TII
MD01-2472
YD H1 H2 H3
H4
H5
H6
H7
20
H8
21
H9
23
H10
24
25
H11
Upper MOW absent at U1386
63-150 µm (wt.-%)
40
0
Zr/Al
10
8
6
4
2
0
6
0
25
50
75
100
125
150
Age (ka)

A

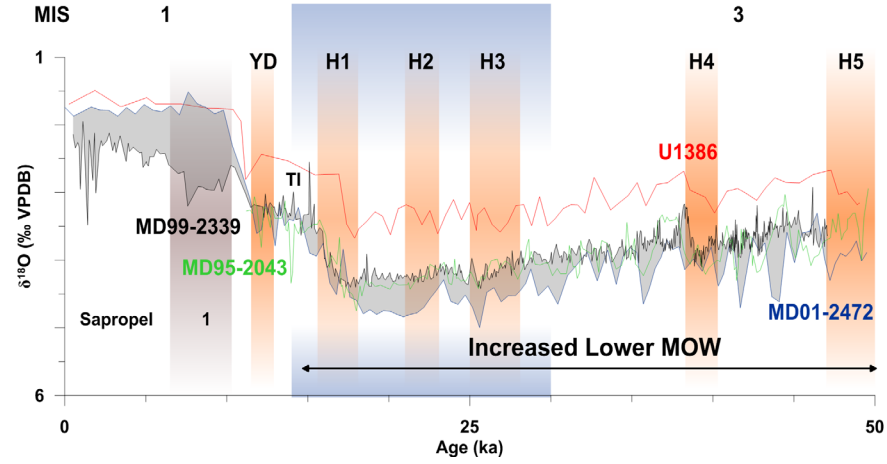
MIS
1
3
YD
H1
H2
H3
H4
H5
δ18O (‰ VPDB)
TI
U1386
MD99-2339
MD95-2043
MD01-2472
Sapropel
1
Increased Lower MOW
1
6
0
25
50
Age (ka)

B

5e, it is possible that the upper MOW core was vertically shifted downward influencing Site U1387 instead of Site U1386.

To explain the increased density of MOW during MIS 3 and MIS 2 Voelker et al. (2006) showed a close correlation between the $\delta^{18}O$ signal of MD99-2339 and the $\delta^{18}O$ record of MD95-2043 (Fig. 2.1B) from the Gulf of Lions (Cacho et al., 2006) on millennial and sub-millennial timescales. MD95-2043 is thought to show changes in Western Mediterranean Deep Water (WMDW) (Cacho et al. 2006). Based on the $\delta^{18}O$ signal correlation as well as the $\delta^{13}C$ comparison of MD99-2339 and MD95-2043 it was argued that WMDW contributions to MOW increased during MIS 3 and MIS 2 (Voelker et al., 2006). The comparison between MD99-2339, MD95-2043 and MD01-2472, within the error margin of the individual age models, shows that LIW is also characterized by very similar MIS 3 variability, and is relatively enriched in $\delta^{18}O$ (Fig. 2.3B). It is therefore possible that a denser LIW, due to the lowered sea level induced salinity increase, instead of WMDW, increased MOW density supplying the lower MOW core during MIS 3 and MIS 2.

2.4.2 Millennial-scale MOW variability

The grain size (63-150 μm) and Zr/Al records of Site U1386 do not show a distinct glacial-interglacial pattern corresponding with the $\delta^{18}O$ variability. The highest grain-size and Zr/Al values occur during interglacials MIS 5 and MIS 1 but are, with the exception of the late Holocene, correlated to sub-millennial high-latitude North Atlantic Climate Oscillations such as Heinrich Events (HE) 10 to 7, Greenland Stadials (GS) 20-25 and the Younger Dryas (YD) (Fig. 2.3A).

On millennial timescales, a coherent relationship between Greenland temperatures and grain size variability in the Gulf of Cadiz was revealed for lower MOW core records, available only during the interval HE6 to HE1 (Cacho et al., 1999; Rogerson et al., 2012; Voelker et al., 2006). It was shown that Heinrich Events correspond to relatively high energy MOW periods and enhanced sand deposition on the middle slope of the Gulf of Cadiz (Rogerson et al., 2005; Toucanne et al., 2007; Voelker et al., 2006). Llave et al. (2006) also recognized HE1, HE2, HE4 and HE6 as horizons depicted with coarse terrigenous debris in the upper MOW branch. At Site U1386 grain-size (63-150 μm) and Zr/Al ratios are also increased during the YD, while HE6 to HE2 are devoid of coarser grains. The interval during HE6 to HE1 coincides with an absent or less enhanced upper MOW influence at Site U1386 which may account for a bias in the grain-size data during this interval. For Site U1387 increased upper MOW flow was also suggested during HE10 to HE1 and the YD (Bahr et al., 2014).

It is noteworthy that the grain-size and Zr/Al variability at Site U1386 seems to be highly sensitive to millennial scale variations during sea level highstands and interglacials MIS 5 and MIS 1. Moreover, a decreasing trend in gran-size (63-150 μm) variability from MIS 5e to 5a, coinciding with lowering sea levels, and an increasing trend from the early MIS 1 to the late MIS 1, coinciding with increasing sea levels, can also be seen.

During HE6 to HE1 (MIS 4-2) when sea level was lower than compared to MIS 5 and MIS 1, Voelker et al. (2006) suggested an increased entrainment of WMDW into the MOW, facilitated by the colder temperatures over the Western Mediterranean Sea. This was argued to explain the increased flow speed along the middle slope. This argument could also been used during HE10 to HE7 (MIS 5) at Site U1386 where an increased entrainment of WMDW into a less dense interglacial MOW could increase the flow strength of the upper MOW core and therefore account for our results during these time periods. It was also argued that changes of the MOW settling depth not only relate to the characteristics of its source water masses but also the degree of mixing with of

al., 2006; Rogerson et al., 2012). Rogerson et al. (2012) emphasized the latter especially for periods of sluggish North Atlantic Deep Water (NADW) formation; such is the case during Heinrich Events. However, these time intervals also coincide with repeated short-lived enrichments in $\delta^{18}O$ at Site U1386 and at MD01-2472 suggesting a density increase of LIW feeding into the MOW at the same time.

2.4.3 Sapropel formation and its influence on Upper MOW variability

Sapropels are a distinct sedimentary feature of the eastern Mediterranean Sea coinciding with periods of precession-induced strong monsoonal rain fall in northern Africa (Cramp and O'Sullivan, 1999; Rossignol-Strick, 1985; Ziegler et al., 2010). These periods coincide with maxima in low latitude summer insolation during precession minima, driving the northward expansion of monsoonal rain belts. Amplified freshwater discharge into the Eastern Mediterranean Sea reduced intermediate and deep water convection, and is argued to have disrupted the North Atlantic-Mediterranean Sea exchange through the Gibraltar gateway causing a reduction in MOW formation, as documented for the Holocene Sapropel 1 (S1) in the Gulf of Cadiz (Cramp and O'Sullivan, 1999; Meijer and Tuenter, 2007; Myers et al., 1998; Rogerson et al., 2012; Rossignol-Strick, 1985; Toucanne et al., 2007; Voelker et al., 2006).

For more insight on the possible precession control on upper MOW variability, we compared the $\delta^{18}O$ records of U1386 and MD01-2472 with the Chinese composite Sanbao and Hulu cave $\delta^{18}O$ speleothem record (Wang et al., 2008, Fig. 2.3A). This record shows East Asian Monsoon activity which is dynamically linked to the African Monsoon system (Yamamoto et al., 2013). Depleted $\delta^{18}O$ values of the Sanbao-Hulu record have been related to maximum intensity of the African monsoon coinciding with an increase in precipitation and river run off over the Eastern Mediterranean Sea (Fig. 2.3A; Ziegler et al., 2010).

In this context, the $\delta^{18}O$ signal comparison of Site U1386 and MD01-2472 is particular interesting since MD01-2472 is directly recording LIW variability originating from the Eastern Mediterranean Basin (Toucanne et al., 2012). During sapropel formation, a freshwater induced reduction of intermediate and deep-water circulation in the Eastern Mediterranean Basin, leading to a reduced MOW, would decrease the supply of denser and therefore isotopically heavier water masses at Site U1386 (see Fig. 2.3A). We would expect Site U1386 to become more influenced by the open ocean signal and hence appear relatively depleted in $\delta^{18}O$ compared to MD01-2472, with the isotopic gradient between these two sites increasing. This is the case for S4 and S3 where the $\delta^{18}O$ of MD01-2472 is enriched and remains relatively depleted at Site U1386. In contrast, S5 and S1 show a decreased isotopic gradient between these sites. The lowered sea-level during MIS 5c and MIS 5a corresponding to S4 and S3 compared to S5 and S1 (MIS 5e and MIS 1) could account for these deviations since the expected salt accumulation during S4 and S3 had a more prominent effect.

Empirical reconstructions and modelling also suggest that thermally driven (Myers, 2002) remnant overturning circulation still occurs even throughout the most extreme surface freshening phases (De Lange et al., 2008; Meijer and Tuenter, 2007; Myers et al., 1998; Rogerson et al., 2012). If true, this argues against a complete collapse of Eastern Mediterranean Sea circulation since LIW formation could still occur; with surface water masses remaining dense enough for intermediate water formation even if deep water formation was halted. This could argue for the formation of a relatively less dense and $\delta^{18}O$ depleted LIW (or better, its equivalent at that time) in the Eastern Mediterranean Sea, creating a less dense MOW which then less vigorously interacted with the Gulf

Cadiz sediments after passing the Gibraltar Gateway. This scenario might also explain the lack of ambient North Atlantic water masses as well as their vertical structure in the Gulf of Cadiz (Llave et sandy contourite on the middle slope within the Gulf of Cadiz (Toucanne et al., 2012; Voelker et al., 2006). The displacement of LIW comparable to present day by intermediate water masses depleted in $\delta^{18}O$ at MD01-2472 during S5 and S1 might also explain our observations.

For the Holocene S1, the proposed reduction of MOW is documented by the absence of sandy contourite layers from the middle slope of the Gulf of Cadiz at MD99-2339 (Voelker et al., 2006) and MD99-2431 (Toucanne et al., 2007). Based on the low grain size values coinciding with decreased magnetic susceptibility Voelker et al. (2006) argued a sudden reduction in flow strength and sediment delivery by the lower MOW core towards MD99-2339 during this time interval, as only an increased bottom flow strength would facilitate an increased deposition of ferromagnetic, lithic grains (Voelker et al., 2006). Toucanne et al. 2007 also argued a flow reduction coinciding with Sapropel 1 at MD99-2341, located on the central slope, based on low grain size values. It was argued that the general inactivity of MOW lead also to the deposition of muddy contourites on the upper slope causing a Gulf-wide "Holocene sandy contourite gap" (Rogerson et al., 2012). The grain-size and Zr/Al values at Site U1386 show slightly increased values during the early phases of S5, and S3p, but are typically low throughout intervals of sapropel formation.

Interestingly, the high amplitude grain-size (63-150 μm) and Zr/Al variations at Site U1386 occurring in-between S4p and S4 and S3p and S3 are inversely related to precession-forced monsoonal freshwater input into the Eastern Mediterranean while also coinciding with high latitude cold events HE8 and HE7 (indicated by small red arrows in Fig. 2.3A). This relationship is not limited to the intervals of S4 and S3 but also present at Site U1386 throughout MIS 5 and MIS 1. Reduced riverine freshwater input into the Levantine Basin might have caused intense intermediate water formation promoted by the intrusion of cold and dry air masses into the eastern Mediterranean related to a strong Siberian High as inferred for the Younger Dryas and Heinrich Events (Kotthoff et al., 2008), and could have enhanced the upper MOW against the background of global ice volume change.

2.5 Conclusions

Our results from Site U1386 suggest a direct influence of the upper MOW during MIS 5e and MIS 1 suggesting LIW to be the main contributor to MOW, these circumstances resemble modern conditions. During the glacial sea-level lowstands the Upper MOW core did not supply Site U1386 due climate paced modification of LIW creating a denser and deeper flowing MOW. During MIS 5d to 5a and MIS 3 the Upper MOW influence at Site U1386 seems to be also reduced or completely absent. Our results suggest that a certain sea level threshold is required for MOW to increase its influence Site U1386.

Grain-size and Zr/Al variability at Site U1386 seems to be highly sensitive to sub-millennial scale variations at Site U1386 during sea level highstands and interglacials MIS 5 and MIS 1 correlating with North Atlantic Cold Events as well as reduced riverine input during reduced Monsoon activity.

Acknowledgements

We thank two anonymous reviewers for providing helpful suggestions for the improvement of the final version of this paper. We acknowledge the Integrated Ocean Drilling Program (IODP) for providing

the samples used in this study as well as A. van Dijk at Utrecht University and R. Gieles at NIOZ for analytical support. This research was funded by NWO-ALW grant (project number 865.10.001) to Lucas J. Lourens. We thank T. Kouwenhoven and F. Hilgen for providing valuable comments on the manuscript.

Chapter 3

Persistent monsoonal forcing of Mediterranean Outflow dynamics during the late Pleistocene

published as: Bahr, A., Kaboth, S., Jiménez-Espejo, F.J., Sierro, F.J., Voelker, A.H.L., Lourens, L., Röhl, U., Reichart, G.J., Escutia, C., Hernández-Molina, F.J., Pross, J., Friedrich, O., 2015. Persistent monsoonal forcing of Mediterranean Outflow Water dynamics during the late Pleistocene. Geology 43, 951–954. doi:10.1130/G37013.1

The mode and vigour of the global oceanic circulation critically depends on the salinity of (sub)surface water masses advected to the loci of deep water formation. Within the Atlantic meridional overturning circulation (AMOC), an important supplier of high-salinity waters is the Mediterranean Outflow Water (MOW), discharging into the North Atlantic via the Strait of Gibraltar. Despite its importance for the North Atlantic salinity budget, the long-term dynamics of MOW production have remained poorly understood. Here, we present high-resolution records of bottom-current velocity from three drill sites within the Gulf of Cadiz that document a persistent low-latitude forcing on MOW flow speed over the past ~150 kyr. We demonstrate that the African Monsoon is the predominant driver of orbital-scale MOW variability via its influence on the freshwater budget in the Eastern Mediterranean. Consequently, MOW formation fluctuates in concert with hemisphere-wide monsoonal systems imposing a strong precession forcing that modulates centennial-scale oscillations of high-latitude origin. We further document that summer insolation minima stimulate maximal injection of MOW-derived salt into the North Atlantic, likely strengthening the intermediate AMOC branch. The direct coupling of MOW formation to low-latitude climate forcing represents a hitherto neglected way of propagating (sub)tropical climate signals into the high northern latitudes.

Introduction

Recent studies have suggested a rather stable overturning circulation prevailed during most of the past 150 kyrs despite considerable variations in the glacial and interglacial boundary conditions (Böhm et al., 2014; Guihou et al., 2011). Hence, efficient negative feedbacks must help to sustain a robust AMOC, although the nature of these feedbacks still awaits clarification (Böhm et al., 2014; Guihou et al., 2011; Rahmstorf, 2002). Because the salinity budget of upper ocean waters in the North Atlantic preconditions the vigor of deep-water formation in the Nordic Seas, much attention has been paid to potential ways enhancing the salinity input into high latitudes. The MOW is an important provider of high salinity waters with a distinct influence on the intermediate depth North Atlantic and a direct influence on the strength of the AMOC (Potter and Lozier, 2004; Schmitz and McCartney, 1993). The absence of MOW would reduces the strength of the AMOC by as much as 15% compared to modern (Rogerson et al., 2012) whereas strong MOW outflow has the potential to invigorate deep-water formation and AMOC strength (Potter and Lozier, 2004; Rogerson et al., 2012, Voelker et al., 2006). However, the long-term dynamics of MOW dispersal

into the North Atlantic remain poorly understood, although abundant evidence exists for strong secular to millennial-scale oscillations (Hernandez-Molina et al., 2014a; Llave et al., 2006; Rogerson et al., 2006; Voelker et al., 2006). This study aims to put constraints on the glacial/interglacial MOW variability and to investigate whether and how variations in MOW output have impacted the North Atlantic hydrography over glacial/interglacial timescales.

Gulf of Cadiz Hydrography

The distinct salinity contrast between relatively fresh Atlantic surface water (~36.5 PSU) (Rogerson et al., 2012) and saline Mediterranean water (~38.5 PSU, Rogerson et al., 2012) drives the exchange of water masses through the Strait of Gibraltar (Rogerson et al., 2012). The key driver of MOW production is Levantine Intermediate Water (LIW), originating from the highly evaporative eastern Mediterranean Sea, which also preconditions the deep and intermediate water formation in the western Mediterranean Sea (Millot, 2014; Rogerson et al., 2012; Toucanne et al., 2012). Here, further contribution to the MOW derives from the Western Mediterranean Deep Water (WMDW), Tyrrhenian Dense Water, and Western Intermediate Water (WIW) (Millot, 2014). When the MOW enters the Gulf of Cadiz (GC), its settling depth is determined by its buoyancy, while the divergence into an upper and lower branch is largely controlled by the sea floor morphology (Fig. 3.1, Rogerson et al., 2012). Paleorecords indicate that the vertical position of the MOW within the GC varied considerably over time (Hernandez-Molina et al., 2014; Rogerson et al., 2012, 2006; Voelker et al., 2006), which has to be considered for interpretations of past MOW fluctuations.

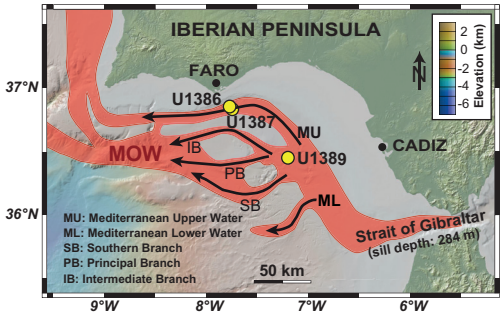

***Figure 3.1**: Main flow paths of the MOW within the GC (Hernández-Molina et al., 2014), including the position of the investigated IODP Expedition 339 Sites.*

Material & Methods

Our study is based on three sites drilled during IODP Expedition 339 within the present-day flow paths of the MOW at the northern margin of the GC (Fig. 3.1, Table DR1 in the GSA Data Repository)[1]. Sites U1386 and U1387 are recovered from Faro Drift situated within the upper MOW core. Site U1386 is positioned closer to the moat generated by the MOW than Site U1387 (Fig. DR1 in the GSA Data Repository[1]). Site U1386 therefore appears to be more sensitive to variations in

[1] GSA Data Repository item 2015xxx, detailed methods, stratigraphy, spectral analysis, DR Figures DR1-DR3 and Tables DR1-DR4, is available online at www.geosociety.org/pubs/ft2015.htm, or on request from editing@geosociety.org or Documents Secretary, GSA, P.O. Box 9140, Boulder, CO 80301, USA

bottom current velocity. Site U1389 is located relatively proximal to the Strait of Gibraltar and, hence, less affected by vertical shifts of the MOW path (Fig. 3.1). Site U1389 is therefore a faithful recorder of the general MOW flow speed whereas the other two sites provide information about potential vertical displacements of the upper MOW core.

Split-core scanning of Sites U1387 and U1389 was performed with the AVAATECH XRF Core Scanner II (Serial No. 2) and III (Serial No. 12), respectively, at the MARUM – University of Bremen (Bahr et al., 2014). Measurements were done in 3 cm intervals, integrated over a 1.2 cm^2 area with a 10 mm down-core slit size performing separate runs with a generator setting of 10, 30, and 50 kV, and currents of 0.2, 1.0, and 1.0 mA, respectively. Sampling time was set to 20 s. Core scanning of Site U1386 was performed using the AVAATECH XRF Core Scanner II (Serial No. 2) at the Royal Netherlands Institute for Sea Research (NIOZ) in 1 cm intervals (1.2 cm2 area, 10 mm down-core slit size), with separate runs of 10, 30, and 50 kV, using a current of 1.5 mA and sampling times of 10, 20 and 40 s, respectively. Relative standard deviations of selected element counts for Site U1386 are listed in GSA Data Repository Table DR2[1].

Chronostratigraphy

The chronostratigraphy of Site U1389 is well constrained by AMS ^{14}C-dating and by matching its planktonic $\delta^{18}O$ record to NGRIP (Seierstad et al., 2014) and the Iberian Margin core MD01 – 2444 (Hodell et al., 2013) (see also the GSA Data Repository[1]). Sites U1386 and U1387 were tied to U1389 and its tuning targets by using normalized XRF-Br records (Bahr et al., 2014). High sedimentation rates, in places in excess of 100 cm/ky allow us to achieve a centennial-scale resolution, hence providing unprecedented insights into the MOW variability (Fig. DR2B in the Data Repository[1]).

Monsoonal impact on MOW dynamics

The Zr/Al ratio represents the accumulation of heavy minerals (e.g., zircon) over alumnosilicates under increasing bottom current flow and has recently been demonstrated to accurately trace relative variations of MOW bottom current velocity within the GC (Bahr et al., 2014). The Zr/Al records, in particular that of Site U1389, reveal a clear inverse correlation with records of African monsoonal strength and summer insolation (Fig. 3.2), with a dominant precessional component in the Site U1389 spectrum (Fig. DR3 in the Data Repository[1]). The synchronicity of MOW fluctuations at all three sites within the GC is remarkable and corroborates the perception that the general MOW dynamics are a direct effect of a common forcing. Notably, even the relative amplitude of Zr/Al variations (i.e., MOW flow speed) reflect the amplitude modulation of low latitude summer insolation (Fig. 3.2F). We therefore propose that monsoon-driven alterations of the freshwater budget within the eastern Mediterranean Sea are the major driver of MOW variability on orbital time scales. A weak MOW flow within the GC is the direct consequence of enhanced run-off into the Mediterranean Sea during summer insolation maxima (Rohling et al., 2015; Rossignol-Strick, 1983) where it obstructs LIW formation (Rogerson et al., 2012; Rohling et al., 2015), and vice versa. This mechanism is coherent with sapropel formation in the Eastern Mediterranean Sea during these periods due to high fresh water input and water column stratification (Rohling et al., 2015; Rossignol-Strick, 1983) (Fig. 3.2). The link between sapropel deposition and a diminished MOW presence within the GC is consistent with studies of the early Holocene sapropel S1 (Rogerson et al., 2012), and can be now be extended back to Marine Isotope Stage (MIS) 5 (sapropels S3, S4 and S5; Fig. 3.2).

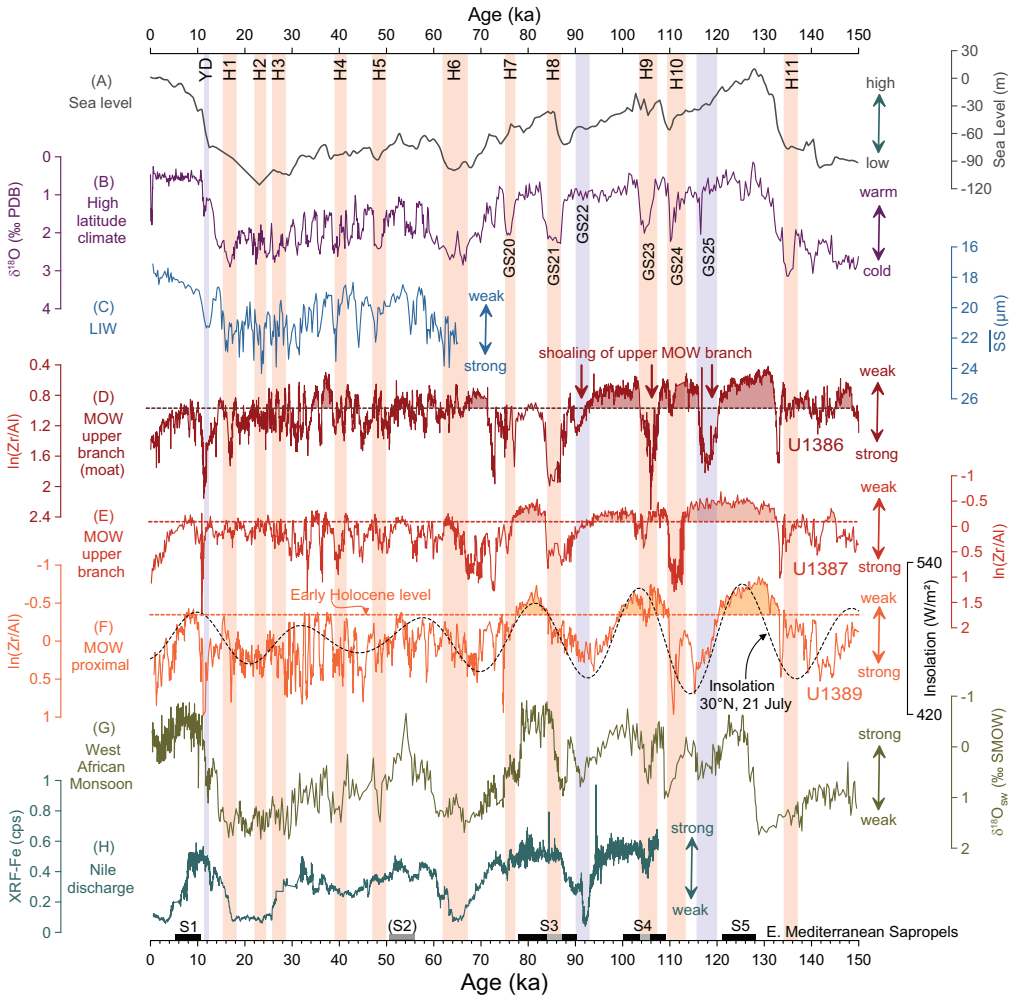

***Figure 3.2**: Mediterranean Outflow Water (MOW) variability in the paleoclimatic context. (**A**) Eustatic sea level (Grant et al., 2012); (**B**) planktic $\delta^{18}O$ from Iberian Margin core MD01 – 2444 (Hodell et al., 2013); (**C**) sortable silt of core MD01 – 2434, Corsica Trough, approximating LIW flow speed (Toucanne et al., 2012); (**D**) Zr/Al ratios reflecting MOW velocity at Sites U1386, (**E**) U1387, and (**F**) U1389 (3 pt. running average, note the inverted scales) with low latitude summer insolation (Laskar et al., 2004); (**G**) Niger Outflow, driven by the West African Monsoon (MD03 – 2707, Weldeab et al., 2007), and (**H**) Nile discharge (MS27-PT, Revel et al., 2010). Indicated are Heinrich Stadials ("H"), the Younger Dryas ("YD"), Greenland Stadials of MIS 5 ("GS"), and eastern Mediterranean Sapropels ("S") (Rohling et al., 2015). All records are plotted on their original stratigraphy.*

Insolation forced LIW formation exerts a predominant control on the orbital-scale MOW production and marginalizes other factors such as long-term eustatic sea level variations. This is unexpected at first sight, because the salinity budget and overturning in the Mediterranean Sea is influenced by the sill depth (284 m) of the Strait of Gibraltar (Alhammoud et al., 2010;

Rogerson et al., 2012). The blocking effect of a low sill depth promotes salinity accumulation in the Mediterranean basin, but at the same time constrains the outflow volume (Alhammoud et al., 2010; Rogerson et al., 2012). However, our data is agreement with numerical simulations that imply a constant bottom flow speed within the Strait of Gibraltar independent of the absolute glacial or interglacial sea level (Alhammoud et al., 2010). A different situation occurs, however, during periods of abrupt sea level change, which are accompanied by strong outflow (Rogerson et al., 2012), evidenced by the synchronous Zr/Al peaks during glacial terminations (Fig. 3.2). Here, freshening in the Atlantic surface waters due to melting ice sheets increased the density contrast between Atlantic and Mediterranean water masses and, thus, promoted a more vigorous MOW production (Rogerson et al., 2012).

Millennial-scale variability

Superimposed on the orbital variations are pulses of increased MOW speed during Greenland Stadials (Toucanne et al., 2007) coinciding with periods of enhanced LIW flow in the western Mediterranean Sea (Fig. 3.2C, Toucanne et al., 2012). Because the African monsoonal systems weakened during high latitude cold events (e.g., Tjallingii et al., 2008; Weldeab et al., 2007; Fig. 3.2G), Nile discharge was low during stadials (Fig. 3.2H, Revel et al., 2010) enhancing LIW formation in and, thus, MOW production. The pronounced millennial-scale variability in the MOW records, particularly during Marine Isotope Stage 3, might have been further amplified by pronounced winter cooling over the Eastern Mediterranean due to a strong Siberian High (Kotthoff et al., 2008) as well as by enhanced contribution of WMDW promoted by intense winter cooling over the Gulf of Lion (Voelker et al., 2006).

Impact of MOW variability on AMOC intensity

Enhanced MOW production likely contributed to the re-invigoration of the sluggish Atlantic thermohaline circulation at the end of Heinrich Events (Rogerson et al., 2012, 2006; Voelker et al., 2006). Our data further suggests that increased outflow of MOW impacted the AMOC mode

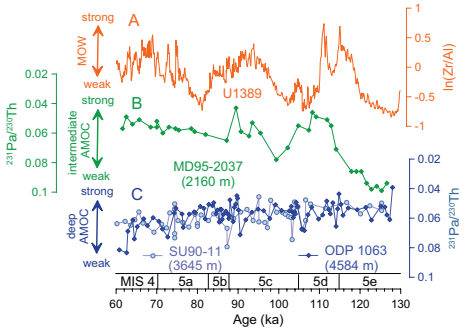

Figure 3.3: *Mediterranean Outflow Water (MOW) dynamics in relation to AMOC intensity during MIS 5. (A) peaks in the Zr/Al ratios (3 pt-average) of Site U1389, reflecting high MOW flow speed, coincided with an enhanced overturning strength in (B) the intermediate Atlantic (core MD95–2037, Guihou et al., 2011), opposed to (C) slightly declining deep circulation (ODP Site 1063, Böhm et al., 2015, and core SU90–11, Guihou et al., 2011) inferred from 231Pa/230Th ratios. Marine Isotope Stages (MIS) are given for reference. All records are plotted on their original stratigraphy.*

and intensity during MIS 5. Both, the long-term increase as well as the MOW velocity peak during the insolation minima of MIS 5, coincided with an intensification of the intermediate Atlantic overturning circulation (Guihou et al., 2011, Fig. 3.3). Notably, deep circulation is slightly declining, hence, a robust AMOC after the climate optimum of MIS 5e is mainly supported by a strong intermediate circulation (Guihou et al., 2011). A vigorous MOW production could have salinified the Atlantic at intermediate depth and thereby stimulated the shallow branch of the AMOC. A strong overturning circulation would not only prolong the prevalence of warm conditions at high latitudes (Potter and Lozier, 2004) but also contribute to initial ice shield growth after MIS 5e (e.g. Grant et al., 2012) by sustaining moisture transport into high latitudes. If confirmed, these findings would imply that increased outflow of MOW into the North Atlantic helps to stabilize high and mid-latitude climate, while at the same time promoting the demise into an ice age.

Summary

Our records of MOW variability over the past 150 kyrs manifest a prime example for low to high latitude teleconnections within the ocean-atmosphere climate system. We document that enhanced MOW production s was promoted by a weak East African Monsoon due to the reduction of freshwater input into the Eastern Mediterranean, and vice versa. Consequently, high amounts of saline MOW discharged into the intermediate depth North Atlantic might have promoted deep water formation and stabilized the meridional overturning circulation.

Acknowledgments

We are greatly indebted to the IODP Expedition 339 Science Party for support onboard the DV Joides Resolution. We kindly acknowledge W. Hale and A. Wülbers (BCR) for core handling and V. Lukies and T. Westerhold, MARUM Bremen, for technical assistance. This manuscript greatly benefitted from the comments of three reviewers. Funding was received through the CTM 2008-06399-C04/MAR (CONTOURIBER), CTM 2012-39599-C03 (MOWER) projects, the Continental Margins Research Group (CMRG) at Royal Holloway University of London (UK), CGL2011-15013-E (MEDITERRANEAN OUTFLOW IODP-EXPEDITION 339) projects to F.J. H.-M., the German Research Foundation (DFG) (BA 3809/4 to A.B. and RO 1113/6 to U.R.) and the Fundação de a Tecnologia e a Cência (FCT) (project MOWCADYN, PTDC/MAR-PRO/3761/2012 to A.V.).

Chapter 4

Paleoceanographic history of the Gulf of Cadiz during the past ~570 kyr: Inferences from IODP 339 Site U1386

Stefanie Kaboth, Bas de Boer, André Bahr, Christian Zeeden and Lucas J. Lourens

The Gulf of Cadiz constitutes a prime area to study Mediterranean Outflow Water (MOW) variability which is considered an important modulator of the North Atlantic heat and salt budget. However, its paleoceanographic evolution is poorly constrained due to the lack of high-resolution proxy records that pre-date the last glaciation. Here we present the first continuous and high-resolution (~ 1 kyr) benthic δ18O and δ13C as well as grain-size records from IODP Site U1386 representing the last ~570 kyr. We find three distinct phases of MOW variability throughout the Late Pleistocene at Site U1386 associated with distinct shifts in its composition and flow strength. During Phase I, comprising the last ~130 kyr, MOW influence is strengthened during interglacial periods (MIS 5 and 1) coinciding with sea-level highstands whereas strongly reduced or absent during glacial periods (MIS 4 and 2). During Phase II between ~475 to ~130 kyr (MIS12 to 6) MOW flow strength seems to be generally reduced independent from the prevalent climatic background conditions contrasting the MOW behaviour observed in Phase I. During Phase III, between ~475 and ~570 ka, MOW influence seems increased again, but in contrast to phase I, both during interglacial (i.e. MIS 13 and 15) and glacial (i.e. MIS 14) periods. Although the MOW flow strength is reduced during Phase II, a small δ18O isotopic gradient between Site U1386 and the Mediterranean Sea signal at Site ODP 967/968 yields strong indication that MOW influence prevailed during this time interval. The Late Pleistocene pattern of MOW variability is mimicked by changes in the δ13C record at Site U1386 possibly indicating a distinct shift in water mass sourcing of the MOW during Phase II towards predominately Mediterranean intermediate water whereas for the younger and older interval stronger contributions of the denser Western Mediterranean Deep-Water might have played a more prominent role. Superimposed on the long-term change in water mass sourcing is the occurrence of distinct and precession paced δ18O enrichment events, which contrast the pattern of global ice volume change as inferred from the global mean δ18O signal (i.e. LR04), but mimics that of the adjacent Mediterranean Sea. We attribute these enrichment events to a profound temperature reduction and salinity increases of the MOW, aligning with similar changes in the Mediterranean source region, possibly increased ice volume as inferred from significant sea level drops recorded in the Red Sea or increased influence of North Atlantic intermediate water masses when MOW influence was absent at Site U1386.

4.1 Introduction

The most striking hydrographic feature of the Gulf of Cadiz (Fig. 4.1) is the Mediterranean Outflow Water (MOW) shaping the sedimentary depositional system along its upper (our study area;

~500 water depth) and middle slope (~1000 m water depth) (Baringer and Price, 1997; Borenäs et al., 2002; Hernández-Molina et al., 2013). The MOW constitutes of warm and relatively saline water masses exiting the Mediterranean Sea through the Strait of Gibraltar (Ambar and Howe, 1979; Bryden and Stommel, 1984; Bryden et al., 1994). The present-day Atlantic-Mediterranean exchange through the Gibraltar Gateway is driven by the evaporation loss of the Mediterranean Sea itself (Bryden et al., 1994; Sankey, 1973). These water masses are sourced predominately of intermediate water masses from the Levantine basin in the Eastern Mediterranean Sea and changeable parts of western Mediterranean deep-water originating in the Alboran and Tyrrhenian Sea (Millot, 2014, 2009; Millot et al., 2006). As such, the Gulf of Cadiz is hydrographically directly linked to changes in the Mediterranean Sea source region through the MOW (Bahr et al., 2015; Kaboth et al., 2015; Voelker et al., 2006). The saline water masses of the MOW are thought to be an important modulator of the North Atlantic salt budget at intermediate water levels and proposed to precondition Atlantic Meridional Overturning Circulation (AMOC; Voelker et al., 2006). Above the MOW, the intermediate water column is influenced by subtropical water masses originating from the northern boundary of the eastern Azores Current branch that extends into the Gulf of Cadiz (Peliz et al., 2009, 2005). During spring and summer, colder and fresher subsurface water masses can be traced along the upper slope region in the Gulf of Cádiz related to the upwelling systems along the Iberian Margin (Fiúza et al., 1998). With the relaxation of the upwelling (in the late fall to winter) the Iberian Poleward Current/Navidad Current establishes along northern Spain transporting the subtropical water masses at surface and subsurface levels also along the Iberian

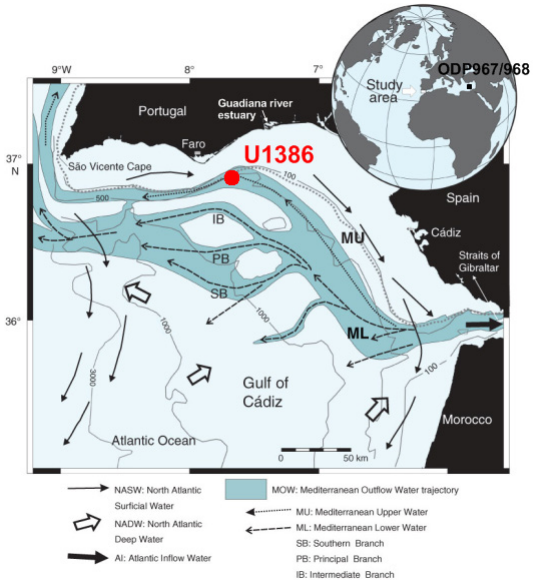

Figure 4.1: *Study area; Location map of the Gulf of Cadiz showing the recent flow pattern of MOW modified after (Hernández-Molina et al., 2013; Stow et al., 2013). Site location of U1386 (Upper MOW core, this study) is marked.*

Margin (Peliz et al., 2005; Stevenson, 1977).

Deciphering the interplay of the various water masses within the Gulf of Cádiz and their associated driving mechanisms over long geological time scales has so far presented a challenge to

the scientific community due to the lack of long sedimentary records from the area pre-dating the last climatic cycle (Hernández-Molina et al., 2006; Llave et al., 2006; Rogerson et al., 2005; Voelker et al., 2006). Plio-/Pleistocene contourite drift sequences from the Gulf of Cádiz have been recently recovered during the IODP Expedition 339 (Hernández-Molina et al., 2013; Stow et al., 2013) allowing for a better understanding of the Gulf of Cadiz current system and climatic evolution.
Taking advantage of the unique hydrographic setting of the Gulf of Cadiz and its inferred sensitivity to Mediterranean and North Atlantic climate variability we aim to investigate the orbital and sub-Milankovitch-scale variability of its intermediate water masses over the last five glacial-interglacial cycles (~570 kyr). For this, we have established the first benthic foraminifera $\delta^{18}O$ and $\delta^{13}C$ record of shallow marine (~560 m water depth) IODP Site U1386 located on the upper slope in the Gulf of Cadiz (see Fig. 4.1). We compare our results to the benthic oxygen isotope record of the ambient Mediterranean Sea, derived from the eastern basin (Konijnendijk et al., 2015). This study is a contribution to deepen our understanding of the glacial-interglacial induced changes of the intermediate water mass structure in the Gulf of Cadiz, the climatic response of MOW throughout Late Pleistocene, and the significance of the observed variability to climatic oscillations beyond the scope of the Gulf of Cadiz.

4.2 Materials &Methods

4.2.1 Site location

Integrated Ocean Drilling Program (IODP) Site U1386 was drilled during Expedition 339 in November 2011 to January 2012 and is located southeast of the Portuguese Margin mounded on the Faro Drift along the Alvarez Cabral Moat at 36°49.68'N; 7°45.32'W in 561 m water depth (see Fig. 4.1). The Faro drift is part of the Contourite Depositional System (CDS) of the Gulf of Cadiz (Stow et al., 2013). At recent, Site U1386 is directly influenced by the upper MOW flow core (Baringer and Price, 1997; Borenäs et al., 2002; Hernández-Molina et al., 2013). The composite depth scale (meters composite depth, MCD) was developed from parallel holes at Site U1386 (Hernández-Molina et al., 2013).

4.2.2 Stable isotope measurements and interspecies correlation

For this study, 658 sediment samples were analysed for $\delta^{18}O$ at 30 cm intervals between 0 to 187.51 mcd (~570 kyr) resulting in an approximately 1 kyr resolution. The freeze-dried sediment samples were wet sieved into three fractions: (>150 μm, >63 μm and >38 μm); residues were oven dried at 40°C. Stable oxygen isotope analyses were carried out on 4 to 6 specimens of the preferably epifaunal living foraminifera species *Planulina ariminensis* from the >150 μm size fraction. In the absence of *P. ariminensis* we selected specimen of the likewise preferably epifaunal living foraminifera *Cibicides ungerianus* (Schönfeld, 2002a). All selected specimens were crushed, sonicated in ethanol and dried at 35˚C. Stable isotope analyses were carried out on a CARBO-KIEL automated carbonate preparation device linked to a Thermo-Finnigan MAT 253 mass spectrometer at Utrecht University. The precision of the measurements is ±0.08‰ and ±0.03 for $\delta^{18}O$ and $\delta^{13}C$, respectively. The results were calibrated using the international standard NBS-19, and the in-house standard NAXOS. Isotopic values are reported in standard delta notation (δ) relative to the Vienna Pee Dee Belemnite (VPDB).

P. ariminensis was absent in 40 samples; resulting gaps were filled with *C. ungerianus*. The $\delta^{18}O$ values were corrected for interspecies induced isotopic offsets. The calculation of the interspecies isotopic offsets is based on 20 paired oxygen and carbon isotope measurements of both benthic species. The interspecies offsets were determined by applying a least square linear regression equation. The Pearson correlation coefficient (R^2) between both species shows high correlation of 0.97 and 0.89 for $\delta^{18}O$ and $\delta^{13}C$, respectively. For $\delta^{18}O$ the calculated slope of linear relationship is ~1 with an intercept of -0.17 ‰ between *P. ariminensis* and *C. ungerianus* at Site U1386 which is slightly lower than the -0.3 ‰ isotopical shift in $\delta^{18}O$ reported by Zahn et al. (1987) between *P. ariminensis* and deeper-dwelling *C. wuellerstorfi* from the Gulf of Cadiz. For $\delta^{13}C$ the calculated

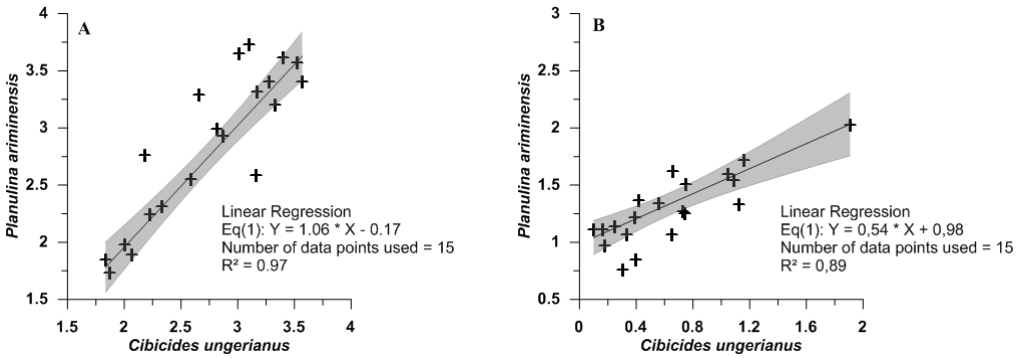

Figure 4.2: *The $\delta^{18}O$ (A) and $\delta^{13}C$ (B) interspecies correlation between benthic foraminifera Cibicides ungerianus and Planulina ariminensis at Site U1386 for the Late Pleistocene. The correction is based on parallel measurements throughout the investigated interval. Linear square regression (black line) equation and Pearson correlation coefficient (R^2) are shown.*

slope of linear relationship is ~0.5 with an intercept of ~1 ‰ between *P. ariminensis* and *C. ungerianus* at Site U1386 which is higher than the isotopical shift in $\delta^{13}C$ reported by Zahn et al. (1987) between *P. ariminensis* and deeper-dwelling *C. wuellerstorfi* from the Gulf of Cadiz.

4.2.3 Grain-size

The oxygen isotope sample preparation was used to obtain Weight percentages (%-wt) of the grain-size fractions >150 µm, 150-63µm, 63-38 µm and <38 µm for the investigated samples were obtained during sample preparation for isotope analyses. We concentrate on the grain-size fraction between 63-150 µm which has been used previously as indicator for flow strength changes in the Gulf of Cadiz attributed to MOW variability (Rogerson et al., 2005). We disregard the size-fraction >150 µm to reduce the bias caused by IRD contributions. Even though untreated weight percentages hold a bias it has been shown for the last climatic cycle that weight percentages mirror major peaks in Zr/Al records, considered a reliable recorder of MOW flow strength variability (Bahr et al. 2014), and thus can be used to trace patterns of MOW variability (Kaboth et al., 2015).

4.2.4 Mg/Ca paleothermometry

5-7 specimen of *U. peregrina* from the >150 µm fraction (~250 µg) were gently crushed between two glass plates to open the chambers and then cleaned following the procedure of Barker et al.

(2003). The major steps of this method are (1) several water and ethanol washings to remove clay, (2) hydrogen peroxide treatment in a boiling water bath to eliminate organic matter and (3) a short (30 s) dilute acid leaching with 0.001 M nitric acid to eliminate any adsorbed contaminants from test fragments. Prior to measurement, samples are dissolved in 350 ml of 0.075 M nitric acid, centrifuged to separate insoluble residues and analysed with a Varian Vista PRO simultaneous inductively coupled plasma atomic emission spectrometer (ICP-AES) at the Godwin Laboratory at Cambridge University. The Mg/Ca ratios were transferred into temperature estimates following Cacho et al. (2006). This calibration is based on western Mediterranean Sea deep-water top core samples and temperature adjusted to fit recent bottom water conditions in the region. We have applied this equation as other available transfer equations (e.g. Bryan and Marchitto, 2008; Elderfield et al., 2012) produced unrealistic cold temperatures at Site U1386 during glacial periods of 1 to 3°C. Additionally, we monitored in particular Mn and Fe element concentrations for the identification of potential contamination from clays or Mn-rich coatings. Long-term instrumental precision of the Mg/Ca ratio data, determined by replicate analyses of a standard solution, was ±0.33%. Uncertainty of the temperature estimates are based on parallel measurements and range between 1 to 1.5°C.

4.2.5 Chronology

The chronology is based on the visual correlation of the benthic $\delta^{18}O$ record at Site U1386 to the global mean benthic isotope stack LR04 (Lisiecki and Raymo, 2005; see Fig. 4.3A). To facilitate best correlation we monitored the average sedimentation rate ~0.3 m/kyr (Hernández-Molina et al., 2013; Stow et al., 2013) of Site U1386 throughout the correlation process. The transitions T_I-T_V were used as initial tie points for the correlation. In addition, we utilized the maxima of the glacials and interglacials, respectively. The chronology of the MIS follows Lisiecki and Raymo (2005). The applied correlation tie points are shown in Table 4.1.

Table 4.1: *Age calibration points for the visual tuning of benthic $\delta^{18}O$ record of Site U1386 to the global mean benthic $\delta^{18}O$ stack of LR04 (Lisiecki and Raymo, 2005).*

MCD	Age (ka)
0.0	0
2.0	9
4.0	18
9.1	29
27.8	60
30.2	87
35.5	112
44.0	123
45.0	135
69.5	185
79.0	210
81.3	223
85.5	230
86.3	237
89.6	252
105.0	286
114.5	324
117.4	341
136.0	401
138.5	405
144.0	431
172.0	508
187.2	570

4.2.6 Spectral analysis

For the spectral analysis we applied the Multi Taper Method as implemented in the 'astrochron' R package (Meyers, 2014; Rahim et al., 2014; Thomson, 1982). The data was evenly spaced at 1 kyr resolution and linear detrended prior to analysis.

4.2.7 Stable oxygen isotope comparison between Sites U1386 and ODP967/968

To evaluate changes in Mediterranean Outflow influence at Site U1386 during the last ~570 kyr, we compared the $\delta^{18}O$ record from Site U1386 in the Gulf of Cadiz to the $\delta^{18}O$ stack of ODP Sites 967 and 968 in the eastern Mediterranean Sea (Konijnendijk et al., 2015). Due to the lack of sufficient long stable oxygen isotope records at

intermediate water depth from the Mediterranean Sea during the Late Pleistocene we are limited to the Eastern Mediterranean Sea deep-water record for comparison. Adjacent sites ODP 967 and 968 are located south of Cyprus near the Eratosthenes seamount at a water depth of 2554 m, and bath in Eastern Mediterranean Deep-Water (EMDW). Although, EMDW is not directly contributing to MOW it is interconnected due to convection and admixing to the overlying intermediate water masses e.g. Levantine Intermediate Water (LIW) which is the predominant contributor to MOW (Millot, 2009; Millot et al., 2006; Rogerson et al., 2012).

For our comparison, we first corrected the two $\delta^{18}O$ records for interspecies offsets to equilibrium with the ambient water. The $\delta^{18}O$ stack at ODP Sites 967/968 is placed on a baseline of *Gyroidina altiformis* and *Gyroidina neosoldanii* (Konijnendijk et al., 2015). *Gyroidina* spp. is considered to calcify its $\delta^{18}O$ composition in equilibrium with the ambient water mass, therefore setting the baseline for our comparison (Shackleton and Cita, 1979). Our oxygen isotope record of Site U1386 is placed on a *P. ariminensis* baseline with *C. ungerianus* values spliced in (see Chapter 2.2). For the interspecies correction we followed the approach described in Kaboth et al. (2015). As there are no direct correction values available for *P. ariminensis* we followed Zahn et al., 1987 who showed a small offset of -0.3‰ for $\delta^{18}O$ between *P. ariminensis* and wider researched *Cibicides wuellerstorfi*. To align Site U1386 to ODP 967/968 we adjusted the $\delta^{18}O$ values first to *C. wuellerstorfi* by -0.3 ‰ following Zahn et al. (1987), and secondly to equilibrium by adding 0.64 ‰ following (Shackleton and Hall, 1984).

4.3 Results

4.3.1 Chronology and sedimentation rate

The U1386 $\delta^{18}O$ record exhibits the major glacial-interglacial variability present in LR04 (Lisiecki and Raymo, 2005) over the past ~570 kyr (Fig. 4.3B). The estimated mean sedimentation rate for Site U1386 (see Fig. 4.3C) is ~0.4 m/kyr which differs from the relatively uniform sedimentation rate of ~0.25 m/kyr that has been calculated from shipboard stratigraphy for the past 1.8 Myr (Hernández-Molina et al., 2013; Stow et al., 2013). The resulting sedimentation rates vary between ~0.1 and ~0.8 m/kyr over the last ~570 kyr. With a sample spacing of approximately 0.3 m the resulting resolution of the composite benthic isotope record from Site U1386 is ~1 kyr. A doubling of the sedimentation rate coincides with the transition of MIS 12 to MIS 11 (~400 ka), MIS 8 to MIS 7 (~220 ka) and MIS 6 to MIS 5 (~125 ka). Three intervals exhibit relatively low sedimentation rates of <0.1 m/kyr: ~65 to 85 ka, ~132 ka and ~230 ka.

4.3.2 Stable oxygen and carbon isotopes

Figure 4.3B shows the comparison between the normalized $\delta^{18}O$ record of Site U1386 with the global mean $\delta^{18}O$ stack LR04 (Lisiecki and Raymo, 2005). Evidently, IODP Site U1386 has been strongly influenced by global ice volume changes. This is made apparent by the good signal correlation of these records for the last ~570 kyr, and highlights the ice volume induced glacial-interglacial variability at Site U1386 (Fig. 4.3B).

On glacial-interglacial timescales Site U1386 shows lightest values (~1.20-1.68 ‰) during interglacials MIS 5 and 13 and glacial enrichment in $\delta^{18}O$ (~2.95-3.72 ‰) during MIS 14 and MIS 12. Terminations T_{IV} to T_I show depletions ranging between ~1.80 ‰ and ~2.19 ‰ (see Fig. 4.2B).

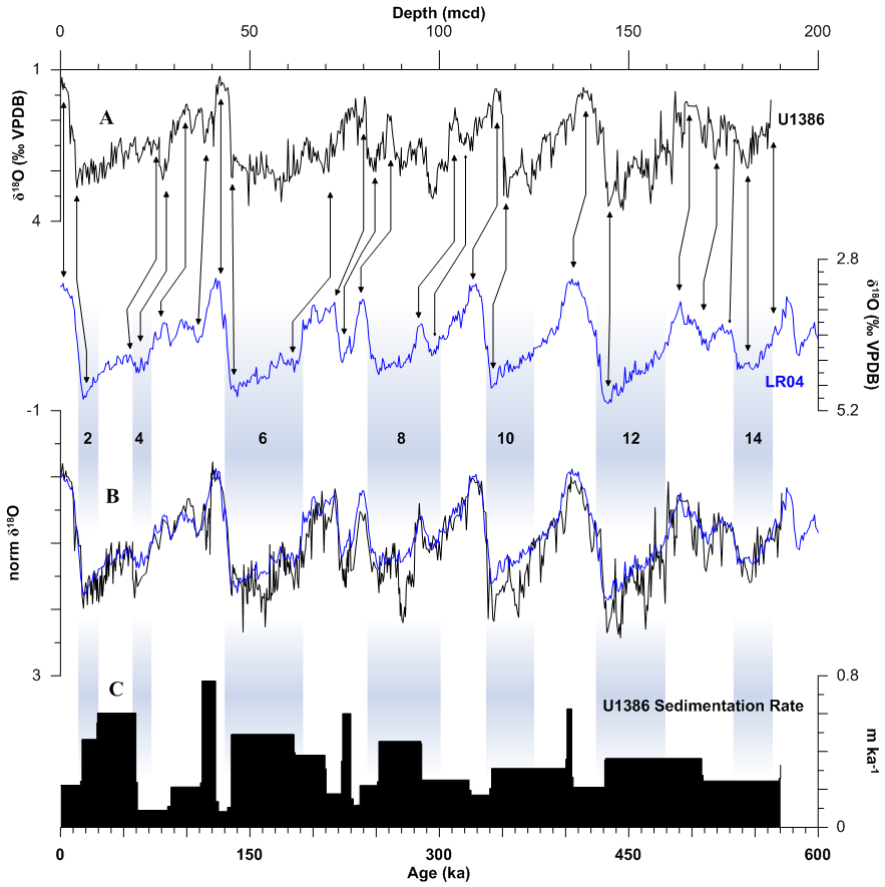

Figure 4.3: *Chronology of Site U1386; Blue columns represent MIS stages following (Lisiecki and Raymo, 2005). (**A**) Correlation of $\delta^{18}O$ record on shipboard MCD scale correlated to the benthic $\delta^{18}O$ LR04 stack (Lisiecki and Raymo, 2005). Lines with arrows indicate selected tie points used for the age model (a full list of tie points is available in Table 4.1). (**B**) Comparison of the normalized benthic $\delta^{18}O$ record of Site U1386 on the time scale according to our tuning, and normalized $\delta^{18}O$ LR04 stack on its age model (Lisiecki and Raymo, 2005). (**C**) Sedimentation rate for Site U1386.*

While the $\delta^{18}O$ signal of Site U1386 and LR04 are coherently in-phase, $\delta^{18}O$ amplitude variations between these two signals are visible especially during glacial periods (Fig. 4.2B). These periods at Site U1386 are marked by a series of millennial-scale oscillations of triangular shape preceding the glacial maxima (see MIS 12, 10, 8, 6 and partially 4). These perturbations are of the order of up to ~1 ‰ (e.g. MIS 8) compared to the global mean $\delta^{18}O$. Similar $\delta^{18}O$ enrichment cannot be observed during MIS 2.

The $\delta^{13}C$ record at Site U1386 is shown in Figure 4.4A. Lightest values of -0.42 ‰ coincide with the transition MIS10/9, and the heaviest values (~2.03 ‰) coincide with MIS 13. The $\delta^{13}C$ record shows a strong long-term trend starting from around ~475 kyr when a shift towards lighter $\delta^{13}C$ occurs compared to the older interval of the record (on average ~0.8 ‰). The trend is reversed around ~130 kyr when $\delta^{13}C$ values increase on average ~0.3 ‰.

4.3.3 Grain-size

The mean grain-size values (63-150 µm fraction) throughout the last ~570 kyr is ~2.5 %-wt. Highest values of up to ~33 %-wt. are correlated with MIS 5 (Fig. 4.4A). The grain-size record shows glacial-interglacial variability with decreased values during glacial periods, and generally high amplitude variations during interglacial periods. Interglacial grain-size variability is however not uniform throughout the interglacial periods with highest values during MIS 5 and MIS 1 (~15 %-wt.) and lowest (~5 %-wt) variations during MIS 11.

4.3.4 Mg/Ca paleothermometry

The benthic Mg/Ca values range from on average 1.52 to 2.01 mmol/mol on glacial interglacial timescales. The resulting temperatures following Cacho et al. (2006) range from ~11°C during MIS 1 (interglacial conditions) to on average 8°C during the glacial periods of the last ~570 kyr (see Fig. 4.4C).

4.4 Discussion

4.4.1 MOW influence at Site U1386 during the Late Pleistocene

The stable isotope and grain-size records at Site U1386 show three distinct phases of MOW variability over the past 570 kyr. The last ~130 kyr (Phase I, see Fig. 4.4A) have been already presented and discussed in Kaboth et al. (2015). For this interval, strong MOW activity at Site U1386 was suggested during sea level high-stands (MIS 5 and MIS 1) as indicated by high-amplitude grain-size variability (Fig. 4.4A). The largest grain-size amplitude changes, indicating a strengthening of MOW flow at Site U1386, were shown to correlate to North Atlantic cold spells during the interglacial periods MIS 5 and MIS 1 (Kaboth et al. 2015). However, the authors also suggested the reduction or lack of MOW influence at Site U1386 during the full glacials MIS 4 and MIS 2 correlating with sea-level low stands. These findings support previous suggestions of glacial MOW flowing deeper along the middle slope of the Gulf of Cadiz during the LGM (Hernandez-Molina et al., 2014; Llave et al., 2007; Rogerson et al., 2005; Schönfeld and Zahn, 2000; Voelker et al., 2006, 2009).

Accordingly, the strongly decreased grain-size variability and substantial shift in $\delta^{13}C$ towards lighter values in Phase II between ~475 kyr (MIS13/12) and ~130 kyr (MIS6/5) would suggest that MOW influence at Site U1386 was genuinely reduced or absent prior to the upper Pleistocene during both glacial and interglacial periods (Fig. 4.4A). The substantial shift in the carbon isotopic composition of the waters at Site U1386 during this interval could hence point to a long-term change in water mass sourcing from dominant Mediterranean mode, i.e. heavy $\delta^{13}C$ values, to most likely an ambient North Atlantic intermediate water masses signal characterized by relative lighter $\delta^{13}C$ values (Voelker et al., 2006). The comparison between the $\delta^{18}O$ records of Site U1386 and that of ODP Sites 967/968 in the Eastern Mediterranean Sea (Konijnendijk et al., 2015) my point however to a different scenario (Fig. 4.4B). This comparison yield an isotopic gradient of the past ~130 ka, similar as found between Site U1386 and Site MD01-2472 in the Western Mediterranean Sea (Kaboth et al., 2015; Toucanne et al., 2012), and a strongly reduced gradient, both during glacial and interglacial periods prior to 130 ka. The absence of a clear gradient indicates that the isotopic composition of the water and temperature conditions were almost similar at Site U1386 and Sites

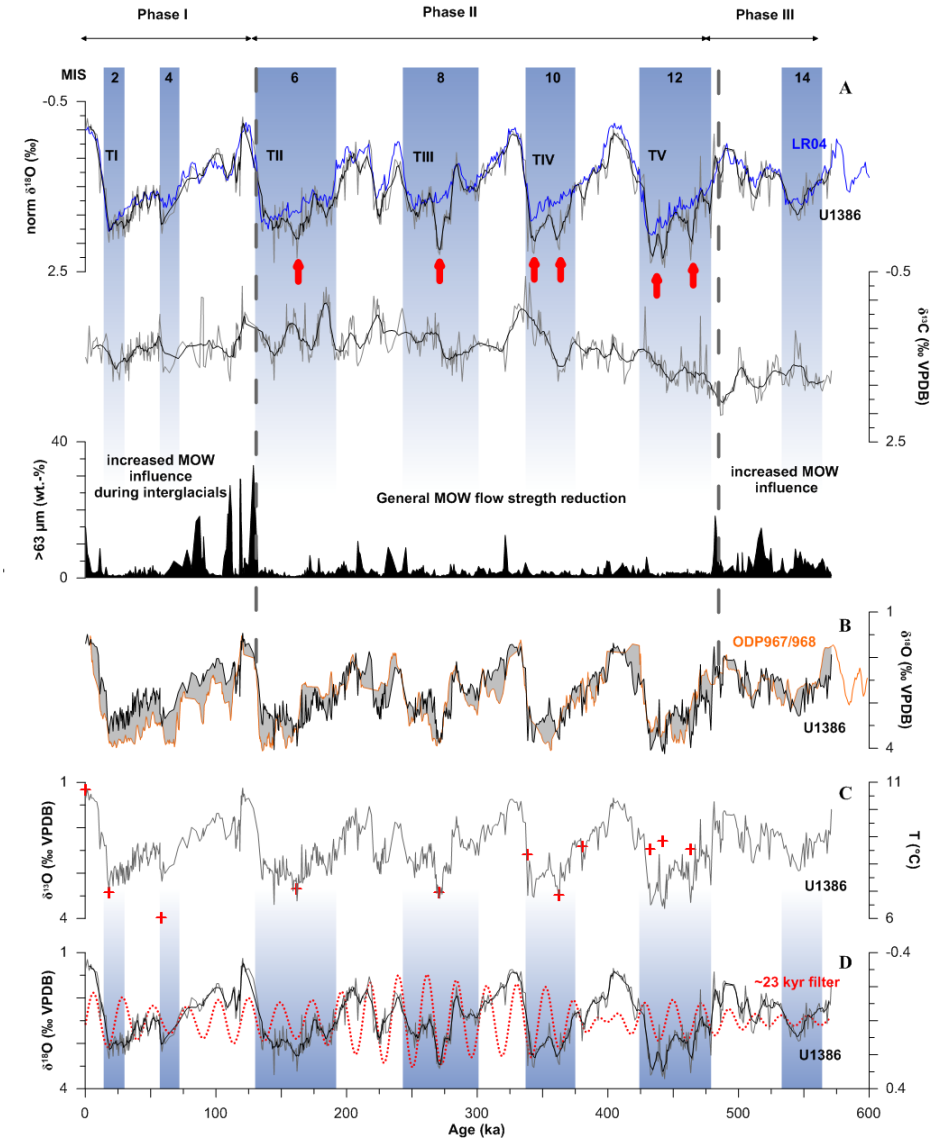

Figure 4.4: *Discussion. (**A**) Comparison of the normalized benthic $\delta^{18}O$ signal of Site U1386 (black) and the global mean LR04 stack (blue) (Lisiecki and Raymo, 2005), with the $\delta^{13}C$ record and the grain-size (63-150 µm fraction) at Site U1386. The glacial $\delta^{18}O$ enrichment events are marked by small red arrows. MIS stages (blue columns) follow (Lisiecki and Raymo, 2005) (**B**) Comparison of the interspecies corrected $\delta^{18}O$ signals between Site U1386 (black line) and ODP sites 967 and 968 (orange line; Konijnendijk et al. 2015). Isotopic gradient marked as grey shaded area. (**C**) U. peregrina Mg/Ca based mean temperature estimates (red crosses) for the glacial $\delta^{18}O$ enrichment events relative to the recent at Site U1386. For visual reference the benthic $\delta^{18}O$ record (grey line) at Site U1386 is also given. (**D**) The ~23 kyr filter (red dotted line) of the benthic $\delta^{18}O$ signal overimposed on the stable oxygen isotope signal at Site U1386.*

967/968, suggesting a permanent MOW influence at Site U1386 between 130 and 570 ka.. Evidently, this MOW influence must have largely ceased during the glacial periods of the last climatic cycle to explain the occurrence of the isotopic gradient between U1386 and the Mediterranean sites. The substantial change in $\delta^{13}C$ between Phase II and I may hence point towards a shift in the major source regions (i.e. western vs. eastern Mediterranean Sea basins) of MOW rather than a switch in water mass sourcing from the Mediterranean to North Atlantic intermediate water masses. This implies that MOW is predominantly composed of an Mediterranean intermediate water mass characterized by a reduced density and lighter $\delta^{13}C$ signature during Phase II, while significant portions of denser WMDW characterized by heavier $\delta^{13}C$ might have played a greater role during Phase I as suggested for the LGM (Voelker et al., 2006). A denser MOW then fed more dominantly into the lower MOW core at greater depth along the middle slope during the last climatic cycle and reduced the upper MOW core at Site U1386 during glacial periods aligning with the increased isotopic gradient between Site U1386 and ODP 967/968 (Fig. 4.4B).

As grain-size variability is a proxy for MOW flow strength and in extension its density rather than its presence the lack of profound grain-size variability during Phase II might be explained by a change in the interactions with a less dense MOW due to a predominant sourcing from intermediate water masses aligning with the reduced isotopic gradient between U1386 and the Mediterranean Sea. Additionally, a renewed tectonic activity from ~600 kyr to ~300 kyr (Hernández-Molina et al., 2015) could have caused a modification of the MOW pathway along the upper slope and a reduction in MOW flow strength resulting in a general fining of the sediment. Site U1386 is also closely located to the moat generated by the MOW (Hernández-Molina et al., 2013; Stow et al., 2013) making it most sensitive to variations in bottom current velocity as it probably represents the upper boundary layer of the MOW (Bahr et al., 2015). Nevertheless, the presence of at least short-term, interglacial MOW variability can be traced in the grain-size changes at Site U1386 during MIS 11, 9 and 7 (Fig. 4.4A).

For the oldest interval (Phase III) of our records between ~570 ka and ~475 ka, relatively heavy $\delta^{13}C$ values, and high grain-size amplitude changes, i.e. similar to the last climatic cycle, point again to a stronger MOW flow strength at Site U1386 at the end of the Mid-Pleistocene transition (Fig. 4.4A). The heavier $\delta^{13}C$ values could be an indication of more pronounced WMDW contributions to MOW, though a clear oxygen isotopic gradient between Site U1386 and ODP967/968, as found for Phase I, did not occur during the glacial period of MIS 14 (Fig. 4.4B), indicating that MOW influence remain present at Site U1386 during Phase III. This interpretation is supported by the large variability found in the grain-size record. Most likely, the less severe climate conditions and associated higher sea level stands during MIS 14 compared to MIS 2 and 4 did not lead to a significant reduction in MOW flow speed along Site U1386.

4.4.2 Glacial $\delta^{18}O$ enrichment events at Site U1386 and their relation to precession

The $\delta^{18}O$ record of Site U1386 reveals, prominent enrichments (up to ~1‰ e.g. MIS 8, Fig. 4.4A) during the full glacial periods between MIS 12 and MIS 6, and the transitional climate conditions (MIS13/12 and MIS11/10), i.e. the time period encompassing the shift in water mass composition at Site U1386 between ~470 and 130 ka, that are clearly absent in the LR04 global stack (Fig. 4.4A). The power spectrum (Fig. 4.5) and filtered ~23 kyr signal both give strong indication that these observed strong glacial $\delta^{18}O$ enrichment events are seemingly related to precession variability (Fig. 4.4D).

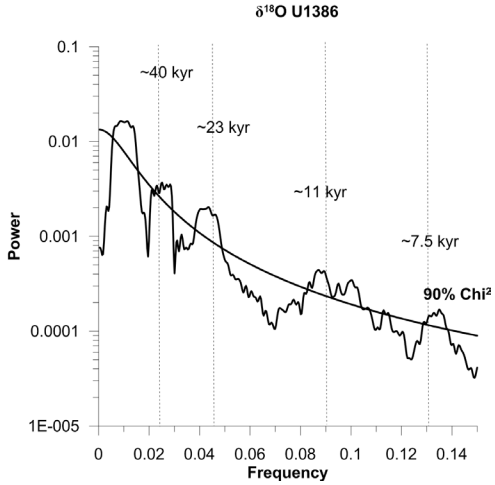

Figure 4.5: *Power spectrum of $\delta^{18}O$ record of Site U1386 with 90% confidence interval. The main frequency of obliquity (~40 kyr), precession (~23 kyr), semi-precession (~11 kyr) and a third precession (~7.5 kyr) are marked.*

The comparison between Site U1386 and the Mediterranean Sea (Fig. 4.4B) might provide the most straightforward explanation for these precession-related enrichment events as glacial enrichment events similar in amplitude can also be found in the eastern Mediterranean Sea (Konijnendijk et al., 2015). It was suggested that these perturbations (e.g. within MIS 8) reflect a sea-level drawdown and associated temperature drop in extension to major ice volume advances as similar excursions were also identified in the Red Sea sea-level reconstructions (Grant et al., 2014; Rohling et al., 2009; Siddall, 2004). If the $\delta^{18}O$ enrichment events at Site U1386 coincide with MOW influence it seems feasible that the Mediterranean sea-level signal was eventually transported to Site U1386. This suggests that the $\delta^{18}O$ enrichment events might, in fact, represent an imprint of ice volume-related changes that are not depicted in the global mean stack. A fraction of the glacial $\delta^{18}O$ enrichment events at Site U1386 might also derive directly from MOW influence which could also explain their seemingly precession paced behavior as a distinct precession-related signal was found in the high-resolution XRF records of various drill sites within the Gulf of Cádiz over the past 150 ka (Bahr et al., 2015). These authors interpreted this variability to changes in bottom-current velocity of MOW linked to a low-latitude forcing mechanism, such as the African monsoon, that caused changes in the freshwater budget of the eastern Mediterranean Sea. In particular, during times of (predominantly) precession-driven sapropel formation in the eastern Mediterranean, MOW was reduced, causing a decline of the flow speed within the major branches of MOW in the Gulf of Cádiz. Hence, besides a possible glacio-eustatic forcing mechanism, these $\delta^{18}O$ enrichment events could also reflect a direct response to insolation driven hydrographic changes in the Mediterranean source area (Bahr et al., 2015; Kaboth et al., 2015). Such a scenario is in accordance with climate modeling experiments showing that MOW is generally increased during precession maxima when dryer and colder climate background conditions prevailed over the Mediterranean region (Bosmans et al., 2014). This aligns with our findings as the strongest $\delta^{18}O$ enrichment events throughout the Late Pleistocene (e.g. MIS 8 and 6) exclusively coincide with precession maxima.

Our bottom water temperature estimates of ~6-8 °C based on benthic Mg/Ca measurements for the enrichment events at Site U1386 are similar to that of the LGM (Fig. 4.4C). This indicates

that bottom water temperatures dropped on glacial-interglacial timescales by ~3 to 5°C, i.e. in accordance with the global mean (Köhler et al., 2010). It becomes apparent that the glacial induced temperature decrease did substantially contribute to the increase of $\delta^{18}O$ during the glacial periods but provide no indication that a more profound cooling occurred during the peaks of the $\delta^{18}O$ enrichment events relative to the LGM conditions at Site U1386. As a similar decrease in temperature is also expected for the Mediterranean Sea it seems possible that our bottom water temperature estimates might represent glacial MOW properties. The rather steady temperature decrease between the peaks of the $\delta^{18}O$ enrichment events during e.g. MIS 8 and 6 compared to the LGM also stands in contrast to the glacial depiction of the LR04 where MIS 8 and 6 are not just related to higher sea-level than compared to the LGM but in association also to a smaller glacial reduction in deep-water temperature (de Boer et al. 2014). This indicates that a substantial part of the relative $\delta^{18}O$ discrepancy between Site U1386 and LR04 derives from the fact that the LR04 represents global mean deep-water temperature conditions which do not match the pattern of glacial temperature decrease we observe at Site U1386.

An alternative explanation for the strong precession cyclicity and the occurrence of these glacial $\delta^{18}O$ enrichment events might also be seen in the influence of subtropical water in the Gulf of Cadiz during glacials. In this scenario, a significant part of the recorded $\delta^{18}O$ signal during these enrichment events could relate to an increased salinity of the subtropical water masses (Schmidt et al., 2006) and not to MOW influence. Initially it was suggested that the prevalence of subtropical intermediate and surface water masses along the Iberian Margin and in extension the Gulf of Cadiz is predominately glacioeustatic driven (Rogerson et al., 2004; Voelker and de Abreu, 2011; Voelker et al., 2009). However, recent suggestions made by Amore et al. (2012) for the Iberian Margin indicate a precession related migration pattern overimposed on glacial-interglacial variability. The authors argued that northward increase of subtropical waters are caused by prolonged negative North Atlantic Oscillation (NAO)-like conditions coinciding with precession maximum (LGM coincides with precession maximum at 20 ka). In this case, the weaker Azores high – Icelandic low pressure system is shifted southward, due to the decreased warming in the Northern Hemisphere in response to insolation as well as emergence of a circumpolar high-pressure belt. As a consequence of the decreased pressure gradient the equatorward wind stress decreases aiding the northward expansion of subtropical water masses (Moreno, 2002; Yin et al., 2009).

4.5 Conclusions

We find three distinct phases of MOW variability throughout the Late Pleistocene at Site U1386. During Phase I (last climatic cycle) MOW influence is strengthened predominately during interglacial periods and sea-level highstands whereas it is reduced or absent during glacial periods of MIS 2 and 4. During Phase II (~130475 to ~130 ka), MOW flow strength is generally low, though prevailed at Site U1386, and largely unaffected by the prevalent glacial-interglacial-related climatic background conditions. During Phase III (~475 to ~570 ka) MOW influence at Site U1386 is generally strengthened and persistent during MIS 14. The overall pattern of MOW variability through these three phases is mimicked by changes in the $\delta^{13}C$ record at Site U1386, possibly indicating distinct shifts in the relative contributions of Mediterranean intermediate water (Phase II) vs. WMDW (Phases I and III).

Keeping pace with the change in MOW sourcing is the occurrence of distinct and precession paced $\delta^{18}O$ enrichment events contrasting the pattern of glacial behaviour depicted in the global mean $\delta^{18}O$ signal (LR04). These $\delta^{18}O$ enrichment events most likely reflect a combination of (1)

profound temperature reduction and salinity increases of the MOW, since it aligns with similar changes in the Mediterranean source region, (2) increased ice volume, since these events are accompanied by significant sea level drops as reconstructed from Red Sea sediments, and (3) the increased influence of North Atlantic intermediate water masses when MOW influence is highly reduced or even absent at Site U1386.

Acknowledgements

We acknowledge the Integrated Ocean Drilling Program (IODP) for providing the samples used in this study as well as A. van Dijk at Utrecht University and J. Nicolson at Cambridge University for analytical support. This research was funded by NWO-ALW grant (project number 865.10.001) to Lucas J. Lourens. B. de Boer receives funding from the European Union's Horizon 2020 research and innovation program under the Marie Sklodowska-Curie grant agreement No 660814.

Chapter 5

On the origin of prolonged $\delta^{18}O$ excursions during MIS 6 and 8

Stefanie Kaboth, André Bahr and Lucas J. Lourens

Distinct mid-glacial $\delta^{18}O$ enrichment events found at Site U1386 in the Gulf of Cadiz during Marine Isotope Stages 6 and 8 represent a striking feature absent in most deep-sea benthic δ18O records studied worldwide. These $\delta^{18}O$ enrichment events are closely related to periods of maximum precession and aligned with previous findings from the Mediterranean and Red Seas. Here we present paired planktic and benthic stable isotope ($\delta^{18}O$ and $\delta^{13}C$) and Mg/Ca-based temperature records of Site U1386 of the last 300.000 years. Our results show that these $\delta^{18}O$ enrichment events are recorded in both subsurface and bottom water masses and pre-date the largest cooling events along the Iberian Margin and associated European sourced meltwater pulses of the Drenthe and Fuhne major ice-sheet advances, suggesting that they instead correspond to periods of maximum ice volume extend in Europe.

5.1 Introduction

High-resolution records of bottom-current velocity from various drill sites within the Gulf of Cádiz have documented a persistent low-latitude forcing mechanism of Mediterranean Outflow Water (MOW) flow speed changes over the past ~150 kyr (Bahr et al., 2015; Kaboth et al., 2015). It was argued that the dominant driver of orbital-scale MOW variability is the African monsoon via its influence on the freshwater budget of the eastern Mediterranean Sea. In particular, during times of (predominantly) precession-driven sapropel formation in the eastern Mediterranean, MOW was reduced, causing a decline of the flow speed within the major branches of MOW in the Gulf of Cádiz. Besides, pulses of increased MOW flow speed occurred during Greenland stadials, coinciding with periods of enhanced Levantine Intermediate Water (LIW) flow in the western Mediterranean Sea (Bahr et al., 2015; Toucanne et al., 2012). It has been suggested that these enhancements were linked to periods of a weakened African monsoonal activity, and hence generally reduced Nile River discharge (Bahr et al., 2015 and references therein). In addition, it has been suggested that the pronounced millennial-scale variability found in the MOW records of the past 150 kyr from the Gulf of Cádiz, in particularly during MIS 3, might have been amplified by severe winter cooling over the eastern Mediterranean due to a strong Siberian High as well as by an enhanced contribution of Western Mediterranean Deep Water promoted by intense winter cooling over the Gulf of Lion (Bahr et al., 2015 and references therein). Thus, MOW formation fluctuates in concert with orbital precession, buts is overprinted by millennial-scale variability. Because MOW is an important provider of high-salinity waters with a distinct impact on the intermediate-depth North Atlantic, i.e. the absence of MOW reduces AMOC intensity by as much as 15% compared to present-day conditions (Rogerson et al., 2012), a strong MOW outflow has the potential to

invigorate deep-water formation and AMOC strength (Potter and Lozier, 2004; Rogerson et al., 2012). Consequently, precession-forced Northern Hemisphere summer insolation minima probably have stimulated maximal injection of MOW into the North Atlantic, thereby strengthening the intermediate AMOC branch (Bahr et al., 2015; Kaboth et al., 2015).

In this paper, we elaborate on the millennial-scale and precession-forcing mechanisms of MOW flow speed changes within the upper core of the Gulf of Cádiz over the past ~300 kyr. In particular, we will focus on the occurrence of two significant $\delta^{18}O$ enrichments (of up to 1‰) reflected in the benthic isotope record of Site U1386 during MIS 6 and MIS 8 (Kaboth et al., *in prep*), which are clearly lacking in the LR04 global mean benthic $\delta^{18}O$ stack of Lisiecki and Raymo (2005). Emphasis will be on the timing and potential driving mechanism of these events, ranging from a local temperature decline to a weakening of the monsoon system to global ice volume increases. For this purpose, we combine stable oxygen and carbon isotope measurements from both planktic and benthic foraminifera with benthic and planktic Mg/Ca-based sea water temperature estimates, and compared our results to published proxy records from the ambient Iberian Margin and the Bay of Biscay (Fig. 5.1). We aim to provide an in-depth analysis of the origin, driving mechanism and significance of the glacial $\delta^{18}O$ enrichment events at Site U1386 and beyond the scope of the Gulf of Cadiz as well as its relation to European Ice sheet dynamics.

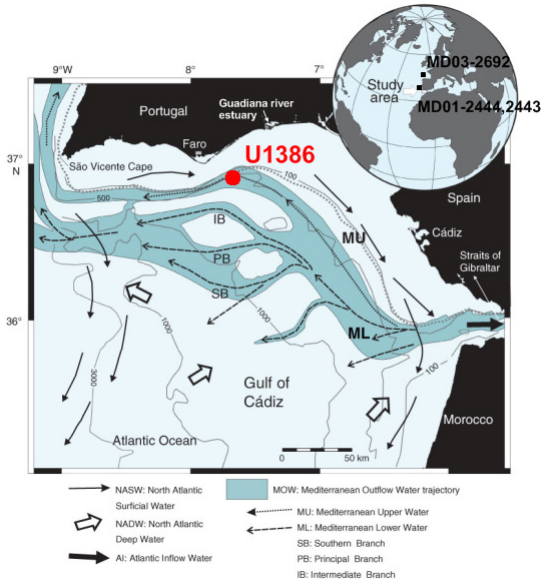

Figure 5.1: *Study area. Location of Site U1386 (upper MOW core) is marked in red. Sites MD01-2444, 2443 (Hodell et al., 2013; Martrat et al., 2007) at the Iberian Margin and Site MD03-2692 (Toucanne et al., 2009) located in the Bay of Biscay are marked in black.*

5.2 Material & Methods

Stable oxygen isotope analyses were carried out on 4-6 specimens of the preferably epifaunal living foraminifera species *Planulina ariminensis* from the >150 µm size fraction. In the absence of *P. ariminensis* we selected specimen of the likewise preferably epifaunal living foraminifera *Cibicides*

ungerianus (Schönfeld, 2002b) For the planktic record we utilized 10-15 specimen of *G. bulloides*. All selected specimens were crushed, sonicated in ethanol and dried at 35˚C. Stable isotope analyses were carried out on a CARBO-KIEL automated carbonate preparation device linked to a Finnigan MAT 253 mass spectrometer at Utrecht University. The precision of the measurements is ±0.08‰ and ±0.03 for $\delta^{18}O$ and $\delta^{13}C$, respectively. The calculation of the benthic interspecies isotopic offset is based on 15 paired oxygen and carbon isotope measurements of both benthic species. The interspecies offsets were determined by applying a least square linear regression equation. The Pearson correlation coefficient (R^2) between both species shows high correlation of 0.97 for $\delta^{18}O$ (Fig. 5.2) and has been presented in Kaboth et al. (*in prep*.).

5-7 specimen of benthic species *U. peregrina* and 30-35 specimen of planktic species *G. bulloides* from the >150 µm fraction (~250 µg) were gently crushed between two glass plates to open the chambers and then cleaned following the procedure of Barker et al. (2003), including (1) several water and ethanol washings to remove clay, (2) hydrogen peroxide treatment in a boiling water bath to eliminate organic matter and (3) a short (30 s) dilute acid leaching with 0.001 M nitric acid to eliminate any adsorbed contaminants from test fragments. Prior to measurement, samples are dissolved in 350 ml of 0.075 M nitric acid, centrifuged to separate insoluble residues and analyzed with a Varian Vista PRO simultaneous inductively coupled plasma atomic emission spectrometer (ICP-AES) at the Godwin Laboratory at Cambridge University. The benthic Mg/Ca ratios were transferred into temperature estimates following Cacho et al. (2006), and the planktic Mg/Ca ratios were transferred following Elderfield and Ganssen (2000). Uncertainty estimates are based on parallel measurements and range between 1 to 1.5°C for both, planktic and benthic measurements. The chronology is based on the visual correlation of the benthic $\delta^{18}O$ record at Site U1386 to the global mean benthic isotope stack LR04 (Lisiecki and Raymo, 2005) as being presented by Kaboth et al. (*in prep*.).

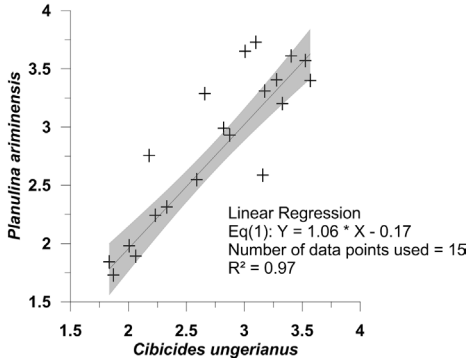

Figure 5.2: *Interspecies correction for $\delta^{18}O$ between C. ungerianus and P. ariminensis at Site U1386. The correction is based on parallel measurements throughout the investigated interval. Linear square regression (black line) equation and Pearson correlation coefficient (R^2) are shown..*

5.3 Results & Discussion

5.3.1 Glacial $\delta^{18}O$ enrichment events during MIS 6 and 8 at U1386

The benthic $\delta^{18}O$ record of Site U1386 reveals strong resemblance with LR04, indicating that the oxygen isotope composition of the bottom water at this location are primarily determined by glacial-interglacial variability in ice volume and temperature (Fig. 5.3). However, the benthic

$\delta^{18}O$ record of Site U1386 clearly differs in shape from LR04, especially during MIS 6 and 8 by the occurrence of prolonged (millennial-scale) and precession-paced $\delta^{18}O$ enrichment events (Kaboth et al., 2015; *in prep.*). They argued that these $\delta^{18}O$ enrichment events most likely reflect a combination of (1) profound temperature reduction and salinity increases of the MOW, since it aligns with similar changes in the Mediterranean source region, (2) increased ice volume, since these events are accompanied by significant sea level drops as reconstructed from Red Sea sediments, or (3) the increased influence of North Atlantic intermediate water masses when MOW influence is highly reduced or even absent at Site U1386.

A comparison between the benthic and planktic $\delta^{18}O$ signal at Site U1386 shows that the $\delta^{18}O$ enrichment events in MIS 6 and 8 are reflected in both bottom and subsurface water masses (Fig. 5.3). This indicates that the increase in $\delta^{18}O$ is not just limited to temperature and/or the isotopic changes within the bottom waters. The benthic and planktic Mg/Ca based temperature estimates of U1386 show furthermore that the temperature of the subsurface and bottom water masses of respectively ~15 and ~7-8°C were almost similar during the LGM, MIS 4 and the $\delta^{18}O$ enrichment events of MIS 8 and 6, and that they were on average ~5 and ~3.5°C colder than during the Holocene (Fig. 5.3). This relatively steady thermocline suggests that the oceanographic structure at Site U1386 was comparable between the LGM, MIS 4 and the $\delta^{18}O$ enrichment events of MIS 8 and 6, and in addition that this precession-paced variability affected the whole water column at Site U1386.

Although the low weight percentage values of the coarse (>63μm) grain-size record of Site U1386 is in agreement with a general reduction in MOW flow speed during MIS 6 and 8, though the absence of a significant $\delta^{18}O$ gradient between the benthic record of Site U1386 and that of Sites 967/968 in the Eastern Mediterranean suggests that MOW nevertheless prevailed as dominant water mass during these events (Kaboth et al., *in prep.*). This might indicate that the enrichment events relate to changes in the temperature/salinity signal of its source region. This is, however, debatable as the upper core of MOW appears to be very sensitive to glacial boundary conditions (Kaboth et al., 2015). In particular, MOW flow speed was probably very low or even absent at Site U1386 during the full glacial conditions of MIS 4 and MIS 2, suggesting that the lowered sea levels (and hence a water depth reduction of ~15% at this site) has driven MOW to flow deeper along the middle slope of the Gulf of Cádiz as was discussed in previous studies (Hernandez-Molina et al., 2014a; Llave et al., 2007; Rogerson et al., 2005; Schönfeld and Zahn, 2000; Voelker et al., 2006, 2009).

A significant part of the precession-paced variability could be related to increased salinity of the subtropical water masses (Schmidt et al., 2006), thereby following Amore et al. (2012) who argued that during precession maxima subtropical waters extended northward due to prolonged negative North Atlantic Oscillation (NAO)-like conditions (see Kaboth et al., *in prep.*). Or secondly, by regional salinity/density changes in the Mediterranean, connected to precession-forced low-latitude climates such as the monsoon (Bahr et al., 2015). Such an interpretation would be in line with a recently published benthic $\delta^{18}O$ record of the eastern Mediterranean, which also showed distinct precession-controlled $\delta^{18}O$ enrichments during MIS 6 and 8 (Konijnendijk et al., 2015) that match the pattern and amplitude variability found at Site U1386 (Kaboth et al., *in prep.*).Finally, it cannot be excluded that ice volume changes may have caused part of the $\delta^{18}O$ enrichments during MIS 6 and 8, which are then evidently not resolved by the LR04 record (Konijnendijk et al., 2015). Evidence for such an explanation comes from the sea level reconstructions based on planktic isotope records of the Red Sea, which clearly indicated a significant sea level low stand corresponding to the $\delta^{18}O$ enrichment event of MIS 8 (Grant et al., 2014; Rohling et al., 2009; Siddall, 2004; Siddall et

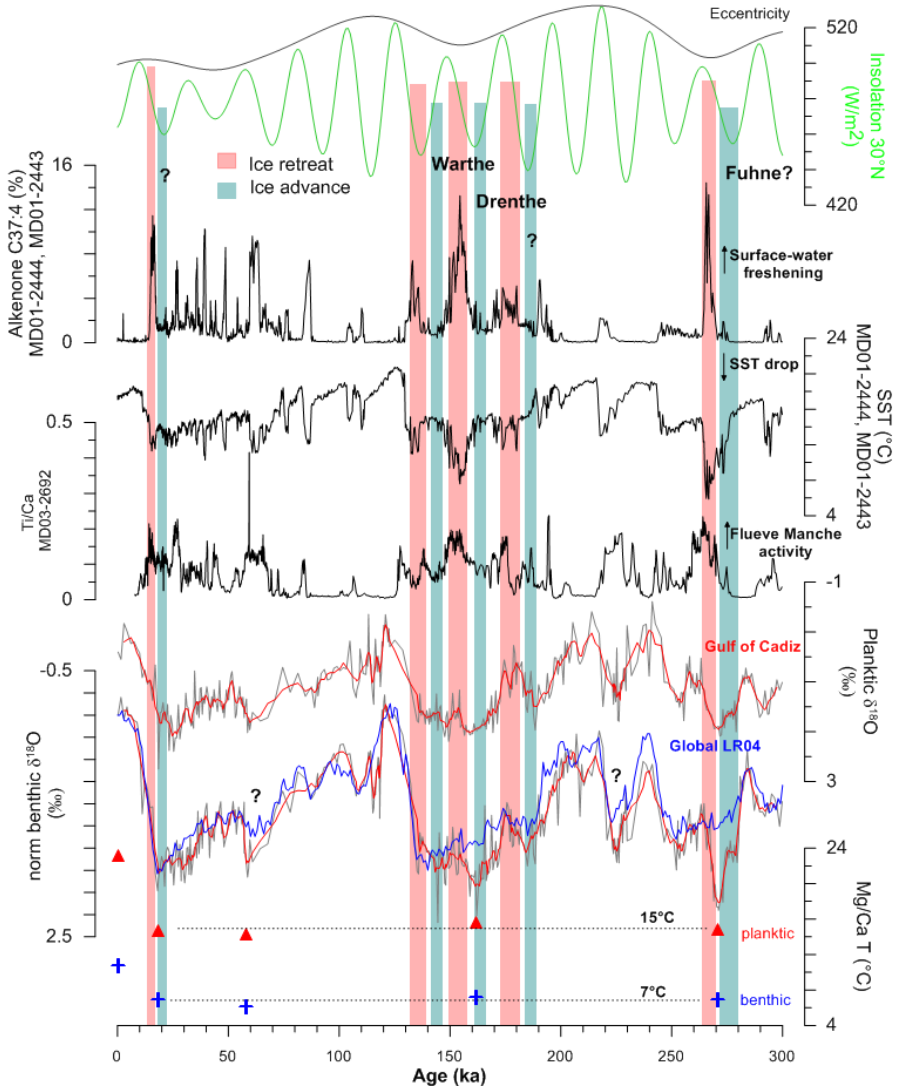

Figure 5.3: *Comparison of benthic and planktic $\delta^{18}O$ and Mg/Ca records of Site U1386 to adjacent proxy records from the Iberian Margin MD01-2444, 24443 (Hodell et al., 2013; Martrat et al., 2007) and the Bay of Biscay MD03-2692 (Toucanne et al., 2009). The age model of Site MD01-2444/2443 is based on the absolute speleothem age model following Hodell et al. (2013), which is an adjustment to the initial age model of Martrat et al. (2007). Thereby, the first climatic cycle was tuned using a combination of radiometric dates and a Monte-Carlo statistical correlation between Iberian Margin proxies and reference isotopic profiles from polar ice of Greenland and Antarctica. For the second and third climatic cycle ages were obtained by relating the benthic $\delta^{18}O$ profile of site MD01-2443 to the Antarctica Dome C isotopic record on the edc2 age-scale. Age models for Site U1386 and MD03-2692 are based on tuning of the respective benthic $\delta^{18}O$ records to the LR04 global mean $\delta^{18}O$ stack (Toucanne et al., 2009; Kaboth et al., in prep; this paper). The age model of MD03-2692 has been revised from 300 to 250 kyr (Toucanne S., pers comm.)*

al., 2003). Since these short-lived excursions are neither as pronounced nor reflected in the open ocean benthic stack LR04, it could be argued that also the planktic isotope records of the Red Sea are influenced by a regional precession-controlled salinity/density change, i.e. similar as that found for the Mediterranean (Konijnendijk et al., 2015) and now for the Gulf of Cadiz (Kaboth et al., in prep; this paper). However, because similar features were also found in the Antarctic EPI Dome C ice core δDeuterium (δD_{ice}) record (Rohling et al., 2009), it has been argued that these excursions are linked to and hence reflect global sea level changes (Grant et al., 2014).

Accordingly, the $\delta^{18}O$ enrichment events could for instance record the substantial continental ice-sheet advances during the Drenthe (at~170-160 ka; Ehlers and Gibbard, 2004; Toucanne et al., 2009) and Fuhne (at ~270 ka; McCann, 2007) periods (Fig. 5.3). Although the continental record for ice advances during MIS 8 (Fuhne cold stage) is less well documented than MIS 6 (Margari et al., 2014; Toucanne et al., 2009), glacial deposits in the Netherlands sector of the North Sea have been linked to mid-MIS 8 suggesting a British Ice Sheet that reached several tens of kilometer into the North Sea basin beyond the extent of the later MIS 2 glaciation (Beets et al., 2005; Bridgland et al., 2014). This is also supported by findings from the Northern German Lowlands suggesting a glacial ice advance similar in its maximum extent as MIS 6 (Roskosch et al., 2015).

5.3.2 Link between $\delta^{18}O$ anomalies and Iberian Margin cold events

Distinct MIS 6 and 8 anomalies of cold water masses have also been reflected in the Iberian Margin sea surface temperature (SST) proxy records (U^{k}_{37} and $C_{37:4}$) of Sites MD01-2444/2443 (Hodell et al., 2013; Martrat et al., 2007). Toucanne et al. (2009) related these Iberian Margin cooling events to the influx of meltwater pulses carried by the Flueve Manche paleoriver from the wasting European continental ice sheets exiting the Bay of Biscay and traveling as a narrow coastal current along the Iberian Margin as far south as ~37°N; effectively the European version of Heinrich events (Fig. 5.3). This hypothesis was based on the robust correlation between increased Ti/Ca ratios (Toucanne et al., 2009) and the abundance of the freshwater algae *Pediastrum* in the Bay of Biscay (Eynaud et al., 2007) with the cooling events along the Iberian Margin. Considering small age uncertainties between the studied records, it appears that the pronounced Flueve Manche activity increases and associated cold climate conditions along the Iberian Margin lag the $\delta^{18}O$ enrichment events found at Site U1386 by ~7-8 kyr (Fig. 5.3). In other words, the reconstructed succession of events suggests that these large melt water pulses characterize the end of the Drenthe and Fuhne periods and hence the termination of large ice-sheet expansions in Europe.

If we take a closer look at Fig. 5.3, it seems that the $\delta^{18}O$ record of Site U1386 is also more enriched during MIS 4, MIS 7.2 and at the onset of MIS 2 with respect to LR04. Similarly, these periods tend to precede distinct pulses of Flueve Manche activity. This succession of events appears to be dominantly precession-controlled with the peak in $\delta^{18}O$ enrichment occurring close to precession maxima (i.e. NH summer insolation minima) and the melt water pulses and associated cold SST conditions at the Iberian Margin following by 5-10 kyr (Fig. 5.3). An explanation for the increased ice-sheet expansions in Europe during precession maximum conditions may come from state-of-the-art high-resolution climate modeling experiments of orbital extremes, which showed that the number of storm tracks in winter over the North Atlantic was considerably higher during precession maximum than during precession minimum configurations (Bosmans et al., 2015). This increase was linked to a larger equator-to-pole insolation gradient, and hence could explain the enhanced moisture transport towards the European ice-sheets during precession maximum configurations In addition, it has been argued that the prevalence of warm subtropical water masses up to ~40°N boost continental ice grow in Northern Europe as the increased thermal

gradient between warm waters at mid-latitudes and cold landmasses invoked the production of moisture (Morley et al., 2014; Sánchez Goñi et al., 2013). The subsequent northward advection of the moisture is triggered by Rossby-wave breaking of the jet stream over Western Europe, which is enhanced due to the presence of the existing Fennoscandian ice shield and the associated semi-permanent blocking circumpolar high, effectively moving the storm tracks farther north (Luetscher et al., 2015)

5.4 Conclusions

Site U1386 in the Gulf of Cadiz record distinct $\delta^{18}O$ enrichment events during MIS 6 and 8 in both subsurface and bottom water masses, which align with previous findings from the Mediterranean and Red Seas. These events potentially reflect substantial ice advance periods on continental Europe (Drenthe and Fuhne) and pre-date "cooling events" along the Iberian Margin linked to European sourced meltwater pulses. Their precession pacing is probably connected to the increased number of storm tracks in winter over the North Atlantic, which enhanced moisture transport towards the European ice-sheets during precession maximum configurations

Acknowledgements
We acknowledge the Integrated Ocean Drilling Program (IODP) for providing the samples used in this study as well as A. van Dijk at Utrecht University and J. Nicolson at Cambridge University for analytical support. We would also like to thank F. Eynaud and S. Toucanne for graciously providing the Bay of Biscay data. This research was funded by NWO-ALW grant (project number 865.10.001) to Lucas J. Lourens.

Chapter 6

Mediterranean Outflow Water variability during the Early Pleistocene climate transition

Stefanie Kaboth, Patrick Grunert and Lucas J. Lourens

Gaining insights into the evolution of Mediterranean Outflow Water (MOW) during the Early Pleistocene climate transition has been so far hampered by the lack of available paleoclimatic archives. Here we present the first benthic foraminifera stable oxygen and carbon isotope records and grain-size data from IODP Expedition 339 Site U1389 presently located within the upper core of the MOW in the Gulf of Cadiz for the time interval between 2.6 and 1.8 Ma. A comparison with an intermediate water mass record from the Mediterranean Sea strongly suggest an active MOW supplying Site U1389 on glacial-interglacial timescales during the Early Pleistocene. We also find indication that the increasing presence of MOW in the Gulf of Cadiz during the investigated time interval aligns with the progressive northward protrusion of Mediterranean sourced intermediate water masses into the North Atlantic, possibly modulating the intensification of the North Atlantic Meridional Overturning Circulation at the same time. Additionally, our results suggest that MOW flow strength was already governed by precession and semi-precession cyclicity during the Early Pleistocene against the background of glacial-interglacial variability dominated by the obliquity cycle of Earth`s inclination axis.

6.1 Introduction

The Mediterranean Outflow Water (MOW) is a distinct hydrographic feature at intermediate water depths in the Gulf of Cadiz, distinguished from other ambient North Atlantic water masses by its warm and saline character (Ambar and Howe, 1979; Bryden and Stommel, 1984; Bryden et al., 1994). In the modern hydro-climatic setting of the Mediterranean Sea the MOW is predominately sourced by Levantine Intermediate Water (~70%), formed in the Eastern Mediterranean Basin, and variable parts of Western Mediterranean Deep Water (WMDW) originating in the Alboran and Tyrrhenian Sea (Millot, 2014, 2009; Millot et al., 2006). After exiting the Strait of Gibraltar, the MOW plume cascades down the continental slope due to its increased density (Ambar and Howe, 1979; Hernandez-Molina et al., 2014a; Hernández-Molina et al., 2006; Mulder et al., 2006). In the Gulf of Cadiz, MOW follows the topography of the continental shelf in two major flow cores at 800-1400 m water depth (lower MOW core), and 500-700 m water depth including our study area (upper MOW core, Fig. 6.1) (Baringer and Price, 1997; Borenäs et al., 2002; Hernández-Molina et al., 2013). After exiting the Gulf of Cadiz, most of MOW flows north along the European continental margin until it mixes with the North Atlantic Current at Rockall Plateau (Hernandez-Molina et al., 2014b).

Beyond the Mediterranean region, MOW has been acknowledged as an important modulator of the North Atlantic salt budget with previous research suggesting that the absence

of MOW may reduce Atlantic Meridional Overturning Circulation (AMOC) by as much as 15% compared to modern (Rogerson et al., 2012). Despite its potential cosmopolitan significance the paleoceanographic history of MOW has so far been only studied for the Pliocene (Khelifi et al., 2009; Khélifi et al., 2014), and during the last climatic cycle (Bahr et al., 2015; Kaboth et al., 2015; Llave et al., 2006; Schönfeld and Zahn, 2000; Schönfeld, 2002a; Toucanne et al., 2007; Voelker et al., 2006). In this light, the reconstruction of MOW variability might be particularly interesting in the broader view of the Pliocene-Pleistocene climate transition. The early Pleistocene period spans the transition from the preceding Pliocene climate optimum with limited ice sheets in the Northern Hemisphere to the cooler Middle and Late Pleistocene climate with rapidly developing continental ice growth in both hemispheres (Raymo et al., 1992; Shackleton and Hall, 1984). Throughout the Early Pleistocene, however, an interruption of the long-term Northern Hemisphere ice volume increase can be observed in concert with a sea-surface temperature stabilization in the high latitude North Atlantic cooling trend (Bell et al., 2015). It was suggested that these changes relate to an increase in AMOC strength, and in extension, an increase in northward heat transport (Bell et al., 2015).

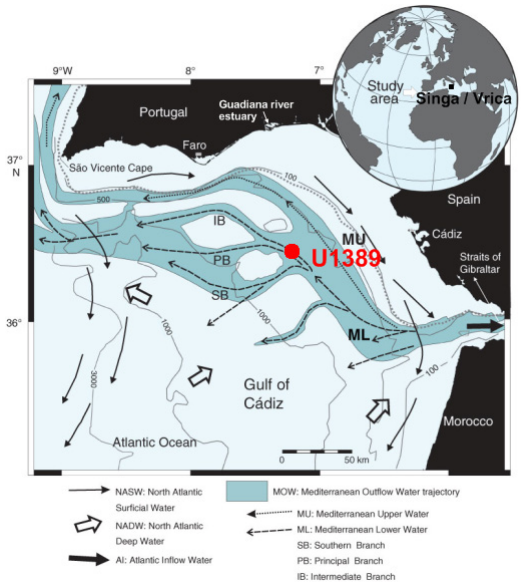

Figure 6.1: *Study area with illustration of modern MOW pathways modified after (Hernández-Molina et al., 2013; Stow et al., 2013). Site location of U1389 (upper MOW core) is marked.*

Here we elaborate on the possible role of MOW on North Atlantic Paleoceanographic changes during the early Pleistocene climate transition by investigating the benthic foraminifera stable oxygen and carbon isotopes and grain-sizes from IODP 339 Site U1389, located on the upper slope of the Gulf of Cadiz (see Fig. 6.1) for two time intervals: 2.6 and 2.4 Ma and 2.1 and 1.8 Ma. We have compared our new data with benthic stable isotope record of the Singa/Vrica sections on Calabria (Italy), representing the intermediate water mass end-member of the Mediterranean Sea (Lourens et al., 1996; unpublished data) that serves as a reference for the source region of MOW during the Early Pleistocene (Fig. 6.1). Our results bridge the gap in our understanding of MOW variability between the wider researched Pliocene and Late Pleistocene. We aim to shed new

light on MOW variability during the Early Pleistocene by analysing hydrographic changes within the Mediterranean source region, investigating the low-latitude control of MOW against the background of dominant obliquity controlled glacial-interglacial cyclicity and documenting the potential influence of MOW variability on long-term climatic oscillations in the North Atlantic.

6.2 Material & Methods

6.2.1 Site U1389

Integrated Ocean Drilling Program (IODP) Site U1389 (36°25.515'N; 7°16.683'W) was drilled in December 2011 and January 2012 during Expedition 339 (Stow et al., 2013). It is located on the southern Iberian Margin ~90 km west of the city of Cadiz and perched on the northwest side of the Guadalquivir diapiric ridge in 644 m water depth (Fig. 6.1). At present, IODP Site U1389 is directly influenced by the upper MOW core (Hernández-Molina et al., 2013; Stow et al., 2013, 2002). For the present study we analysed 423 samples from Site U1389 Hole E which cover the Early Pleistocene (2.6 to 1.8 Ma) time interval at 30 cm intervals between 549.8 to 706.35 mbsf. An expanded hiatus at Hole U1389E between 2.1 and 2.4 Ma (~622-644 mbsf) has been initially related to a phase of highly active MOW (Hernández-Molina et al., 2013; Stow et al., 2013). However, more recent findings link this compressional event to tectonically invoked erosion (Hernández-Molina et al., 2015). As a consequence we present the data split in two intervals (Interval I: 2.6-2.4 Myr and II: 2.1 to 1.8 Myr).

6.2.2 Stable isotope measurements and interspecies correction

The freeze-dried sediment samples were wet sieved into three fractions (>150 μm, >63 μm and >38 μm), and their residues oven dried at 40°C. Stable oxygen ($\delta^{18}O$) and carbon ($\delta^{13}C$) isotope analyses were carried out on 4 to 6 specimens of the epifaunal living foraminiferal species *Planulina ariminensis* and *Cibicides ungerianus* from the >150 μm size fraction. All selected specimens were crushed, sonicated in ethanol, and dried at 35˚C. Stable isotope analyses were carried out on a CARBO-KIEL automated carbonate preparation device linked to a Thermo-Finnigan MAT253 mass spectrometer at Utrecht University. The precision of the measurements is ±0.08‰ for $\delta^{18}O$ and ±0.03 for $\delta^{13}C$. The results were calibrated using the international standard NBS-19, and the in-house standard NAXOS. Isotopic values are reported in standard delta notation (δ) relative to the Vienna Pee Dee Belemnite (VPDB).

P. ariminensis was absent in 100 samples; resulting gaps were filled with *C. ungerianus* values corrected for interspecies isotopic offsets. The calculation of the interspecies offset is based on 62 paired isotope measurements of both benthic species. The $\delta^{18}O$ interspecies offset was determined by applying a least square linear regression equation (Fig. 6.2). The Pearson correlation coefficient (R^2) between both species shows high correlation of 0.79 for $\delta^{18}O$. The calculated slope of this relationship is ~0.97 with an intercept of +0.10 ‰ between *P. ariminensis* and *C. ungerianus*.
In contrast, the $\delta^{13}C$ correlation was insignificant with R^2 of 0.02 between the two benthic species (Fig. 6.2). Therefore, we only present the $\delta^{13}C$ of *P. ariminensis*, considered a valuable basis for $\delta^{13}C$ studies of the paleo-hydrography of the MOW (Zahn et al., 1987).

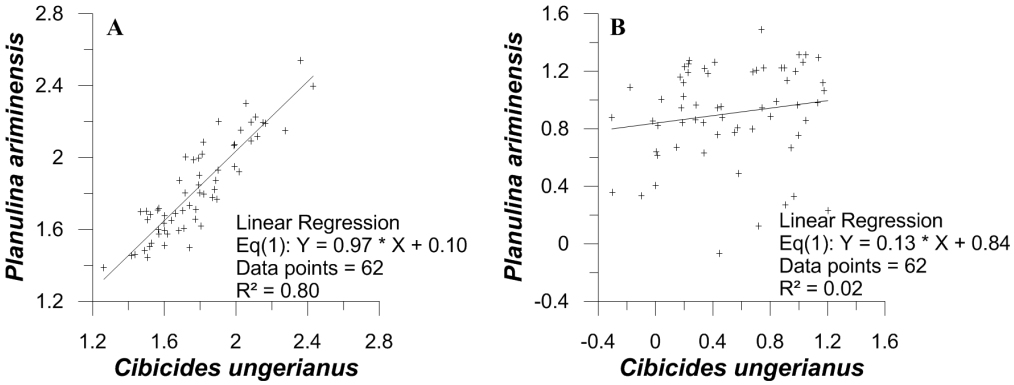

Figure 6.2: *The $\delta^{18}O$ and $\delta^{13}C$ interspecies correlation between benthic foraminifera Cibicides ungerianus and Planulina ariminensis at Site U1389. Parallel measurements were conducted throughout both investigated intervals. Linear square regression equation and Pearson correlation coefficient (R^2) are shown.*

6.2.3 Grain-size analyses

The stable isotope sample preparation was used to obtain weight percentages (wt.-%) of the grain-size fractions >150 µm, 150-63µm, 63-38 µm and <38 µm for the investigated samples were obtained during sample preparation for isotope analyses. We concentrate on the grain-size fraction between 63-150 µm which has been used previously as indicator for flow strength changes in the Gulf of Cadiz attributed to MOW variability (Rogerson et al., 2005). Even though untreated weight percentages hold a bias it has been shown for the last climatic cycle that weight percentages mirror major peaks in Zr/Al records, considered a reliable recorder of MOW flow strength variability (Bahr et al., 2014), and thus can be used to trace patterns of MOW flow strength variability (Kaboth et al., 2015).

6.2.4 Chronology

Primary age constraints are based on paleomagnetic and biostratigraphic tie points as listed in Table 6.1. The secondary age model follows the visual correlation of the benthic $\delta^{18}O$ record at Site U1389 to the benthic $\delta^{18}O$ "MedSea" stack of Lourens et al. (1996, unpublished data) within the investigated time period. The respective tie points of the secondary age model are listed in Table 6.2. The MedSea stack is based on the benthic *C. ungerianus* $\delta^{18}O$ values from the Singa and Vrica sections located in Calabria, Italy used in Lourens et al. (1996, *unpublished data*). The *C. ungerianus* values of the MedSea stack were adjusted to the *P. ariminensis* based $\delta^{18}O$ record at Site U1389 by applying the interspecies correction equation cited under section 6.2.2. The Mediterranean Sea stack $\delta^{18}O$ time series is based on tuning sapropel midpoints to La2004 65° N summer insolation maxima, including a 3-kyr time lag (Lourens, 2004). Monitoring of the sedimentation rate was done to control viability of secondary age model. The designation of MIS stages follows the MedSea stack chronology (Lourens, 2004).

Table 6.1: *Paleomagnetic and biostratigraphic tie points used in the primary age model of Site U1389 based on shipboard data following Hernández-Molina et al. (2013) and Stow et al. (2013). 1 = Gradstein et al. 2004; 2 = Raffi et al., 2006; 3= Lourens et al. 2004; 4 = Grunert P., pers. comm.*

No.	Event	TOP Depth (mbsf)	BOT Depth (mbsf)	Time (Ma)	Reference
1	Top Olduvai	542.00		1.778	1
2	Bottom Olduvai		592.00	1.945	1
3	Matuyama/Gauss	696.00		2.581	1
4	LO *C. macintyrie*	510.09	515.65	1.66	2
5	FO *G. inflata*	627.21	630.21	2.09	3
6	LO *G. puncticulata*	645.02	646.61	2.41	3
7	LO *D. pentradiatus*	674.25	681.98	2.5	2
8	LO *D. scurlus*	681.98	693.70	2.53	2
9	LO *D. tamalis*	~805		2.8-2.87	4

6.2.5 Spectral Analysis

Spectral analysis was performed to test for statistically significant cycles with respect to orbital parameters. For analysis of orbital periodicities, the non-constantly sampled time series were analysed by a Multi Taper Method using the program REDFIT (Schulz and Mudelsee, 2002).

6.3 Results

6.3.1 Age model & Sedimentation rates

The two studied intervals of the Site U1389 $\delta^{18}O$ record exhibit similar glacial-interglacial variability as present in MedSea stack throughout the Early Pleistocene. The estimated mean sedimentation rate for both intervals is ~0.30 m/kyr (Fig. 6.3) which is similar to the sedimentation rate of ~0.25 to ~0.30 m/kyr that has been calculated from shipboard stratigraphy for the past 3.2 Myr (Hernández-Molina et al., 2013; Stow et al., 2013). A doubling of the sedimentation rate coincides with transition of MIS 96 to MIS 95 in Interval I, and ~MIS 73 in Interval II. Condensed sections with low sedimentation rates of ~0.1 m/kyr correlate with the transition between MIS 97 to MIS 96 in Interval I, and MIS 69 and MIS 68 in Interval II, respectively.

Table 6.2: *Age calibration points for the visual tuning (secondary age model) of benthic $\delta^{18}O$ records of Site U1389 to the MedSea benthic $\delta^{18}O$ stack of Lourens et al. 2004, unpublished data.*

Depth (mbsf)	Age (ka)
569.5	1810
572.25	1827
573.36	1841
578.6	1855
579.85	1903
590.00	1930
595.00	1965
600	1975
615.63	2005
623.00	2070
629.1	2092
646	2425
648.75	2435.5
665.1	2462.5
666.3	2486
673	2500
677.45	2517.5
691.8	2565
695.75	2600

6.3.2 Stable oxygen and carbon isotopes

The comparison between both intervals of the $\delta^{18}O$ record at Site U1389 with the benthic $\delta^{18}O$ MedSea stack is shown in Figure 6.4. In Interval I, lightest values of 1.17 and 1.22 ‰ coincide with interglacials MIS 103 and 101, and the strongest glacial enrichment in $\delta^{18}O$ (2.69 ‰) coincides with MIS 100. Transitional

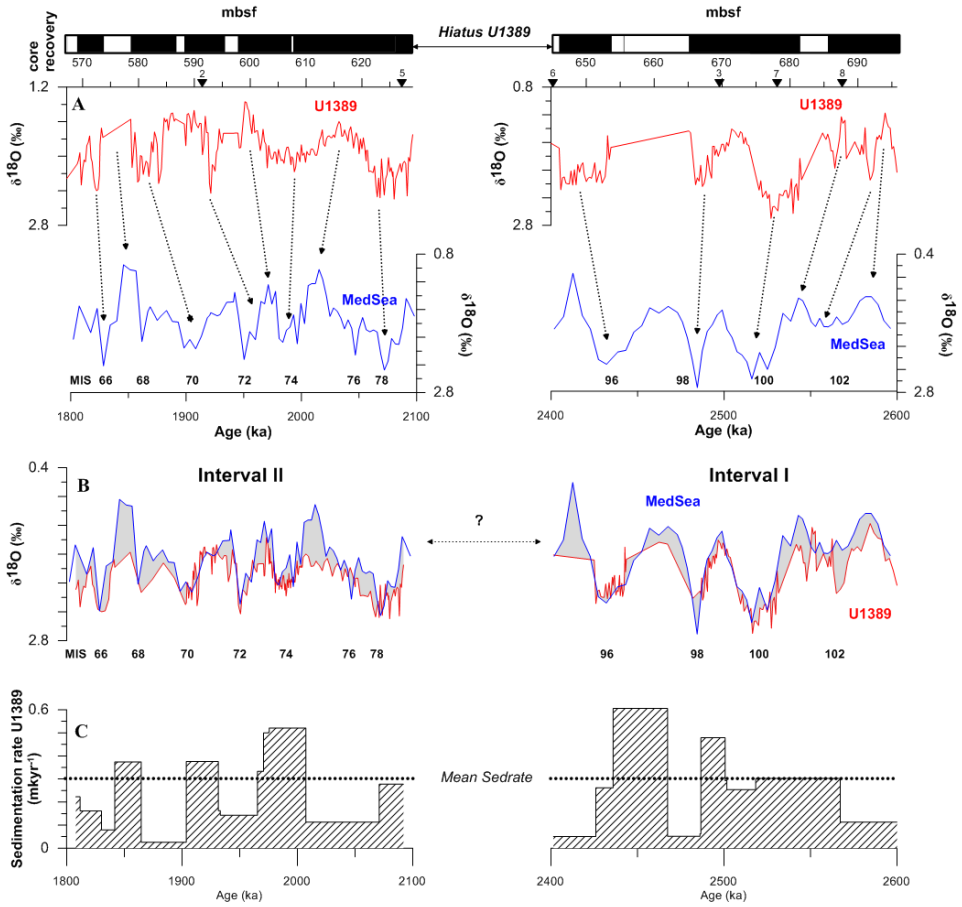

Figure 6.3: *Chronology of Site U1389. Assigned marine isotope stages (MIS) follow Lourens et al. (2004). (**A**) Both intervals of the $\delta^{18}O$ record of Site U1389 on shipboard MCD scale correlated to the benthic $\delta^{18}O$ record of the Mediterranean Sea (MedSea stack) after Lourens et al. (1996, unpublished data). Chronostratigraphy of MedSea stack is based on tuning sapropel midpoints to La2004 65° N summer insolation (Lourens, 2004). Lines with arrows indicate selected tie points used for the age model (a full list of tie points is available in Table 2). Black triangles with numbers indicating used biostratigraphic and paleomagnetic tie points as referenced in Table 6.1. Black and white bar at the top represents core recovery following Hernández-Molina et al. (2013) (**B**) Comparison of the normalized benthic $\delta^{18}O$ record of Site U1389 on new time scale according to our tuning, and normalized benthic $\delta^{18}O$ MedSea stack on its respective age model (Lourens et al. 2004) (**C**) Calculated sedimentation rates for Site U1389. Mean Sedimentation rate is marked by dotted line.*

depletion is on average 0.97 ‰ with highest values (1.29 ‰) in the interval between MIS 101 and 100 (see Fig. 6.4). In Interval II, the lightest values coincide with MIS 73 (1.36 ‰) whereas the strongest glacial $\delta^{18}O$ enrichment can be observed during MIS 72 and 66 with 2.42 % and 2.36 %, respectively (see Fig. 6.4). Transitional depletion is on average 0.82 ‰ with highest values (1.06 ‰) in the interval between MIS 73 and 72. Pronounced amplitude offsets between the $\delta^{18}O$ signal of

Site U1389 and MedSea are visible in both intervals but especially during MIS 102, 77 and 75 (Fig. 6.4). These perturbations are of the order of up to ~0.5 ‰ (e.g. MIS 75).

The comparison between both intervals of the $\delta^{13}C$ record at Site U1389 with the $\delta^{13}C$ MedSea stack is shown in Figure 6.4. During Interval I the $\delta^{13}C$ record at Site U1389 shows strong millennial-scale variability. Lightest values of 0.27 and 0.32 ‰ coincide with MIS 101 and 100, and the heaviest values (~1.27 ‰) coincide with the transition of MIS 102 to MIS 101, MIS 100, and the transition between MIS 99 to MIS 98.

6.3.3 Grain-size

The mean grain-size values (63-150 μm) for both investigated intervals are ~3.0 %-wt. Highest values of both investigated intervals of up to ~21 %-wt. are correlated with early MIS 100 (Fig. 6.4). The grain-size variability is seemingly not related to glacial-interglacial variability. In contrast to the $\delta^{18}O$ records at Site U1389, grain-size values increased during glacial and interglacials periods in both investigated intervals.

6.3.4 Spectral analyses

The grain-size records of Interval I and II at Site U1389 exhibit significance (80% to 90%) variance in the precession (~23 kyr) and semi-precession (~ 11 kyr) frequency band (Fig. 6.5). The obliquity signal is insignificant in the younger Interval II. For interval I we find significant (80%) peak at ~33 kyr which might indicate a weak obliquity influence during this interval.

6.4 Discussion

6.4.1 Glacial-Interglacial MOW variability at Site U1389 during the Early Pleistocene

Site U1389 reveals $\delta^{18}O$ values similar to the MedSea stack during Interval I (2.6-2.4 Ma) and Interval II (2.1-1.8 Ma), which emphasize the direct influence of intermediate Mediterranean water masses on MOW (Fig. 6.4). This suggests that MOW formation during the Early Pleistocene was similar to modern conditions where MOW originates largely from intermediate water masses such as the Levantine Intermediate Water (Millot, 2014, 2009; Millot et al., 2006).

The $\delta^{18}O$ difference between Site U1389 and the Mediterranean Sea is small during glacial periods, suggesting that Site U1389 bathed in MOW during these colder climatic conditions throughout the early Pleistocene time interval (Fig. 6.4). This is particularly interesting in light of the proposed vertical shift of the MOW flow path during glacial periods of the Late Pleistocene fostered by the increased density of the outflowing Mediterranean water masses (Kaboth et al., 2015; Lofi et al., 2015; Toucanne et al., 2007b; Voelker et al., 2006; Rogerson et al., 2005; Schönfeld and Zahn, 2002). This suggests that Site U1389 was not subjected to major glacial-interglacial induced flow path changes during the early Pleistocene, possibly due to its deeper and relatively proximal location to the Strait of Gibraltar, placing it more into the general flow path of upper MOW. These results confirm the inferences derived from Site U1389 of the Late Pleistocene interval where MOW activity was also shown to be largely unaffected by glacial-interglacial variability but instead predominately influenced by insolation driven hydro-climatic changes of its Mediterranean source region (Bahr et al., 2015).

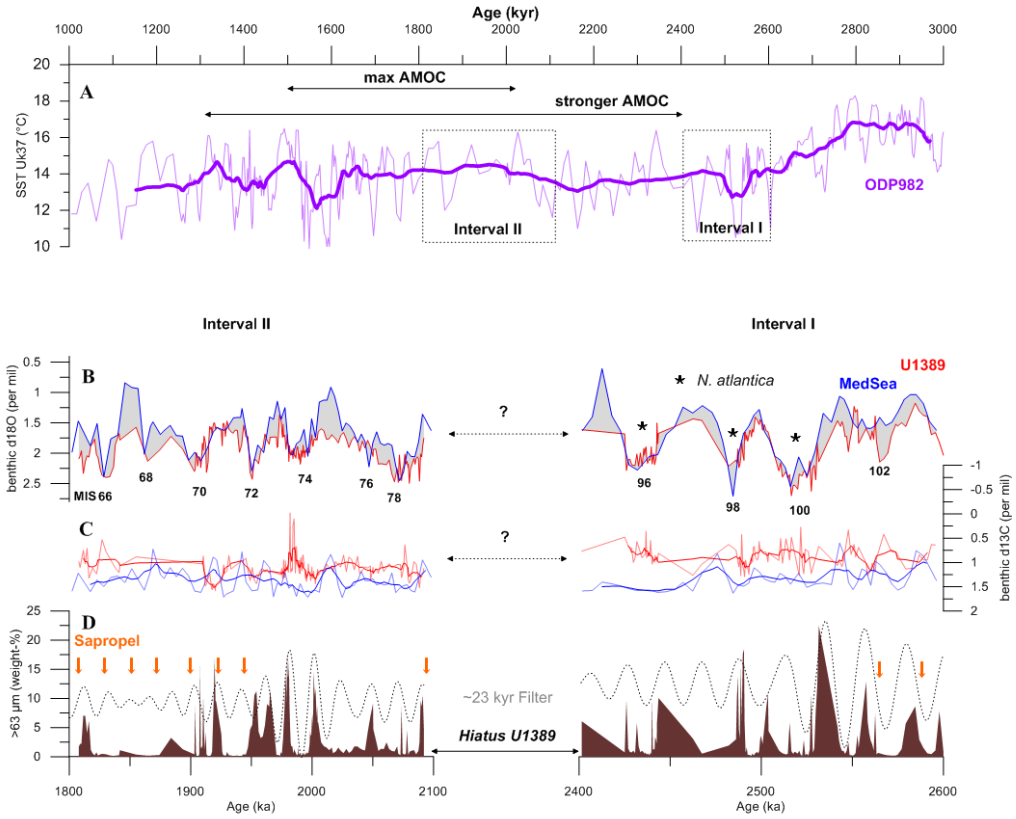

Figure 6.4: *(**A**) UK^{37} based sea-surface temperature (SST) record of North Atlantic Site ODP 982 (Lawrence et al., 2009). The running mean has a band width of 23. AMOC phases are marked by black arrows and follow the chronology of Bell et al. (2015). (**B**) δ^{18}O records of both investigated intervals at Site U1389. Interval I comprises the time frame of 2.6 to 2.4 Ma and Interval II 2.1 to 1.8 Ma. Isotopic gradient between both records is indicated by the grey-shaded area. (**C**) Comparison of δ^{13}C of P. ariminensis for both investigated intervals at Site U1389 and δ^{13}C of the MedSea stack (Lourens et al. 2004, unpublished data). The running means have a band width of 5. The C. ungerianus based δ^{13}C values of the MedSea stack were adjusted to P. ariminensis δ^{13}C values of Site U1389 following the interspecies correction presented in Kaboth et al., (in prep) (**D**) Grain-size (63-150 µm wt.-%) records for both investigated intervals at Site U1389. The filtered ~23 kyr signal of the grain-size signal is indicated by the black dotted-line. Sapropel mid-points are marked by orange arrows and follow the chronology of Emeis et al. (2000).*

In contrast, the interglacial periods of both intervals show a small but relative depletion in the Mediterranean Sea compared to the δ^{18}O signal at Site U1389 which might reflect relatively higher temperatures or lower salinity of the intermediate Mediterranean Sea waters with respect to the MOWs during interglacial periods. The strongest intervals of relative δ^{18}O depletion throughout both investigated time periods correlate with MIS 102, MIS 75, MIS 69 and MIS 67 characterized by a depletion of up to ~0.5 ‰ in the Mediterranean Sea compared to Site U1389. This shift might correspond to a freshening of the Mediterranean Sea intermediate water column during sapropel

formation and a consequently reduction of MOW influence at Site U1389 (Rogerson et al., 2012). In case of MIS 102, 69 and 67 sapropels have been documented in the Eastern Mediterranean Sea basin but not for MIS 75 (Emeis et al., 2000; Lourens, 2004; Lourens et al., 1996b, 1992).

During Interval II, the generally heavier $\delta^{13}C$ values at U1389 are close to those of the Mediterranean Sea values inferring that MOW was in fact the predominant source of bottom water at Site U1389 between 1.8 and 2.1 Ma. In contrast, the older Interval I is characterized by a slightly increased $\delta^{13}C$ gradient between Site U1389 and the Mediterranean Sea suggesting a generally larger contribution of ambient North Atlantic water masses carrying a lighter $\delta^{13}C$ signal to the site. This could indicate a more vigorous MOW or that during Interval I the MOW flow core was less proximal than during Interval II. The later argument seems to be supported by the grain-size and its variability, as Interval II shows a ~10% decrease in mean and amplitude relative to Interval I (Fig. 6.4). This would suggest that during Interval I Site U1389 was less proximal to the flow core albeit more sensitive to flow strength changes whereas during Interval II the MOW plume has settled upon Site U1389.

A distinct increase in the $\delta^{13}C$ gradient can be seen during MIS 96, which may document a particular strong MOW activity. However, the sample resolution during MIS 96 and the subsequent MIS 95 is relatively low so that increase in the $\delta^{13}C$ gradient remains ambiguous.

6.4.2 Precession control on MOW strength during the Early Pleistocene: Similarities to Late Pleistocene MOW behaviour?

Untreated grain-size weight percentages can only give an indication for patterns in flow strength (Kaboth et al., 2015). For the two investigated intervals we find that the 63-150 μm fraction variability is seemingly modulated by a ~23 kyr pacing (Fig. 6.4). This relationship is evident in the power spectrum of the grain-size data which yields for both intervals a dominance in the precession frequency band (~23 kyr); more prominently in the younger than in the older interval (Fig. 6.5). This suggests that the flow strength of MOW was probably directly modulated by precession during the Early Pleistocene, aligning with previous findings based on Zr/Al ratios at Site U1389 from the Late Pleistocene (Bahr et al., 2015). We also find significant semi-precession (~11 kyr) influence indicative for a primarily low-latitude response argued to originate in the tropics (de Winter et al., 2014; Rutherford and D'Hondt, 2000).

The $\delta^{18}O$ signal comparison of Site U1389 and the MedSea stack is also particular interesting in the context of sapropel formation, as the MedSea stack due to its intermediate paleo-water depth was potentially also sensitive to freshwater induced changes in the intermediate water composition. A substantial freshening of the intermediate water masses in the Mediterranean Sea can be inferred from the strongly depleted $\delta^{18}O$ values during MIS 102, 75, 69 and 67 relative to Site U1389 (Fig. 6.4). The potentially reduced MOW supply at Site U1389 at the same time would increase the isotopic gradient between both locations, as Site U1389 could be affected by more open ocean conditions. However, despite the low sample resolution, this seems not a persistent relationship throughout both investigated intervals.

For the Late Pleistocene, it was argued that sea level induced salinity changes in the Mediterranean Sea might have modulated the effect of freshening related to sapropel formation (Kaboth et al., 2015). For the Holocene S1, the proposed reduction in MOW has been documented by the absence of sandy contourite layers from the middle slope of the Gulf of Cadiz indicating a sudden reduction in flow strength and sediment delivery by the MOW (Toucanne et al., 2007; Voelker et al., 2006). The grain-size values throughout both investigated intervals at Site U1389 are

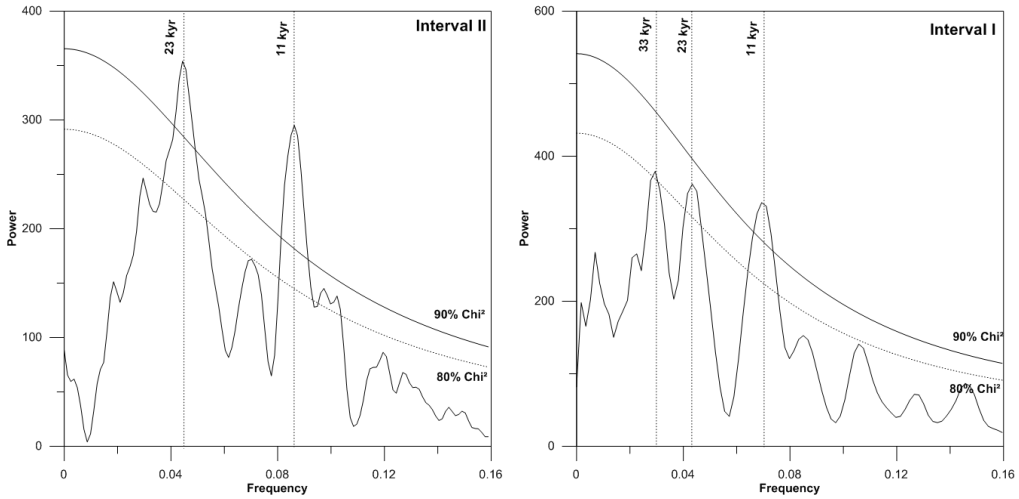

Figure 6.5: *REDFIT Power Spectra of the grain-size values (63-150µm fraction in wt.-%) for both investigated intervals of Site U1389 (Interval I = 2.6-2.4 Ma; Interval II: 2.1-1.8 Ma). The 90% (black line) and 80% (dotted line) confidence levels are given.*

typically low during sapropel formation seemingly supporting the findings from the middle and upper slope during the Late Pleistocene (Kaboth et al., 2015).

6.4.3 Did MOW contribute to the Early Pleistocene climate transition?

Between ~2.8 and 2.4 Ma (Interval I) occurrences of *Neogloboquadrina atlantica* (sin), an extinct polar species, were reported in the Mediterranean Sea during glacial periods suggesting the intrusion of colder water masses into the Mediterranean basin (Becker et al., 2005; Lourens and Hilgen, 1997; Zachariasse et al., 1990). We also find *N. atlantica* (sin) present during glacial periods of Interval I (Fig. 6.4), confirming a more southern delineation of transitional and subpolar water masses during glacial periods of the Early Pleistocene than in recent setting (Voelker et al., 2015). This latitudinal shift might occurred in concert with a more sluggish AMOC at least during the glacial periods if not throughout the whole time interval (Bell et al., 2015). Colder and more arid background conditions in the Mediterranean Sea could foster a stronger MOW analogous to cold spells related to Heinrich Events throughout the last climatic cycle (Bahr et al., 2015, 2014; Kaboth et al., 2015). An intensification of MOW during Interval I would align with the increased $\delta^{13}C$ gradient between Site U1389 and the Mediterranean Sea suggesting a more vigorous MOW which is also reflected by higher grain-size amplitudes compared to Interval II (Fig. 6.4). Our data, however, do not extend further back in time to test whether these conditions coincides with the proposed steady increase of MOW activity in the Gulf of Cadiz since 3.2 Ma as inferred from natural gamma ray logs and seismic profiles (Hernández-Molina et al., 2015), and with the arrival of Mediterranean sourced intermediate water mass at North Atlantic Sites DSDP 548 and 552 and ODP 982 from ~3.6 onwards (Khélifi et al., 2014; Loubere, 1987). This northward protrusion of warm and saline MOW towards high-latitude deep-water convection hot spots is considered an important modulator of the North Atlantic salt budget (Bahr et al., 2015; Rogerson et al., 2006; Voelker et al., 2006). We suggest that steady contributions of MOW throughout Interval I supplied continuously salt into the

North Atlantic and potentially preconditioned the strong AMOC activity phase starting at ~2.4 Ma (Bell et al., 2015) when a tipping point was reached. The Early Pleistocene MOW might therefore have acted as a positive climatic feedback mechanism against the background of increasingly colder temperatures (Fig. 6.4). This stands in contrast to the warm Pliocene setting where it was proposed that MOW contributions to the North Atlantic did not have a significant influence on the AMOC (Khélifi et al., 2014).

The intensification of the AMOC is also in concert with the disappearance of *N. atlantica* (sin) in the Mediterranean Sea and the North Atlantic up to at least 52°N after ~2.4 Ma (Lourens and Hilgen, 1997; Weaver and Clement, 1987). This suggests the reduction in southward protrusion of colder water masses and hence the *N. atlantica* extinction, and a return to a warmer background climate in the Mediterranean region during glacial periods (Lourens, 2008).

The increased AMOC activity is documented by the North Atlantic SST record of Site ODP 982 displaying a plateau starting at ~2.4 Ma indicating more steady climate conditions (Fig. 6.4), and a stagnation in ice sheet growth (Bell et al., 2015; Lawrence et al., 2009). Coinciding with this stabilization of North Atlantic SSTs is a cooling in the South Atlantic attributed to a northward piracy of the tropical warmer water pool by a strong AMOC and implying an active interhemispheric climatic seesaw at that time (Patterson et al., 2014; Etourneau et al., 2010). Despite the lack of data at Site U1389 during the 2.4 to 2.0 Ma hiatus it appears that the MOW settled upon Site U1389 during Interval II and continued if not increased its dominance as indicated by the reduced $\delta^{13}C$ gradient between Site U1389 and the MedSea stack (Fig. 6.4). The reduction in grain-size might also imply more stable MOW behaviour whereas during the transitional phase of the older Interval I MOW was probably more erratic, indicated by the high grain-size variability and the increased $\delta^{13}C$ gradient (Fig. 6.4). Unfortunately, we lack data beyond ~ 2.5 Ma from ODP Sites 549, 552 and 982 to further trace the temporal MOW influence in the high-latitude North Atlantic throughout Interval II but it stands to reason that continued MOW contributions also during Interval II might have contributed to the sustained AMOC activity.

6.5 Conclusions

Based on our results, the supply of MOW to Site U1389 was already established during the Early Pleistocene and not limited to Late Pleistocene climate conditions. In addition, we find indication that the MOW flow strength might have been modulated by precession superimposed on glacial-interglacial change, this aligns with findings from the Late Pleistocene at Site U1389 and suggests that Site U1389 is a true recorder of MOW variability also throughout Early Pleistocene. In the broader view of the Early Pleistocene climate transition we find indication that increased MOW might have contributed to the increased AMOC phases starting from 2.4 Ma, and thus influencing North Atlantic oceanic heat transport.

Acknowledgements

We acknowledge the Integrated Ocean Drilling Program (IODP) for providing the samples used in this study as well as A. van Dijk at Utrecht University for analytical support. This research was funded by NWO-ALW grant (project number 865.10.001) to Lucas J. Lourens and contributes to contributes to project P25831-N29 of the Austrian Science Fund (FWF).

References

Alhammoud, B., Meijer, P.T., Dijkstra, H.A., 2010. Sensitivity of Mediterranean thermohaline circulation to gateway depth: A model investigation. Paleoceanography 25, PA222. doi:10.1029/2009PA001823

Ambar, I., Howe, M.R., 1979. Observations of the mediterranean outflow – II the deep circulation in the vicinity of the gulf of cadiz. Deep Sea Res. Part A. Oceanogr. Res. Pap. doi:10.1016/0198-0149(79)90096-7

Amore, F.O., Flores, J.A., Voelker, A.H.L., Lebreiro, S.M., Palumbo, E., Sierro, F.J., 2012. A Middle Pleistocene Northeast Atlantic coccolithophore record: Paleoclimatology and paleoproductivity aspects. Mar. Micropaleontol. 90-91, 44-59. doi:10.1016/j.marmicro.2012.03.006

Bahr, A., Jiménez-Espejo, F.J., Kolasinac, N., Grunert, P., Hernández-Molina, F.J., Röhl, U., Voelker, A.H.L., Escutia, C., Stow, D.A.V., Hodell, D., Alvarez-Zarikian, C.A., 2014. Deciphering bottom current velocity and paleoclimate signals from contourite deposits in the Gulf of Cadiz during the last 140kyr: an inorganic geochemical approach. Geochemistry, Geophys. Geosystems 15, 3145-3160. doi:10.1002/2014GC005356

Bahr, A., Kaboth, S., Jiménez-Espejo, F.J., Sierro, F.J., Voelker, A.H.L., Lourens, L., Röhl, U., Reichart, G.J., Escutia, C., Hernández-Molina, F.J., Pross, J., Friedrich, O., 2015. Persistent monsoonal forcing of Mediterranean Outflow Water dynamics during the late Pleistocene. Geology 43, 951-954. doi:10.1130/G37013.1

Baringer, M.O., Price, J.F., 1997. Mixing and Spreading of the Mediterranean Outflow. J. Phys. Oceanogr. doi:10.1175/1520-0485(1997)027<1654:MASOTM>2.0.CO;2

Baringer, M.O., Price, J.F., 1999. A review of the physical oceanography of the Mediterranean outflow. Mar. Geol. 155, 63-82. doi:10.1016/S0025-3227(98)00141-8

Barker, S., Greaves, M., Elderfield, H., 2003. A study of cleaning procedures used for foraminiferal Mg/Ca paleothermometry: MG/CA PALEOTHERMOMETRY. Geochemistry, Geophys. Geosystems 4, 9, 8407. doi:10.1029/2003GC000559

Barker, S., Knorr, G., Edwards, R.L., Parrenin, F., Putnam, A.E., Skinner, L.C., Wolff, E., Ziegler, M., 2011. 800,000 Years of Abrupt Climate Variability. Science. 334, 347-351. doi:10.1126/science.1203580

Becker, J., Lourens, L.J., Hilgen, F.J., van der Laan, E., Kouwenhoven, T.J., Reichart, G.-J., 2005. Late Pliocene climate variability on Milankovitch to millennial time scales: A high-resolution study of MIS100 from the Mediterranean. Palaeogeogr. Palaeoclimatol. Palaeoecol. 228, 338-360. doi:10.1016/j.palaeo.2005.06.020

Beets, D.J., Meijer, T., Beets, C.J., Cleveringa, P., Laban, C., van der Spek, A.J.F., 2005. Evidence for a Middle Pleistocene glaciation of MIS 8 age in the southern North Sea. Quat. Int. 133-134, 7-19. doi:10.1016/j.quaint.2004.10.002

Bell, D.B., Jung, S.J.A., Kroon, D., 2015. The Plio-Pleistocene development of Atlantic deep-water circulation and its influence on climate trends. Quat. Sci. Rev. 123, 265-282. doi:10.1016/j.quascirev.2015.06.026

Bersch, M., Yashayaev, I., Koltermann, K.P., 2007. Recent changes of the thermohaline circulation in the subpolar North Atlantic. Ocean Dyn. 57, 223-235. doi:10.1007/s10236-007-0104-7

Böhm, E., Lippold, J., Gutjahr, M., Frank, M., Blaser, P., Antz, B., Fohlmeister, J., Frank, N., Andersen, M.B., Deininger, M., 2014. Strong and deep Atlantic meridional overturning circulation during the last glacial cycle. Nature 517, 73-76. doi:10.1038/nature14059

Borenäs, K.M., Wåhlin, A.K., Ambar, I., Serra, N., 2002. The Mediterranean outflow splitting – a comparison between theoretical models and CANIGO data. Deep Sea Res. Part II Top. Stud. Oceanogr. doi:10.1016/S0967-0645(02)00150-9

Bosmans, J.H.C., Drijfhout, S.S., Tuenter, E., Hilgen, F.J., Lourens, L.J., 2014. Response of the North African summer monsoon to precession and obliquity forcings in the EC-Earth GCM. Clim. Dyn. 44, 279-297. doi:10.1007/s00382-014-2260-z

Bosmans, J.H.C., Drijfhout, S.S., Tuenter, E., Hilgen, F.J., Lourens, L.J., Rohling, E.J., 2015. Precession and obliquity forcing of the freshwater budget over the Mediterranean. Quat. Sci. Rev. 123, 16-30. doi:10.1016/j.quascirev.2015.06.008

Bridgland, D.R., Howard, A.J., White, M., White, T.S. (Eds.), 2014. Quaternary of the Trent. Oxbow Books, Oxford.

Bryan, S.P., Marchitto, T.M., 2008. Mg/Ca-temperature proxy in benthic foraminifera: New calibrations from the Florida Straits and a hypothesis regarding Mg/Li: BENTHIC FORAMINIFERAL Mg/Ca CALIBRATION. Paleoceanography 23, n/a-n/a. doi:10.1029/2007PA001553

Bryden, H.L., Candela, J., Kinder, T.H., 1994. Exchange through the Strait of Gibraltar. Prog. Oceanogr. doi:10.1016/0079-6611(94)90028-0

Bryden, H.L., Stommel, H.M., 1984. Liminting processes thatdetermine basic features of the circulation in the Mediterranean Sea. Oceanol. Acta 7, 289-296.

Cacho, I., Grimalt, J.O., Pelejero, C., Canals, M., Sierro, F.J., Flores, J.A., Shackleton, N., 1999. Dansgaard-Oeschger and Heinrich event imprints in Alboran Sea paleotemperatures. Paleoceanography 14, 698-705. doi:10.1029/1999PA900044

Cacho, I., Shackleton, N., Elderfield, H., Sierro, F.J., Grimalt, J.O., 2006. Glacial rapid variability in deep-water temperature and $\delta^{18}O$ from the Western Mediterranean Sea. Quat. Sci. Rev. 25, 3294-3311. doi:10.1016/j.quascirev.2006.10.004

Cramp, A., O'Sullivan, G., 1999. Neogene sapropels in the Mediterranean: a review. Mar. Geol. 153, 11-28. doi:10.1016/S0025-3227(98)00092-9

De Lange, G.J., Thomson, J., Reitz, A., Slomp, C.P., Speranza Principato, M., Erba, E., Corselli, C., 2008. Synchronous basin-wide formation and redox-controlled preservation of a Mediterranean sapropel. Nat. Geosci. 1, 606-610. doi:10.1038/ngeo283

de Winter, N.J., Zeeden, C., Hilgen, F.J., 2014. Low-latitude climate variability in the Heinrich frequency band of the Late Cretaceous greenhouse world. Clim. Past 10, 1001-1015. doi:10.5194/cp-10-1001-2014

Ehlers, J., Gibbard, P.L., 2004. Quaternary glaciations: Extent and chronology, 2004th ed. Elsevier, Amsterdam.

Elderfield, H., Ferretti, P., Greaves, M., Crowhurst, S., McCave, I.N., Hodell, D., Piotrowski, A.M., 2012. Evolution of Ocean Temperature and Ice Volume Through the Mid-Pleistocene Climate Transition. Science. 337, 704-709. doi:10.1126/science.1221294

Elderfield, H., Ganssen, G., 2000. Past temperature and [delta]18O of surface ocean waters inferred from foraminiferal Mg/Ca ratios. Nature 405, 442-445. doi:10.1038/35013033

Elshanawany, R., Zonneveld, K., Ibrahim, M.I., Kholeif, S.E.A., 2010. Distribution patterns of recent organic-walled dinoflagellate cysts in relation to environmental parameters in the Mediterranean Sea. Palynology 34, 233-260. doi:10.1080/01916121003711665

Emeis, K.-C., Sakamoto, T., Wehausen, R., Brumsack, H.-J., 2000. The sapropel record of the eastern Mediterranean Sea – results of Ocean Drilling Program Leg 160. Palaeogeogr. Palaeoclimatol. Palaeoecol. 158, 371-395. doi:10.1016/S0031-0182(00)00059-6

Etourneau, J., Schneider, R., Blanz, T., Martinez, P., 2010. Intensification of the Walker and Hadley atmospheric circulations during the Pliocene – Pleistocene climate transition. Earth Planet. Sci. Lett. 297, 103-110. doi:10.1016/j.epsl.2010.06.010

Eynaud, F., Zaragosi, S., Scourse, J.D., Mojtahid, M., Bourillet, J.F., Hall, I.R., Penaud, A., Locascio, M., Reijonen, A., 2007. Deglacial laminated facies on the NW European continental margin: The hydrographic significance of British-Irish Ice Sheet deglaciation and Fleuve Manche paleoriver discharges: CONTINENTAL MARGIN LAMINATED FACIES. Geochemistry, Geophys. Geosystems 8, n/a-n/a. doi:10.1029/2006GC001496

Fiúza, A.F.G., Hamann, M., Ambar, I., Díaz del Río, G., González, N., Cabanas, J.M., 1998. Water masses and their circulation off western Iberia during May 1993. Deep Sea Res. Part I Oceanogr. Res. Pap. 45, 1127-1160. doi:10.1016/S0967-0637(98)00008-9

Grant, K.M., Rohling, E.J., Bar-Matthews, M., Ayalon, A., Medina-Elizalde, M., Ramsey, C.B., Satow, C., Roberts, A.P., 2012. Rapid coupling between ice volume and polar temperature over the past 150,000 years. Nature. 491, 744-747. doi:10.1038/nature11593

Grant, K.M., Rohling, E.J., Ramsey, C.B., Cheng, H., Edwards, R.L., Florindo, F., Heslop, D., Marra, F., Roberts, A.P., Tamisiea, M.E., Williams, F., 2014. Sea-level variability over five glacial cycles. Nat. Commun. 5, 5076. doi:10.1038/ncomms6076

Guihou, A., Pichat, S., Govin, A., Nave, S., Michel, E., Duplessy, J.-C., Telouk, P., Labeyrie, L., 2011. Enhanced Atlantic Meridional Overturning Circulation supports the Last Glacial Inception. Quat. Sci. Rev. 30, 1576-1582. doi:10.1016/j.quascirev.2011.03.017

Hernandez-Molina, F.J., Llave, E., Preu, B., Ercilla, G., Fontan, A., Bruno, M., Serra, N., Gomiz, J.J., Brackenridge, R.E., Sierro, F.J., Stow, D.A. V., Garcia, M., Juan, C., Sandoval, N., Arnaiz, A., 2014a. Contourite processes associated with the Mediterranean Outflow Water after its exit from the Strait of Gibraltar: Global and conceptual implications. Geology 42, 227-230. doi:10.1130/G35083.1

Hernández-Molina, F.J., Llave, E., Stow, D.A.V., García, M., Somoza, L., Vázquez, J.T., Lobo, F.J., Maestro, A., Díaz del Río, V., León, R., Medialdea, T., Gardner, J., 2006. The contourite depositional system of the Gulf of Cádiz: A sedimentary model related to the bottom current activity of the Mediterranean outflow water and its interaction with the continental margin. Deep Sea Res. Part II Top. Stud. Oceanogr. 53, 1420-1463. doi:10.1016/j.dsr2.2006.04.016

Hernández-Molina, F.J., Sierro, F.J., Llave, E., Roque, C., Stow, D.A.V., Williams, T., Lofi, J., Van der Schee, M., Arnáiz, A., Ledesma, S., Rosales, C., Rodríguez-Tovar, F.J., Pardo-Igúzquiza, E., Brackenridge, R.E., 2015. Evolution of the gulf of Cadiz margin and southwest Portugal contourite depositional system: Tectonic, sedimentary and paleoceanographic implications from IODP expedition 339. Mar. Geol. doi:10.1016/j.margeo.2015.09.013

Hernández-Molina, F.J., Stow, D., Alvarez-Zarikian, C., Acton, G., Bahr, A., Balestra, B., Ducassou, E., Flood, R., Flores, J.A., Furota, S., Grunert, P., Hodell, D., Jimenez-Espejo, F., Kim, J.K., Krissek, L., Kuroda, J., Li, B., Llave, E., Lofi, J., Lourens, L., Miller, M., Nanayama, F., Nishida, N., Richter, C., Roque, C., Pereira, H., Goñi Fernanda Sanchez, M., Sierro, F.J., Singh, A.D., Sloss, C., Takashimizu, Y., Tzanova, A., Voelker, A., Williams, T., Xuan, C., 2013. IODP Expedition 339 in the Gulf of Cadiz and off West Iberia: Decoding the environmental significance of the Mediterranean outflow water and its global influence. Sci. Drill. 16, 1-11. doi:10.5194/sd-16-1-2013

Hernandez-Molina, F.J., Stow, D.A. V., Alvarez-Zarikian, C.A., Acton, G., Bahr, A., Balestra, B., Ducassou, E., Flood, R., Flores, J.-A., Furota, S., Grunert, P., Hodell, D., Jimenez-Espejo, F., Kim, J.K., Krissek, L., Kuroda, J., Li, B., Llave, E., Lofi, J., Lourens, L., Miller, M., Nanayama, F., Nishida, N., Richter, C., Roque, C., Pereira, H., Sanchez Goni, M.F., Sierro, F.J., Singh, A.D., Sloss, C., Takashimizu, Y., Tzanova, A., Voelker, A., Williams, T., Xuan, C., 2014. Onset of Mediterranean outflow into the North Atlantic. Science. 344, 1244-1250. doi:10.1126/science.1251306

Hodell, D., Crowhurst, S., Skinner, L., Tzedakis, P.C., Margari, V., Channell, J.E.T., Kamenov, G., Maclachlan, S., Rothwell, G., 2013. Response of Iberian Margin sediments to orbital and suborbital forcing over the past 420 ka: IBERIAN MARGIN PALEOCEANOGRAPHY. Paleoceanography 28, 185-199. doi:10.1002/palo.20017

Hodell, D.A., Evans, H.F., Channell, J.E.T., Curtis, J.H., 2010. Phase relationships of North Atlantic ice-rafted debris and surface-deep climate proxies during the last glacial period. Quat. Sci. Rev. 29, 3875-3886. doi:10.1016/j.quascirev.2010.09.006

Iorga, M.C., Lozier, M.S., 1999. Signatures of the Mediterranean outflow from a North Atlantic climatology: 1. Salinity and density fields. J. Geophys. Res. 104(C11), 25985-26009. doi:10.1029/1999JC900115

Jansen, J.H.., Van der Gaast, S.., Koster, B., Vaars, A.., 1998. CORTEX, a shipboard XRF-scanner for element analyses in split sediment cores. Mar. Geol. 151, 143-153. doi:10.1016/S0025-3227(98)00074-7

Kaboth, S., Bahr, A., Reichart, G.-J., Jacobs, B., Lourens, L.J., 2015. New insights into upper MOW variability over the last 150kyr from IODP 339 Site U1386 in the Gulf of Cadiz. Mar. Geol. doi:10.1016/j.margeo.2015.08.014

Khelifi, N., Sarnthein, M., Andersen, N., Blanz, T., Frank, M., Garbe-Schonberg, D., Haley, B.A., Stumpf, R., Weinelt, M., 2009. A major and long-term Pliocene intensification of the Mediterranean outflow, 3.5-3.3 Ma ago. Geology 37, 811-814. doi:10.1130/G30058A.1

Khélifi, N., Sarnthein, M., Frank, M., Andersen, N., Garbe-Schönberg, D., 2014. Late Pliocene variations of the Mediterranean outflow. Mar. Geol. 357, 182-194. doi:10.1016/j.margeo.2014.07.006

Köhler, P., Bintanja, R., Fischer, H., Joos, F., Knutti, R., Lohmann, G., Masson-Delmotte, V., 2010. What caused Earth's temperature variations during the last 800,000 years? Data-based evidence on radiative forcing and constraints on climate sensitivity. Quat. Sci. Rev. 29, 129-145. doi:10.1016/j.quascirev.2009.09.026

Konijnendijk, T.Y.M., Ziegler, M., Lourens, L.J., 2015. On the timing and forcing mechanisms of late Pleistocene glacial terminations: Insights from a new high-resolution benthic stable oxygen isotope record of the eastern Mediterranean. Quat. Sci. Rev. 129, 308-320. doi:10.1016/j.quascirev.2015.10.005

Kotthoff, U., Pross, J., Müller, U.C., Peyron, O., Schmiedl, G., Schulz, H., Bordon, A., 2008. Climate dynamics in the borderlands of the Aegean Sea during formation of sapropel S1 deduced from a marine pollen record. Quat. Sci. Rev. 27, 832-845. doi:10.1016/j.quascirev.2007.12.001

Laskar, J., Fienga, A., Gastineau, M., Manche, H., 2011. La2010: a new orbital solution for the long-term motion of the Earth. Astron. Astrophys. 532, A89. doi:10.1051/0004-6361/201116836

Lawrence, K.T., Herbert, T.D., Brown, C.M., Raymo, M.E., Haywood, A.M., 2009. High-amplitude variations in North Atlantic sea surface temperature during the early Pliocene warm period: VARIABLE PLIOCENE NORTH ATLANTIC SSTS. Paleoceanography 24, PA2218. doi:10.1029/2008PA001669

Lisiecki, L.E., Raymo, M.E., 2005. A Pliocene-Pleistocene stack of 57 globally distributed benthic $\delta^{18}O$ records. Paleoceanography 20, 1-17. doi:10.1029/2004PA001071

Llave, E., Hernández-Molina, F.J., Stow, D.A. V, Fernández-Puga, M.C., García, M., Vázquez, J.T., Maestro, A., Somoza, L., Díaz del Río, V., 2007. Reconstructions of the Mediterranean Outflow Water during the quaternary based on the study of changes in buried mounded drift stacking pattern in the Gulf of Cadiz. Mar. Geophys. Res. 28, 379-394. doi:10.1007/s11001-007-9040-7

Llave, E., Schönfeld, J., Hernández-Molina, F.J., Mulder, T., Somoza, L., Díaz Del Río, V., Sánchez-Almazo, I., 2006. High-resolution stratigraphy of the Mediterranean outflow contourite system in the Gulf of Cadiz during the late Pleistocene: The impact of Heinrich events. Mar. Geol. 227, 241-262. doi:10.1016/j.margeo.2005.11.015

Loubere, P., 1987. Changes in mid-depth North Atlantic and Mediterranean circulation during the Late Pliocene – Isotopic and sedimentological evidence. Mar. Geol. 77, 15-38. doi:10.1016/0025-3227(87)90081-8

Lourens, L.J., 2004. Revised tuning of Ocean Drilling Program Site 964 and KC01B (Mediterranean) and implications for the $\delta^{18}O$, tephra, calcareous nannofossil, and geomagnetic reversal chronologies of the past 1.1 Myr: PLEISTOCENE ASTRONOMICAL TIMESCALES. Paleoceanography 19, PA3010. doi:10.1029/2003PA000997

Lourens, L.J., 2008. On the Neogene-Quaternary debate. Episodes 31, 239-242.

Lourens, L.J., Antonarakou, A., Hilgen, F.J., Van Hoof, A.A.M., Vergnaud-Grazzini, C., Zachariasse, W.J., 1996a. Evaluation of the Plio-Pleistocene astronomical timescale. Paleoceanography 11, 391-413. doi:10.1029/96PA01125

Lourens, L.J., Hilgen, F.J., 1997. Long-periodic variations in the earth's obliquity and their relation to third-order eustatic cycles and late Neogene glaciations. Quat. Int. 40, 43-52. doi:10.1016/S1040-6182(96)00060-2

Lourens, L.J., Hilgen, F.J., Gudjonsson, L., Zachariasse, W.J., 1992. Late Pliocene to early Pleistocene astronomically forced sea surface productivity and temperature variations in the Mediterranean. Mar. Micropaleontol. 19, 49-78. doi:10.1016/0377-8398(92)90021-B

Lourens, L.J., Hilgen, F.J., Raffi, I., Vergnaud-Grazzini, C., 1996b. Early Pleistocene chronology of the Vrica Section (Calabria, Italy). Paleoceanography 11, 797-812. doi:10.1029/96PA02691

Luetscher, M., Boch, R., Sodemann, H., Spötl, C., Cheng, H., Edwards, R.L., Frisia, S., Hof, F., Müller, W., 2015. North Atlantic storm track changes during the Last Glacial Maximum recorded by Alpine speleothems. Nat. Commun. 6, 6344. doi:10.1038/ncomms7344

Maldonado, A., Nelson, C.H., 1999. Interaction of tectonic and depositional processes that control the evolution of the Iberian Gulf of Cadiz margin. Mar. Geol. 155, 217-242. doi:10.1016/S0025-3227(98)00148-0

Margari, V., Skinner, L.C., Hodell, D.A., Martrat, B., Toucanne, S., Grimalt, J.O., Gibbard, P.L., Lunkka, J.P., Tzedakis, P.C., 2014. Land-ocean changes on orbital and millennial time scales and the penultimate glaciation. Geology 42, 183-186. doi:10.1130/G35070.1

Martrat, B., Grimalt, J.O., Shackleton, N.J., de Abreu, L., Hutterli, M.A., Stocker, T.F., 2007. Four climate cycles of recurring deep and surface water destabilizations on the Iberian margin. Science 317, 502-507. doi:10.1126/science.1139994

McCann, T., 2007. The Geology of Central Europe Volume 2, Mesozoic and Cenozoic. Geological Society of London.

Meijer, P.T., Tuenter, E., 2007. The effect of precession-induced changes in the Mediterranean freshwater budget on circulation at shallow and intermediate depth. J. Mar. Syst. 68, 349-365. doi:10.1016/j.jmarsys.2007.01.006

Meyers, S.R., 2014. astrochron: An R Package for Astrochronology.

Millot, C., 2009. Another description of the Mediterranean Sea outflow. Prog. Oceanogr. 82, 101-124. doi:10.1016/j.pocean.2009.04.016

Millot, C., 2014. Heterogeneities of in- and out-flows in the Mediterranean Sea. Prog. Oceanogr. 120, 254-278. doi:10.1016/j.pocean.2013.09.007

Millot, C., Candela, J., Fuda, J.-L., Tber, Y., 2006. Large warming and salinification of the Mediterranean outflow due to changes in its composition. Deep Sea Res. Part I Oceanogr. Res. Pap. 53, 656-666. doi:10.1016/j.dsr.2005.12.017

Moreno, A., 2002. Saharan Dust Transport and High-Latitude Glacial Climatic Variability: The Alboran Sea Record. Quat. Res. 58, 318-328. doi:10.1006/qres.2002.2383

Morley, A., Rosenthal, Y., deMenocal, P., 2014. Ocean-atmosphere climate shift during the mid-to-late Holocene transition. Earth Planet. Sci. Lett. 388, 18-26. doi:10.1016/j.epsl.2013.11.039

Mulder, T., Lecroart, P., Hanquiez, V., Marches, E., Gonthier, E., Guedes, J.-C., Thiébot, E., Jaaidi, B., Kenyon, N., Voisset, M., Perez, C., Sayago, M., Fuchey, Y., Bujan, S., 2006. The western part of the Gulf of Cadiz: contour currents and turbidity currents interactions. Geo-Marine Lett. 26, 31-41. doi:10.1007/s00367-005-0013-z

Myers, P.G., 2002. Flux-forced simulations of the paleocirculation of the Mediterranean. Paleoceanography. 17(1). doi:10.1029/2000PA000613

Myers, P.G., Haines, K., Rohling, E.J., 1998. Modeling the paleocirculation of the Mediterranean: The Last Glacial Maximum and the Holocene with emphasis on the formation of sapropel S_1. Paleoceanography 13, 586-606. doi:10.1029/98PA02736

Nelson, C., Baraza, J., Maldonado, A., 1993. Mediterranean undercurrent sandy contourites, Gulf of Cadiz, Spain. Sediment. Geol. 82, 103-131. doi:10.1016/0037-0738(93)90116-M

Nelson, C.H., Baraza, J., Maldonado, A., Rodero, J., Escutia, C., Barber, J.H., 1999. Influence of the Atlantic inflow and Mediterranean outflow currents on Late Quaternary sedimentary facies of the Gulf of Cadiz continental margin. Mar. Geol. 155, 99-129. doi:10.1016/S0025-3227(98)00143-1

Peliz, Á., Dubert, J., Santos, A.M.P., Oliveira, P.B., Le Cann, B., 2005. Winter upper ocean circulation in the Western Iberian Basin – Fronts, Eddies and Poleward Flows: an overview. Deep Sea Res. Part I Oceanogr. Res. Pap. 52, 621-646. doi:10.1016/j.dsr.2004.11.005

Peliz, A., Marchesiello, P., Santos, A.M.P., Dubert, J., Teles-Machado, A., Marta-Almeida, M., Le Cann, B., 2009. Surface circulation in the Gulf of Cadiz: 2. Inflow-outflow coupling and the Gulf of Cadiz slope current. J. Geophys. Res. 114. doi:10.1029/2008JC004771

Potter, R.A., Lozier, M.S., 2004. On the warming and salinification of the Mediterranean outflow waters in the North Atlantic. Geophys. Res. Lett. 31. doi:10.1029/2003GL018161

Rahim, K.J., Burr, W., Thomson, D.J., 2014. Applications of Multitaper Spectral Analysis to Nonstationary Data – Appendix A.

Rahmstorf, S., 2002. Ocean circulation and climate during the past 120,000 years. Nature 419, 207-214. doi:10.1038/nature01090

Rahmstorf, S., Box, J.E., Feulner, G., Mann, M.E., Robinson, A., Rutherford, S., Schaffernicht, E.J., 2015. Exceptional twentieth-century slowdown in Atlantic Ocean overturning circulation. Nat. Clim. Chang. 5, 475-480. doi:10.1038/nclimate2554

Raymo, M.E., Hodell, D., Jansen, E., 1992. Response of deep ocean circulation to initiation of northern hemisphere glaciation (3-2 MA). Paleoceanography 7, 645-672. doi:10.1029/92PA01609

Revel, M., Ducassou, E., Grousset, F.E., Bernasconi, S.M., Migeon, S., Revillon, S., Mascle, J., Murat, A., Zaragosi, S., Bosch, D., 2010. 100,000 Years of African monsoon variability recorded in sediments of the Nile margin. Quat. Sci. Rev. 29, 1342-1362. doi:10.1016/j.quascirev.2010.02.006

Richter, T.O., van der Gaast, S., Koster, B., Vaars, A., Gieles, R., de Stigter, H.C., De Haas, H., van Weering, T.C.E., 2006. The Avaatech XRF Core Scanner: technical description and applications to NE Atlantic sediments. Geol. Soc. London, Spec. Publ. 267, 39-50. doi:10.1144/GSL.SP.2006.267.01.03

Rogerson, M., Rohling, E.J., Bigg, G.R., Ramirez, J., 2012. Paleoceanography of the Atlantic-Mediterranean exchange: Overview and first quantitative assessment of climatic forcing. Rev. Geophys. 50, RG2003. doi:10.1029/2011RG000376

Rogerson, M., Rohling, E.J., Weaver, P.P.E., 2006. Promotion of meridional overturning by Mediterranean-derived salt during the last deglaciation: PROMOTION OF MERIDIONAL OVERTURNING. Paleoceanography 21, PA4101. doi:10.1029/2006PA001306

Rogerson, M., Rohling, E.J., Weaver, P.P.E., Murray, J.W., 2004. The Azores Front since the Last Glacial Maximum. Earth Planet. Sci. Lett. 222, 779-789. doi:10.1016/j.epsl.2004.03.039

Rogerson, M., Rohling, E.J., Weaver, P.P.E., Murray, J.W., 2005. Glacial to interglacial changes in the settling depth of the Mediterranean Outflow plume: CHANGES IN THE MEDITERRANEAN OUTFLOW. Paleoceanography 20, 1-12. doi:10.1029/2004PA001106

Rohling, E.J., Grant, K., Bolshaw, M., Roberts, A.P., Siddall, M., Hemleben, C., Kucera, M., 2009. Antarctic temperature and global sea level closely coupled over the past five glacial cycles. Nat. Geosci. 2, 500-504. doi:10.1038/ngeo557

Rohling, E.J., Marino, G., Grant, K.M., 2015. Mediterranean climate and oceanography, and the periodic development of anoxic events (sapropels). Earth-Science Rev. 143, 62-97. doi:10.1016/j.earscirev.2015.01.008

Roskosch, J., Winsemann, J., Polom, U., Brandes, C., Tsukamoto, S., Weitkamp, A., Bartholomäus, W.A., Henningsen, D., Frechen, M., 2015. Luminescence dating of ice-marginal deposits in northern Germany: evidence for repeated glaciations during the Middle Pleistocene (MIS 12 to MIS 6): Luminescence dating of ice-marginal deposits, N Germany. Boreas 44, 103-126. doi:10.1111/bor.12083

Rossignol-Strick, M., 1983. African monsoons, an immediate climate response to orbital insolation. Nature 304, 46-49. doi:10.1038/304046a0

Rossignol-Strick, M., 1985. Mediterranean Quaternary sapropels, an immediate response of the African monsoon to variation of insolation. Palaeogeogr. Palaeoclimatol. Palaeoecol. 49, 237-263. doi:10.1016/0031-0182(85)90056-2

Rutherford, S., D'Hondt, S., 2000. Early onset and tropical forcing of 100,000-year Pleistocene glacial cycles. Nature 408, 72-75. doi:10.1038/35040533

Sánchez Goñi, M.F., Bard, E., Landais, A., Rossignol, L., d'Errico, F., 2013. Air – sea temperature decoupling in western Europe during the last interglacial – glacial transition. Nat. Geosci. 6, 837-841. doi:10.1038/ngeo1924

Sanchez Goñi, M.F., Harrison, S.P., 2010. Millennial-scale climate variability and vegetation changes during the Last Glacial: Concepts and terminology. Quat. Sci. Rev. 29, 2823-2827. doi:10.1016/j.quascirev.2009.11.014

Sankey, T., 1973. The formation of deep water in the northwestern Mediterranean,. Prog. Oceanogr. 6, 159-179.

Schmidt, M.W., Vautravers, M.J., Spero, H.J., 2006. Rapid subtropical North Atlantic salinity oscillations across Dansgaard-Oeschger cycles. Nature 443, 561-564. doi:10.1038/nature05121

Schmitz, W.J., McCartney, M.S., 1993. On the North Atlantic Circulation. Rev. Geophys. 31, 29. doi:10.1029/92RG02583

Schönfeld, J., 1997. The impact of the Mediterranean Outflow Water (MOW) on benthic foraminiferal assemblages and surface sediments at the southern Portuguese continental margin. Mar. Micropaleontol. 29, 211-236. doi:10.1016/S0377-8398(96)00050-3

Schönfeld, J., 2002a. A new benthic foraminiferal proxy for near-bottom current velocities in the Gulf of Cadiz, northeastern Atlantic Ocean. Deep. Res. Part I Oceanogr. Res. Pap. 49, 1853-1875. doi:10.1016/S0967-0637(02)00088-2

Schönfeld, J., 2002b. Recent benthic foraminiferal assemblages in deep high-energy environments from the Gulf of Cadiz (Spain). Mar. Micropaleontol. 44, 141-162. doi:10.1016/S0377-8398(01)00039-1

Schönfeld, J., Zahn, R., 2000. Late Glacial to Holocene history of the Mediterranean outflow. Evidence from benthic foraminiferal assemblages and stable isotopes at the Portuguese margin. Palaeogeogr. Palaeoclimatol. Palaeoecol. 159, 85-111. doi:10.1016/S0031-0182(00)00035-3

Schulz, M., Mudelsee, M., 2002. REDFIT: estimatingred-noise spectra directly from unevenly spaced paleoclimatic time series. Comput. Geosci. 28, 421-426.

Seierstad, I.K., Abbott, P.M., Bigler, M., Blunier, T., Bourne, A.J., Brook, E., Buchardt, S.L., Buizert, C., Clausen, H.B., Cook, E., Dahl-Jensen, D., Davies, S.M., Guillevic, M., Johnsen, S.J., Pedersen, D.S., Popp, T.J., Rasmussen, S.O., Severinghaus, J.P., Svensson, A., Vinther, B.M., 2014. Consistently dated records from the Greenland GRIP, GISP2 and NGRIP ice cores for the past 104 ka reveal regional millennial-scale δ18O gradients with possible Heinrich event imprint. Quat. Sci. Rev. 106, 29-46. doi:10.1016/j.quascirev.2014.10.032

Shackleton N.J., Cita M.B., 1979. 12. Oxygen and Carbon Isotope Stratigraphy of Benthic Foraminifers at Site 397: Detailed History of Climatic Change during the Late Neogene, in: Initial Reports of the Deep Sea Drilling Project 47, 433-445 U.S. Government Printing Office.

Shackleton, N.J., Hall, M.A., 1984. Oxygen and carbon isotope stratigraphy of the deep sea drilling project hole 552A: Plio-Pleistocene glacial history. Initial Reports DSDP 81, 599-609.

Siddall, M., 2004. Understanding the Red Sea response to sea level. Earth Planet. Sci. Lett. 225, 421-434. doi:10.1016/j.epsl.2004.06.008

Siddall, M., Rohling, E.J., Almogi-Labin, A., Hemleben, C., Meischner, D., Schmelzer, I., Smeed, D.A., 2003. Sea-level fluctuations during the last glacial cycle. Nature 423, 853-858. doi:10.1038/nature01690

Sierro, F.J., Flores, J.A., Baraza, J., 1999. Late glacial to recent paleoenvironmental changes in the Gulf of Cadiz and formation of sandy contourite layers. Mar. Geol. 155, 157-172. doi:10.1016/S0025-3227(98)00145-5

Stevenson, R.E., 1977. Huelva Front and Malaga, Spain, eddy chain as defined by satellite and oceanographic data. Dtsch. Hydrogr. Zeitschrift 30, 51-53. doi:10.1007/BF02226082

Stow, D.A. V., Faugeres, J.-C., Gonthier, E., Cremer, M., Llave, E., Hernandez-Molina, F.J., Somoza, L., Diaz-Del-Rio, V., 2002. Faro-Albufeira drift complex, northern Gulf of Cadiz. Geol. Soc. London, Mem. 22, 137-154. doi:10.1144/GSL.MEM.2002.022.01.11

Stow, D.A. V., Hernández-Molina, F.J., Alvarez-Zarikian, C., 2013. Expedition 339 Summary. Exped. 339 Summ. Proceedings of the Integrated Ocean Drilling Program. doi:10.2204/iodp.proc.339.104.2013

Thomson, D.J., 1982. Spectrum estimation and harmonic analysis. Proc. IEEE 70, 1055-1096. doi:10.1109/PROC.1982.12433

Thorpe, S.A., 1976. Variability of the mediterranean undercurrent in the Gulf of Cadiz. Deep Sea Res. Oceanogr. Abstr. 23, 711-IN1. doi:10.1016/S0011-7471(76)80016-2

Tjallingii, R., Claussen, M., Stuut, J.-B.W., Fohlmeister, J., Jahn, A., Bickert, T., Lamy, F., Röhl, U., 2008. Coherent high- and low-latitude control of the northwest African hydrological balance. Nat. Geosci. 1, 670-675. doi:10.1038/ngeo289

Toucanne, S., Jouet, G., Ducassou, E., Bassetti, M.-A., Dennielou, B., Angue Minto'o, C.M., Lahmi, M., Touyet, N., Charlier, K., Lericolais, G., Mulder, T., 2012. A 130,000-year record of Levantine Intermediate Water flow variability in the Corsica Trough, western Mediterranean Sea. Quat. Sci. Rev. 33, 55-73. doi:10.1016/j.quascirev.2011.11.020

Toucanne, S., Mulder, T., Schönfeld, J., Hanquiez, V., Gonthier, E., Duprat, J., Cremer, M., Zaragosi, S., 2007. Contourites of the Gulf of Cadiz: A high-resolution record of the paleocirculation of the Mediterranean outflow water during the last 50,000 years. Palaeogeogr. Palaeoclimatol. Palaeoecol. 246, 354-366. doi:10.1016/j.palaeo.2006.10.007

Toucanne, S., Zaragosi, S., Bourillet, J.F., Cremer, M., Eynaud, F., Van Vliet-Lanoë, B., Penaud, A., Fontanier, C., Turon, J.L., Cortijo, E., 2009. Timing of massive "Fleuve Manche" discharges over the last 350kyr: insights into the European ice-sheet oscillations and the European drainage network from MIS 10 to 2. Quat. Sci. Rev. 28, 1238-1256. doi:10.1016/j.quascirev.2009.01.006

Voelker, A., Lebreiro, S., Schonfeld, J., Cacho, I., Erlenkeuser, H., Abrantes, F., 2006. Mediterranean outflow strengthening during northern hemisphere coolings: A salt source for the glacial Atlantic? Earth Planet. Sci. Lett. 245, 39-55. doi:10.1016/j.epsl.2006.03.014

Voelker, A.H.L., Colman, A., Olack, G., Waniek, J.J., Hodell, D., 2015. Oxygen and hydrogen isotope signatures of Northeast Atlantic water masses. Deep Sea Res. Part II Top. Stud. Oceanogr. 116, 89-106. doi:10.1016/j.dsr2.2014.11.006

Voelker, A.H.L., de Abreu, L., 2011. A Review of Abrupt Climate Change Events in the Northeastern Atlantic Ocean (Iberian Margin): Latitudinal, Longitudinal, and Vertical Gradients, in: Rashid, H., Polyak, L., Mosley-Thompson, E. (Eds.),. American Geophysical Union, Washington, D. C., pp. 15-37.

Voelker, A.H.L., de Abreu, L., Schönfeld, J., Erlenkeuser, H., Abrantes, F., 2009. Hydrographic conditions along the western Iberian margin during marine isotope stage 2: IBERIAN MARGIN HYDROGRAPHY DURING MIS 2. Geochemistry, Geophys. Geosystems 10. doi:10.1029/2009GC002605

Wang, Y., Cheng, H., Edwards, R.L., Kong, X., Shao, X., Chen, S., Wu, J., Jiang, X., Wang, X., An, Z., 2008. Millennial- and orbital-scale changes in the East Asian monsoon over the past 224,000 years. Nature 451, 1090-1093. doi:10.1038/nature06692

Weaver, P.P.E, Clement, B.M., 1987. Magnetobiostratigraphy of planktonic foraminiferal datums: Deep Sea Drilling Project Leg 94, North Atlantic, in: Initial Reports of the Deep Sea Drilling Project 94, 815-829. U.S. Government Printing Office. doi: 10.2973/dsdp.proc.84.120.1987

Weldeab, S., Lea, D.W., Schneider, R.R., Andersen, N., 2007. 155,000 Years of West African Monsoon and Ocean Thermal Evolution. Science (80-.). 316, 1303-1307. doi:10.1126/science.1140461

Yamamoto, M., Sai, H., Chen, M.-T., Zhao, M., 2013. The East Asian winter monsoon variability in response to precession during the past 150 000 yr. Clim. Past 9, 2777-2788. doi:10.5194/cp-9-2777-2013

Yin, Q.Z., Berger, A., Crucifix, M., 2009. Individual and combined effects of ice sheets and precession on MIS-13 climate. Clim. Past 5, 229-243. doi:10.5194/cp-5-229-2009

Zachariasse, W.J., Gudjonsson, L., Hilgen, F.J., Langereis, C.G., Lourens, L.J., Verhallen, P.J.J.M., Zijderveld, J.D.A., 1990. Late Gauss to Early Matuyama invasions of Neogloboquadrina Atlantica in the Mediterranean and associated record of climatic change. Paleoceanography 5, 239-252. doi:10.1029/PA005i002p00239

Zahn, R., Sarnthein, M., Erlenkeuser, H., 1987. Benthic isotope evidence for changes of the Mediterranean outflow during the Late Quaternary. Paleoceanography 2, 543-559. doi:10.1029/PA002i006p00543

Ziegler, M., Lourens, L.J., Tuenter, E., Hilgen, F., Reichart, G.-J., Weber, N., 2010. Precession phasing offset between Indian summer monsoon and Arabian Sea productivity linked to changes in Atlantic overturning circulation. Paleoceanography 25, PA3213. doi:10.1029/2009PA001884

Ontrafelen van de paleoceanografische en paleoklimatologische veranderingen in de Golf van Cádiz in de laatste 2.6 miljoen jaar

Samenvatting in het Nederlands

Het doel van dit proefschrift is om nieuwe inzichten te verschaffen over de klimaat-gestuurde evolutie van de Mediterrane Uitstroom Water (het water dat vanuit de Middellandse Zee richting de Atlantische Oceaan stroomt; "Mediterranean Outflow Water" afgekort: MOW) tijdens het Pleistoceen tijdperk, dat de laatste ~2.6 miljoen jaar omvat. Een belangrijk kenmerk van de evolutie van het klimaat van het noordelijk halfrond tijdens de geologische geschiedenis is intensiteit van de Noord-Atlantische Diepwaterpomp die zorgt voor de noordwaartse verplaatsing van warmte via de Golfstroom. De intensiteit van de Diepwaterpomp is direct gekoppeld aan variaties in het zoutgehalte van de Noord Atlantische Oceaan, dat weer wordt gestuurd door het warme en zeer zoute water van de Middellandse Zee dat de Noord Atlantische Oceaan binnenstroomt via de smalle en ondiepe Straat van Gibraltar. Ondanks de potentiele wereldwijde significantie wordt variatie in de MOW, gedreven door verschillende achterliggende klimaat condities, tot nu toe nog slecht begrepen. Tijdens de laatste paar decennia is de sterkte van de Noord-Atlantische diepwaterpomp substantieel afgenomen door een toename aan zoetwater transport vanuit de Arctische Oceaan en vanaf Groenland, aangestuurd door antropogene klimaat verandering. Daardoor wordt kennis over de werking van de MOW nog belangrijker gezien de kritische rol dat deze water massa speelt in dit proces.

De formatie van de MOW wordt gedreven door de warme en droge condities van de oostelijke Middellandse Zee, wat zorgt voor een hoog zout gehalte in het oppervlakte water. Tijdens de winter koelt dit water af en zinkt het hierdoor naar een grotere diepte en vervolgens naar het westen, richting de Straat van Gibraltar. Naast de intermediaire water massa's van de oostelijke Middellandse Zee bestaat de MOW ook uit veranderende delen van het diepwater van de westelijke Middellandse Zee. Wanneer de MOW de Straat van Gibraltar verlaat, stort het naar beneden volgens de morfologie van de zeebodem richting de bovenste en middelste hellingen van de Golf van Cadiz, waarbij het richting het noordwesten de Noord-Atlantische waterkolom op intermediaire diepte penetreert. Door de directe interactie van het MOW water met een hoge dichtheid en het sediment langs de continentale helling van de Golf van Cadiz worden hier uiteindelijk de klimaat gestuurde variaties van de MOW opgeslagen in het sediment.

Om het effect van het klimaat op de variabiliteit van de MOW op geologische tijdschalen goed te begrijpen, werd er in dit proefschrift gefocust op sediment kernen die werden geboord op twee locaties (U1386 en U1389) langs de bovenste en middelste hellingen van de Golf van Cadiz tijdens Ocean Discovery-Program (IODP) expeditie 339. Het onderzoek concentreerde zich op geochemische (bijv. stabiele zuurstof en koolstof isotopen metingen van planktische en benthische foraminiferen, Mg/Ca paleothermometrie) en sedimentologische (bijv. x-ray fluorescentie metingen van de elementsamestelling van de sedimenten, korrelgrote analyse) methoden. Deze resultaten werden besproken in de context van de invloed van korte en lange klimaat variabiliteit op het gedrag van de MOW (bijv. Milankovitch cyclussen, Heinrich Events), de relatie tussen de MOW en de klimaat gestuurde variabiliteit van het oorsprong gebied (bijv. sapropel formatie) evenals

de reactie van de MOW op de forcering van hoge-breedtegraden (bijv. ijs volume en daardoor zeespiegel variatie) en lage-breedtegraden (bijv. moesson).

De bevindingen in dit proefschrift laten zien dat er tijdens het late Pleistoceen en het Holoceen (de laatste 600.000 jaar) drie uitgesproken fases van MOW compositie en stoomsnelheid veranderingen zijn geweest langs de bovenste helling van de Golf van Cadiz (Hoofdstuk 2 tot en met 4). Aan de ene kant worden deze veranderingen geassocieerd met de dichtheid toename van de MOW tijdens ijstijden, gedreven door het ondieper worden van de Straat van Gibraltar en het daardoor zouter worden van de Middellandse Zee. Aan de andere kant kunnen de geobserveerde veranderingen ook gekoppeld worden aan de verschillen in de oorsprong van de MOW, bijvoorbeeld door grotere contributies van het Middellandse Zee diepwater met een hogere dichtheid en door een potentiele tektonische modulatie van de MOW stromingsrichting binnen de Golf van Cadiz. Bovendien laten de resultaten een inverse relatie zien tussen de MOW en de instroom van zoetwater in de oostelijke Middellandse Zee gedreven door moessons, wat tegelijkertijd weer wordt geforceerd door de precessie van de rotatie as van de aarde (met tijdschalen van ~23.000 jaar; vooral beschreven in hoofdstuk 3). Een sterkere Oost Afrikaanse Moesson kan leiden tot een sterkere afvoer van de Nijl dat het ontstaan van de MOW belemmert.

De resultaten laten ook zien dat kenmerkende pieken in de stabiele zuurstof isotoop curves in het tijdsinterval tussen 150.000 en 300.000 jaar geleden samen vallen met periodes van grootschalige ijskap-uitbreidingen in continentaal Europa (Drenthe en Fuhne). Ook komen ze net vooraf aan de “afkoel gebeurtenissen” langs de Iberische Marge, die gelinkt worden aan smeltwater pulsen vanuit Europa.

Tenslotte suggereren de resultaten in dit proefschrift dat er tijdens het vroege Pleistoceen al sprake was van afvloei water afkomstig uit de Middellandse Zee en dat het toen voornamelijk zijn oorsprong vond in de intermediaire water massa’s van de oostelijke Middellandse Zee, vergelijkbaar met de huidige situatie (Hoofdstuk 6). De gedocumenteerde toename van de MOW in de Golf van Cadiz tijdens het Vroege Pleistoceen is mogelijk gerelateerd aan het sterker worden van de Noord Atlantische Diepwaterpomp dat op het zelfde moment plaatsvond.

Die Entschlüsselung der paläozeanographischen und paläoklimatologischen Veränderungen im Golf von Cádiz der vergangenen 2,6 Millionen Jahre

Zusammenfassung in deutscher Sprache

Die vorliegende Arbeit untersucht die klimaabhängige Dynamik des Mittelmeerausstroms im Verlauf des Pleistozäns (die letzten 2,6 Millionen Jahre). Ein entscheidender Faktor für die Ausprägung der klimatischen Bedingungen der Nordhemisphäre sowohl der geologischen Vergangenheit als auch der Gegenwart ist in der Intensität der Umwälzungszirkulation des Atlantischen Ozeans zu finden und den daran gekoppelten, nordwärts gerichteten Wärmetransport durch den Golfstrom. Die Intensität dieses „ozeanischen Wärmefließbands" hängt dabei im besonderen Maße vom Salzhaushalt des Atlantischen Ozeans ab. In diesem Zusammenhang kommt den salzreichen und relativ warmen Wassermassen des Mittelmeersaustroms, die durch die Straße von Gibraltar in den angrenzenden Nord Atlantik fließen und dessen Salzhaushalt modulieren, eine besondere Rolle zu und macht die Untersuchung der Entwicklung des Mittelmeerausstroms während unterschiedlicher Klimabedingungen der geologischen Vergangenheit unerlässlich. Dies gilt besonders im Hinblick auf die prognostizierte Abschwächung des Golfstroms durch die verstärkte Zufuhr von Schmelzwasser aus der Arktis und aus Grönland als Konsequenz der anthropogenen Klimaerwärmung.

Angetrieben wird der Mittelmeerausstrom vorwiegend durch die trockenen und heißen Bedingungen im östlichen Mittelmeer, die einen hohen Salzgehalt im Oberflächenwasser hervorrufen. Im Winter kühlen diese Wassermassen ab, werden dichter und fließen in größerer Tiefe Richtung Westen, wo sie das Mittelmeer ganzjährig durch die schmale und flache Straße von Gibraltar verlassen. Neben den intermediären Wassermassen des östlichen Mittelmeeres trägt auch Tiefenwasser, das im westlichen Mittelmeer gebildet wird, zum Ausstrom bei. Nach dem Verlassen der Straße von Gibraltar sinkt der salzreiche und damit dichte Mittelmeerausstrom ab und folgt der Meeresbodentopografie entlang des oberen und mittleren Kontinentalhangs im Golf von Càdiz, während er weiter nach Norden vorstößt und sich, in der Folge, in mittlerer Tiefe innerhalb des Nordatlantiks einschichtet. Durch die Interaktionen des relativ dichten Mittelmeerausflusses mit den abgelagerten Sedimenten entlang des Kontinentalhangs sind die klimatisch bedingten Veränderungen seiner Dynamik schlussendlich "archiviert" worden.

Um die Dynamik des Mittelmeerausstroms besser verstehen zu können, wurden im Rahmen dieser Arbeit Bohrkerne von zwei Lokationen entlang des oberen (U1386) und mittleren (U1389) Kontinentalhangs im Golf von Càdiz untersucht, die im Rahmen des International Ocean Discovery-Programms (IODP) während Expedition 339 auf dem Schelfhang vor Südspanien und Portugal gewonnen wurden. Dabei lag der Schwerpunkt auf geochemischen (z.B. stabile Sauerstoff- und Kohlenstoffisotopenmessungen an planktischen und benthischen Foraminiferen sowie Mg/Ca Paläothermometrie) und sedimentologischen (z.B. Röntgenflouressenzmessungen der elementaren Zusammensetzung der Sedimente, Korngrößenbestimmung) Untersuchungsmethoden. Die Ergebnisse wurden im Zusammenhang des Mittelmeerausstroms zu kurz- und langfristigen

Klimavariabilität (z.B. Milankovitć-Zyklen, Heinrich Events), seiner Abhängigkeit zu hydrografischen Veränderungen im Mittelmeer (z.B. Sapropelentwicklung) und den klimatischen Einfluss der Hohen Breiten (z.B. Eisvolumen und daran gekoppelte Meeresspiegelschwankungen) und der niedrigen Breiten (z.B. Monsun) diskutiert.

Die Resultate dieser Arbeit zeigen, vor dem Hintergrund der klimatischen Entwicklungen im Spätpleistozän und Holozän (die letzten 600.000 Jahre), drei ausgeprägte Variabilitäsphasen der Wassermassenzusammensetzung und der Fließgeschwindigkeit des Mittelmeerausstroms entlang des oberen Kontinentalhangs im Golf von Càdiz (Kapitel 2 bis 4). Angetrieben werden diese Veränderungen zum einen durch die glaziale Dichtezunahme des Mittelmeerausflusses forciert durch die glaziale Meeresspiegelabsenkung, die die Zirkulation zwischen dem Nord Atlantik und dem Mittelmeer stark begrenzt, was wiederum zu einer Salzerhöhung dieses Binnenmeeres führt, und zum anderen in einer Veränderung der Wassermassenzusammensetzung des Mittelmeerausstroms durch einen größeren Zufluss an dichterem, im westlichen Teil des Mittelmeeres gebildetem, Tiefenwasser oder tektonisch verursachten Modifikationen des Strömungsbereiches des Ausstroms im Golf von Càdiz. Darüber hinaus ist ebenfalls festzustellen, dass die Glazial-Interglazial forcierten Variationen des Mittelmeerausstroms überlagert werden durch die Beziehung zwischen Änderungen der Präzession der Erdrotationsachse (die Kreiselbewegung der Erdachse) und dem Frischwasserbudget des Mittelmeeres (speziell Kapitel 3).

Die Ergebnisse zeigen eine ausgeprägte inverse Korrelationen zwischen der Stärke des Ausstroms und der Intensität des afrikanischen Monsuns auf Präzessionszeitskalen (~23.000 Jahre). Hierbei führt starker Monsun-Niederschlag in Nordostafrika zu einem erhöhten Frischwassereinstrom ins östliche Mittelmeer über den Nil, welcher die Bildung des Mittelmeerausstroms abschwächt.

Des Weiteren deuten die Resultate daraufhin, dass die mit-glaziale Anreicherung stabiler sauerstoffisotopen im Zeitintervall zwischen 150.00 bis 300.000 Jahren im direktem Zusammenhang stehen mit den Eisschildvorstößen der Drenthe und Fuhne Kaltzeiten und den Schmelzwasserabfluss des „Flueve Manche“ entlang der Iberischen Küstenlinie (Kapitel 5).

Abschließend zeigt sich, dass der Mittelmeerausstrom bereits im Frühpleistozän (1,7 bis 2,6 Millionen Jahre) entlang des mittleren Kontinentalhangs aktiv war und sich dominant aus intermediären Wassermassen des östlichen Mittelmeeres zusammensetze ähnlich gegenwärtigen Bedingungen. Die dokumentierte Intensivierung des Mittelmeerausstroms während des Frühpleistozäns steht potenziell in Verbindung mit der Verstärkung der Nord Atlantischen Umwälzungszirkulation im selben Zeitraum (Kapitel 6).

Acknowledgements

".... und am Ende der dunklen Gasse erstrahlt die gelbe Wand."

(aus dem Liedtext "Wir sind alle am Borsigplatz geboren", Liedautor unbekannt)

There are many people near and far I would very much like to thank for their unwavering support, encouragement, believe, trust, friendship, motivational speeches, kick-in-the-butt when needed and more importantly a huge amount of joyful hours during the past four years without this thesis would have never come to pass.

First off I would like to thank my supervisor/promotor and co-author Luc for giving me this great opportunity 4 years ago. I never understood whether my fierce presentation of Arctic forams or the lunch hour after my interview which I spent solely discussing football was what convinced you to give me this job but I am sure glad you did. I want to thank you for your passions, for being there when the shit-hit-the-fan, for the freedom to follow my own ideas and your support for letting me go wherever I wanted to go - not everyone would have done so - thus I am truly grateful you did. I will keep fond memories of my years working with you, the hangover day in Seville, the cactus "incident" and the bike ride through San Francisco come to mind.

Tanja, there are not enough words in the English, Dutch or German language to describe how eternally grateful I am for your support throughout the last 4 years. Without you I would have gone mad half way through this! Danke für alles!!

I would also like to thank my committee members for taking the time to assess my thesis: Antje Voelker, Frederike Wagner-Cremer, David Hodell, Franciesco Sierro, Gert-Jan Reichert and Andrè Bahr.

At Utrecht University, I would like to thank all my colleagues from Strat&Pal who have supported me throughout my PhD with their friendship, scientific discussions, laughter and it-will-be-fine speeches: Cindy, Joyce, Tiuri, Vittoria, Helen, Antonio, Martin, Margreet, Wilma, Marjolein and Hemmo. Thank you Maria for being a wonderful office mate. Frits, thank you for making me hate running more than I already did before and all your help with my thesis! Christian, vielen lieben Dank für all die wissenschaftlichen Gespräche, emotionalen Aufmunterungen und gemeinsame Stunden in Wien. Furthermore, I would like to give thanks to people from various other working groups of UU: Andrew, I am sure going to miss your dark British humor; Dirk, du und dein positives Lebensbild waren mir stets ein Quell der Inspiration; Derya, Anne-Christine and Suzanne.

I would like to thank Dominika and Arnold for all the technical support at UU with the organization, supplies, washing and isotope measurements! Thanks also go to Rineke Giles at the NIOZ and John Nicolson at Cambridge University for analytical support with the XRF and Mg/Ca measurements.

In these 4 years I have also met some wonderful people outside of science in Utrecht who supported and encouraged me to get this PhD done. In particular I would like to thank Maartje, you are a truly wonderful person and I feel blessed to call you my friend. Sebastian and Dave, thanks so much for all the climbing throughout the years which sometimes seemed the only way to take my mind of things. I will miss you guys!

Also abroad there are a huge amount of people from the two Urbino Summer Schools and the two Arctic Expeditions onboard the FS "Heinke" and "Polarstern" that I participated in that which I would like to thank for their support and friendship.

Kirstin, it all started with you and a bottle of wine on a fateful Friday evening in March 2012 when you helped me to write my application letter for Utrecht. Since then you always have been there when I needed you the most and I would like to thank you so much for it!

Zu guter Letzt möchte ich noch meiner Familie und meinen Freunden danken, die mich bereits seit Jahrzehnten begleiten und ohne die diese Arbeit kaum möglich gewesen wäre. Ich danke euch für all die emotionale Unterstützung, aufbauenden Worte, Fußspiele, Urlaube, Postkarten, Besuche, Feiern, endlosen Skypegespäche und WhatsAppnachrichten, die stets dafür gesorgt haben, dass ich egal, wo ich bin, mich nie alleine fühle.

Katrin, Nadja und Annett, ihr verrückten Hühner, danke dass ihr Teil meines Lebens seid!
Mama und Papa, ich habe es geschafft!

Curriculum vitae

Stefanie Kaboth was born March 14th 1985 in Mühlhausen/Thüringen in Germany. She finished her secondary education (Abitur) at the Albert-Schweitzer-Gymnasium in Mühlhausen where she graduated in summer 2003. From 2003 to 2004 she conducted a Freiwilliges Ökologisches Jahr (Voluntary Ecological Year) working at the Kali-Umwelttechnik Sonderhausen in Germany in the division for Geoökologie (Geoecology). She started studying Geoecology at the Technische Universität Bergakademie Freiberg in Germany in October 2004 specialising in hydrology, meteorology & climatology and environmental engineering. Her Diplomarbeit (MSc thesis) was in collaboration with the Alfred-Wegener-Institute for Marine and Polar Research (AWI) in Bremerhaven documenting glacial-interglacial variations in the deep-water regime of the central Arctic Ocean. After graduating in December 2011 from Freiberg she continued to work at the AWI as research assistant until she started her PhD project in the stratigraphy and palaeontology workgroup at Utrecht University in autumn 2012 of which this thesis is the result. Throughout her time at the AWI and Utrecht University she has participated in four sea-going expeditions to Arctic and Antarctic in 2011, 2012 and 2014. From May to August 2016 she has also conducted an ECORD funded research project in collaboration with Université du Québec à Montréal in Canada.